DESIGN, DEVELOPMENT AND PERFORMANCE EVALUATION OF A DYNAMIC KNEE SIMULATOR

by

C.A. McLean

A thesis submitted to the Faculty of Graduate Studies and Research in partial fulfillment of the requirements for the Degree of Master of Engineering

Department of Mechanical Engineering

McGill University

Montreal, Quebec

July 1990

ABSTRACT

This study reports on the design, development and evaluation of a dynamic simulator for the human knee joint. The simulator was designed to facilitate the study of knee mechanics corresponding to dynamic functional activities (e.g., walking, stair ascent and descent). The simulator can be programmed to apply specified load histories to a knee specimen, in an unconstrained manner, such that the normal physiological response of the joint is reproduced.

The simulator comprises of four actuators. Two stepping motors, acting as the main muscle groups, control the flexion angle histories of the joint through steel cables. Two electrohydraulic actuator systems apply the two main components of the foot-to-floor reaction; the flexing/extending moment and the tibial axial force. Actuation control and data acquisition are performed separately through two microcomputer/interface systems.

Satisfactory function reproduction, corresponding to walking gait, was obtained within the following ranges and error margins for a gait cycle time of 1.25 sec: Flexion Angle: 70 $\pm$ 5°; Flexing Moment: 55 $\pm$ 5 Nm; Tibial Axial Force: 670 $\pm$ 67 N.

RESUME

Ce mémoire présente la conception, le développement et l'évaluation d'un simulateur dynamique pour l'articulation du genou humain. Le simulateur fut conçu pour faciliter l'étude de la mécanique du genou dans des activités dynamiques fonctionnelles, telles que: marcher, monter ou descendre des escaliers. Le simulateur peut être programmé pour appliquer à des spécimens in-vitro, des cycles spécifiques de charge de façon non-contraignante, de sorte que la réponse physiologique et normale de l'articulation soit respectée.

Le simulateur consiste en quatre actuateurs. Deux moteurs pas-à-pas remplacent les groupes musculaires principaux, soit les fléchisseurs et les extenseurs, et contrôlent par l'entremise de câbles d'acier, l'angle de flexion de l'articulation Finalement, les deux composantes principales de la réaction au sol, soit le moment fléchisseur/extenseur et la force axiale sur le tibia, sont appliquées à l'aide de deux systèmes d'actuateurs électrohydrauliques. Deux micro-ordinateurs avec interfaces sont utilisés pour le contrôle de la simulation et l'acquisition de données.

Une reproduction satisfaisante des fonctions cycliques prédéterminées, correspondant à la démarche, a pu être obtenue, atteignant les caractéristiques suivantes: flexion, 70 $\pm$ 5°; moment de flexion, 55 $\pm$ 5 Nm; force axiale sur le tibia, 670 $\pm$ 67 N; pour une période de marche, 1.25 sec.

ACKNOWLEDGEMENTS

I wish to thank: Dr. A.M. Ahmed for thesis supervision and guidance; Celia Williams for her relentless collaboration and support; Alex Hyder, John Kelly and staff, Arthur Clement and staff, George Dedic and George Tewfik for their technical assistance; Shaolin Shi and Françoise Marchand for their expertise and finally, Anna Cianci for her patience in typing this manuscript.

Contents

List of Figures

List of Tables

Chapter 1

INTRODUCTION

1.1 General Introduction

The knee joint is one of the more complicated and larger joints in the human musculoskeletal system. It acts as the articulating junction between two long lever arms, the thigh and the shank, through which the upper body interacts with the ground surface. It is a necessary element in both normal bipedal ambulation and simple support.

During functional activity, the knee joint must transmit large reaction loads while allowing large relative displacements between the joint members. Because of this, the joint is susceptible to both structural damage (injury) and articular surface degeneration (arthritis). In either case, surgery may be performed to restore the joint's normal biomechanical function including the replacement of the articular surfaces with prosthetic implants. The success of surgical interventions depends largely on a clear understanding of the joint's mechanical characteristics which are partly obtained from biomechanical research. In view of the joint's importance during dynamic functional activity (e.g. ambulation), the establishment of the joint's characteristics under dynamic conditions is of interest. In-vitro simulation of these conditions on a knee joint specimen under controlled laboratory conditions, allowing the investigator the possibility of using various invasive instrumentation techniques, is an appropriate approach for the study of the joint's characteristics. The subject of the present study is the design, development and implementation of a research tool capable of simulating, in-vitro, common dynamic functional activities on a human knee specimen.

1.2 Motivation

In general, biomechanical research is performed in either the static or dynamic regimes, i.e., the joint is subjected to either a constant load or to a time-varying load function, while the joint response characteristics of interest are measured. Each of these approaches can be undertaken either under in-vitro or in-vivo conditions. There are advantages and disadvantages associated with each combination.

The static regime is simpler than the dynamic one and requires therefore less sophisticated hardware. However, functional activity is dynamic in nature and the correlation of statically obtained data to a normal dynamic physiological situation is difficult in view of the complexities of the joint and the time-dependent material characteristics of biological tissues.

For in-vivo testing, whether static or dynamic, the investigator is restricted to non-invasive instrumentation techniques in constrast to the case of in-vitro testing. In-vivo studies yield data concerning qualitative forces of superficial muscles acquired electromyographically, approximate relative displacements of joint bone components measured externally using photographic techniques or electro-mechanical goniometers, and foot-to-floor (ground) reactions measured via force plates. The lower limb incorporates 31 muscles and thus to obtain the joint reaction forces or other joint forces (ligament forces ...), objective functions are developed to render the problem determinate and verified with the recorded data. These objective functions are derived from intuitive criteria and are therefore, a source of uncertainties.

Dynamic in-vitro testing offers the capability of directly measuring the joint characteristics since joint components can be made more easily accessible as required. Furthermore, since studies are performed under dynamic conditions, the data obtained applies directly to the simulated activity with the time-dependent aspects of the biological tissues taken into account. Such advantages warrant the development of a dynamic in-vitro simulator.

In this study, it is proposed to design, fabricate and test a facility which applies dynamic loads to amputated or cadaver knee joint specimens. The applications of this simulator are manifold:

i. studies of the knee joint under dynamic conditions can be undertaken with the use of a full complement of instrumentation techniques. For instance, the direct measurement of ligament loads, external joint forces and spatial displacements between joint members are possible.

ii. the biomechanical consequences of corrective surgical procedures can be evaluated by monitoring their effects under dynamic activity, avoiding the risks associated with in-vivo experiments.

iii. the biomechanical performance of knee joint prosthetic implants can be evaluated including the effects of their misalignment.

1.3 Previous Investigations

A series of dynamic knee loading devices have been reported in the literature [Shaw and Murray (1973), Richards Manufacturing Co. (1978), Greer (1979), Pappas and Buechel (1979), Szklar (1985), Szklar and Ahmed (1987)]. Only one of these simulators [Szklar (1985), Szklar and Ahmed (1987)] is of direct significance in this study. The remaining similators were designed as life-cycle testing machines to determine the rate and nature of wear of prosthetic components. In view of their intended application, simple constrained loading schemes were employed which did not allow normal physiologically constrained joint responses. Joint wrench reactions and/or relative displacements were applied directly as control inputs. In the normal physiological situation consistent with a given functional activity, the joint reaction forces and relative displacements are induced by muscle forces and ground reaction forces while being passively controlled by each joint's geometrical and structural chacteristics in a unique fashion. Hence, the joint forces and relative displacements can not be expected to be 'normal' in these life-cycle testing machines. Although these facilities serve a useful function for which they were designed, they are inadequate for joint biomechanical research.

The only unconstrained simulator reported in the literature is that by Szklar (1985) and, Szklar and Ahmed (1987). This was the first simulator of its type and is the prototype on which the simulator discussed in the present study is based. The simulator reported in the present study is actually an extended and modified version of the 'Szklar' simulator. Many of the hardware components have been either re-implemented unchanged or modified depending on their performance, and new components have been added as necessary to improve or supplement the original simulator's features. Many references will be made to the previous simulator hereafter under the term 'prototype'.

Because of the technical complexities of true dynamic simulation, the prototype was limited to simulating the dynamics of the joint by using only two muscle forces, the extensor and flexor lumped muscle group forces, without the independent application of the ground reaction force. While the femur was held fixed to a force plate, the muscle forces were applied to a freely moveable tibia by two electro-hydraulic servo-actuators acting through flexible cables. The extensor cable was attached to the patella, thus including the patellofemoral joint reaction contribution to the overall joint mechanics. Individual action of the actuators was used to control active flexion/extension, while their simultaneous action was used to control the joint compressive force. A microprocessor under real-time control coupled with an interface card was used to simultaneously send reference command signals to the hydraulic actuators and to record the knee flexion angle as well as the joint reaction time-histories, measured respectively using a two degrees-of-freedom goniometer and the force plate.

Although the prototype design provided a scheme by which the action of the two main muscle groups affecting the knee during normal functional activities could be mechanically simulated without constraining the natural and conjunct passive motions of the knee, the application of the total axial joint compressive forces through the muscle cables resulted in the presence of large non-physiological forces. For example, the extensor loads partly included the tibial axial component of the ground reaction force resulting in parasitic patellofemoral reaction loads. Normally, the tibial axial component of the ground reaction force is transmitted up the tibia to the joint without the active interactions of the extensor or flexor muscles. The muscular activity which affects the knee should only be in response to the components of the ground reaction force, as well as the inertial and gravity forces, which are tending to rotate the shank with respect to the thigh in such a manner that the motions associated with functional activity are obtained. Therefore, to avoid the generation of non-physiological forces on the joint, the ground reaction force and moment components should be applied to the joint members separately from the muscle forces.

Another problem which limited the usefulness of the prototype, and which stemmed from an unforeseen problem within the actuation system, was its inability to reproduce gaits of frequencies and flexion ranges beyond .5 Hz and 40^{o} respectively. Such a limited range of operation precluded the simulation of most functional activities.

Although these problems were significant, the performance of the prototype was sufficiently encouraging to promote further design development to circumvent the above limitations.

1.4 Specific Objectives, Basic Design Approach

Ideally, a dynamic loading simulator should be capable of applying to a joint specimen all the forces affecting the joint (viz.,muscle forces, ground reaction, inertia, gravity) in a manner such that their time-histories correspond to the functional activity under simulation. Moreover, the method of application of the forces should be such as not to constrain the resultant response of the joint.

Given that the aforementioned dynamic load functions are applied to a knee joint specimen, then the resulting motions and joint reaction forces will be those intrinsically defined by the biomechanical characteristics of the specimen. Thus the relative motions and joint reaction forces are not inputs to the simulator but a result of the inputs. Such physiologically controlled dynamics are termed 'unconstrained'. This criterion is adhered to in this study.

Due to the technical complexities involved in the realization of an ideal simulator, to render the design feasible, certain simplifications must be adopted without undue compromise of the applicability of the simulator. In the prototype, each of the extensor and flexor muscle groups were lumped resulting in a two-muscle force simulation in such a manner that their lines of action were theoretically equivalent to that of the resultants of the various muscles which control flexion/extension. This mode of actuation has also been employed in the present study.

The other simplification which was used in the prototype was to include the ground reaction force in the muscle loads to obtain the axial joint reaction. As was mentioned in the previous section, this resulted in large parasitic forces. The ground reaction force should be separately applied to restrict the muscle loads to amounts which are physiologically correct and commensurate with the activity simulated. Hence, it is the purpose of this study to extend the prototype such that the ground reaction may be separately applied (Figure 1.1). Such an undertaking implies the design and implementation of independent ground reaction actuating mechanisms, control systems and instrumentation. A complete re-design of the given prototype and its user interface system to incorporate the new subsystems is also entailed.

The ground reaction (foot-to-floor) may be defined by three mutually perpendicular forces defined by the plane of motion and the tibial long axis. The component along the tibial long axis is in general at least 5 times larger than the remaining two components during normal functional activities (walking gait, stair gaits, etc ...). This force is transmitted up along the tibia to result directly in a compressive force at the tibio-femoral junction. Another major contributor to knee joint mechanics is the moment generated by the off-axis component of the ground reaction force in the plane of motion (the flex./ext. moment). This component is significant in that the flexing/extending muscle forces generated during functional activity are to a large extent directly attributable to this moment. The muscle forces must in effect generate a moment about the knee's central axis to sustain or overcome the ground moment in order to produce the required motion. These two components of the ground reaction are in the plane of motion. The remaining important contributor to knee joint mechanics is the moment component of the ground reaction which is tending to deviate the shank out-of-plane relative to the thigh (abducting/adducting).

In view of the foregoing, only the tibial axial and moment components of the ground reaction in the plane of motion are considered in the present study (Figure 1.1). To also simulate the out-of-plane moment component of the ground reaction would require additionally the simulation of the abductor/adductor muscle groups.

Two specially designed actuating systems have been implemented to apply the described ground reaction components. The electro-hydraulic actuators that were used as the muscle load actuators in the prototype have been selected here to provide the actuating forces. They were shown to be ideal as force applicators in the prototype as is necessary in this instance. The hardware problem which limited the operating range of these actuators in the prototype has been resolved to ensure that it doesn't hinder the presently proposed simulation. The designs of these actuating systems as presented in this study are such that the natural and conjunct passive motions of the knee are unconstrained.

As to the muscle load actuation scheme, a two axis stepping motor actuation system has been implemented to replace the hydraulic actuation system. Loads are applied through steel cables to maintain the unconstrained condition as was achieved in the prototype. The extensor cable is again directly attached to the patella thus reproducing the patellofemoral contribution to the knee joint mechanics. Stepping motors have been chosen in view of their suitability in positional control applications. It has been decided in the present study to input the displacement time-histories of the muscle cables to specifically and actively control the flexion angle time-histories associated with the functional activity under study. Since the ground reaction forces are applied separately, the forces generated in the muscle cables should inherently be physiological.

Hence, it is proposed to actively control the joint flexion angle through the flexing/extending lumped muscle groups while concurrently and separately applying the two described components of the ground reaction. The remaining degrees of freedom are passively controlled only by knee geometry and ligamentous structure. The contributions of the inertial and gravitational forces are only partially maintained. Only the relative accelerations of the shank with respect to the thigh are reproduced since the femur is held fixed to a force plate as in the prototype. The gravitational forces are only approximated since again the femur is held fixed in an average upright position. Although not exactly reproduced, these contributions are much smaller than the muscle and ground reaction contributions to knee joint mechanics.

The simulator must be capable of simulating a variety of functional activities. However, the design of the actuation system considers only level walking gait and stair gaits (both ascent and descent). It is felt that given this range of possible activities, other activities such as ramp ascent and descent may also be considered. Due to the page constraints of this report and the time limitation of this study, the simulator presented in this study was only evaluated under the conditions of level walking since it is by far the most common and clinically relevant functional activity which the joint must sustain.

In the prototype, both actuation control and data acquisition were performed by a single microprocessor with a limited possibility for system expansion. In the present study, actuation is controlled by a microcomputer which is entirely programmable such that other activities may be simulated. A dedicated data acquisition system has been implemented to measure the simulators performance which may also be reprogrammed as required to allow the measurement and logging of knee joint characteristics.

In summary, the specificic objectives were to design, fabricate and implement a dynamic simulator for the knee joint. In order to fufill the requirements, a four actuator scheme was adopted. In correlation to a specified activity, the flexion angle and the tibial axial force and flexing/extending moment components of the ground reaction are reproduced. The flexion angle is controlled through the actions of the flexor and extensor muscle forces while the two ground reaction loads are applied independently. All loading is such that the natural and conjunct passive motions of the knee are unconstrained The femur is held fixed to a force plate while the forces are applied to a freely moveable tibia. The extensor force is applied through the patella and thus, both the tibiofemoral and patellofemoral articulations which form the knee are left intact. The design and/or selection of the simulator components (i.e., actuators, mechanical components, instrumentation, control systems, ...) took into consideration the requirements corresponding with walking and stair gait simulations to ensure the possibility of simulating a wide range of functional activities. The simulator's hardware and user interface system are redesigned separating the controller and data acquisition components in a manner to facilitate use and system expansion. New control and data acquisition software is implemented and designed to ensure ease in system programmability. Finally, sample results of a walking gait simulation are obtained for two specimens in order to evaluate the performance of the simulator.

1.5 Thesis Organization

To achieve the design of a knee simulator, the system with which the simulator interacts (i.e. the knee) must be first clearly understood. An anatomical study of the joint and its behaviour during functional activity are the subjects of Chapter 2.

Then the adopted overall design and its various features are described in Chapter 3. Included in this chapter are the reference input functions which were chosen to be simulated and the method of specimen preparation.

In Chapter 4, the implemented actuating systems and their components are described. System modelling, component selection criteria and performance characteristics are included.

The instrumentation used to measure the joint characteristics and the performance of the actuating systems are described in Chapter 5.

The microcomputers and various subsystems used to control the simulator and perform the data acquisition functions are described in the first part of Chapter 6. The remaining part of the chapter is dedicated to the various procedures and software techniques, utilized to generate the command functions, control the actuating systems for a simulation run and perform the data acquisition functions.

The results of a simulation run performed on two specimens will be presented and discussed in Chapter 7.

The final chapter is a concluding chapter in which the achievements of the simulator design criteria are evaluated. The scope of the experimentation capabilities of the simulator as well as recommendations for future development are also included.

The Appendices are reserved for secondary information. They include the dynamic equilibrium equations and parameter value estimations used to model the ground reaction actuation systems. The source listing of the operating routine is also included.

Chapter 2

JOINT ANATOMY AND MECHANICS

2.1 Introduction

In this chapter, the knee joint anatomy and physiology will be presented. The discussion on anatomy will be limited to those aspects which are relevant to the design of the dynamic simulator. The important aspects of anatomy which determine the joint's functional behaviour are the geometry of its articular surfaces, the ligamentous structure and the musculature. Having described the elements which form the knee joint, its resulting behaviour under prescribed functional activities will be presented in terms of muscular activity, joint kinematics and reaction forces. The functional activities which will be examined are level walking and stair ascent and descent gait activities.

A greater emphasis will be placed on level walking since the simulator has been tested and validated under those conditions. Stair gaits will be briefly examined since the actuator scheme and other simulator components have been designed to also accommodate the simulation of these more stringent activities.

2.2 Joint Anatomy

2.2.1 Articular Surface Geometry

At first impression, the knee joint may appear to act as a pin-joint having a single rotary degree of freedom. In actuality, there is no mechanical interlocking of the bony components themselves and the mating surfaces are highly irregular. Furthermore, the knee joint is comprised of two articulations as can be seen in Figure 2.1 One is the tibiofemoral articulation between the tibia and the femur and the other is the patellofemoral articulation between the patella and the femur. The femoral articulating surfaces are formed by two nearly spherical surfaces called the condyles which mate with two virtually flat surfaces separated by an eminence on the proximal end of the tibia. The articulating surfaces of the tibia are called the tibial plateaus The articulating path for the patella on the femur is a notch between the femoral condyles called the 'patellar' surface. This surface also forms a bearing surface for the attached quadriceps tendon. The irregular mating geometries and the incongruencies of the articulations imply that the relative displacements between the joint bone components are a function of the geometry and flexion angle in addition to the applied loads Hence, the relative displacements depend upon the activity performed Furthermore, an important consideration is that each knee joint is unique (biological variance) and presents a variable geometry. Relative displacements may then be expected to vary somewhat between specimens under identical loading conditions.

2.2.2 Ligamentous Structure

As was noted in the previous section, the geometric characteristics of the articular surfaces are insufficient to provide the joint with adequate stability. The ligamentous structure serves to passively restrain the non-compressive relative displacements between the articulating surfaces.

Ligaments are bands of fibrous tissue which serve to join or connect adjacent bones in a joint. Although, upon dissection, the joint is seen to be totally encapsulated by a single ligamentous structure, its thickness varies locally such that discrete ligaments may be defined (Figure 2.2).

The medial and lateral collateral ligaments are oriented vertically on each side of the knee joint between the tibia and femur, and the fibula and femur, respectively. They provide lateral and rotary stability for the knee. In the middle of the knee, starting between the femoral condyles and ending at the eminence of the tibia and forming an x-pattern, are the anterior and posterior cruciate ligaments. Their disposition is such that backward motion of the tibia relative to the femur is restrained by the posterior cruciate ligament while the opposite motion is restrained by the anterior cruciate ligament.

The other ligament to be considered is the patellar ligament. This ligament has a tendon-like function and is often called the patellar tendon. It connects the patella to the front of the tibia and serves to transmit to the tibia, through the patella, the muscle forces from the front of the thigh.

Ligaments are tensile members which display viscoelastic behaviour. This characteristic will result in their response being a function of their load-time histories. Hence, relative displacements and stress distribution between the articular surfaces are not only a function of the activity performed but also of the rate at which they are performed.

2.2.3 Musculature

The lower limb comprises the hip, knee and ankle joints, all of which are capable of multiple motions. To control these multiple degrees of freedom, the lower limb is equipped with 31 muscles. Each of these may span one or two joints and they are hence capable of producing multiple actions on the joint bone components such as flexion, abduction, axial rotation, etc. Table 2.1 lists only those muscles and actions which are pertinent to this study. The primary degree of freedom of the knee joint is flexion/extension. The quadriceps group at the front of the thigh is responsible for extension. As was mentioned in the previous section, all quadriceps group muscles

Table 2.1: Pertinent Muscles of The Knee Joint (Szklar, 1985).

Action	Muscle	Origin (Proximal Attachment)	Insertion (Distal Attachment)
Knee Extension	Quadriceps		
	Rectus Femoris	Ilium	
	Vastus Lateralis	Femur	Patella
	Vastus Medialis		
	Vastus Intermedialis		
Knee Flexion	Hamstrings		
	Biceps Femoris	Ilium & Femur	
	Semitendinosis	Ilium	
	Semimembranosis	Ilium	Tibia
	Gracilis	Pubis	
	Sartorius	Ilium	
Foot Flexion	Gastrocnemius		
	Medial Head	Condyles of Femur	
	Lateral Head		Heel
	Soleus	Tibia & Fibula	
	Peroneus Longus	Tibia & Fibula	
	Peroneus Brevis	Fibula	
	Tibialis Posterior	Membrane between Tibia & Fibula	Foot
	Flexor Digitorum Longus	Tibia	

act through the patella. Flexion is produced mainly by the hamstrings at the back of the thigh. The gastrocnemius group are the main ankle actuating muscles (foot extensors). They have also been included in this study since they also span the knee joint and are known to be important contributors in locomotion as will be elaborated in a further section (Section 2.3.2).

The areas of attachment of the aforementioned muscles are depicted in Figures 2.3, 2.4 and 2.5. These are necessary in the determination of the lines of action of the contributing muscles as is required in the next chapter (Section 3.2).

The other degrees of freedom of the knee joint beyond flexion/extension will be discussed in the later section on joint kinematics (Section 2.3.4).

2.3 Gait Analysis

2.3.1 Introduction

The response of the knee during functional activity is the result of the actions of many forces which are in dynamic equilibrium. A free body diagram of the joint is depicted in Figure 2.6. Starting distally, there is the ground reaction force which is transmitted up the tibia from the ankle and foot. Then in relation to the movement and position of the lower limb, there are the inertial and gravitational forces which act upon the lower limb. The muscle forces act next upon the knee bone components as prime movers to actively produce the overall motion associated with locomotion. All these forces are in equilibrium with the joint reaction forces (articular contact forces and ligament forces), and result in the relative displacements between the joint members.

2.3.2 Gait Descriptions

Stick figure representations of single cycles of walking and stair ascent and descent gaits are depicted in Figure 2.7. There are two distinct phases during a single step of walking or stair gait: the stance phase which is initiated when the foot contacts the ground (i.e. "heel strike" for walking); and the swing phase which is initiated when the foot leaves the ground surface. The ratio of swing to stance is about 60%:40% to 65%:35% for the gaits depicted. Since the ratio is not even, there is a period during which both feet are in contact with the ground and this portion is defined as double-legged stance. Stance is opposite in nature to swing. It is the weight bearing period during which the lower leg is in contact with the ground and the knee joint must sustain the ground reaction forces which are transmitted from the ankle along the tibia in addition to the muscle forces During swing, the period during which the foot is not in contact with the ground, the knee joint need only sustain the smaller inertial and gravitational loads of the lower leg. Furthermore, minimal knee flexion is observed during stance relative to swing during level walking. However, during stair gaits, the ranges of flexion, as well as the magnitudes of the flexion rates, are approximately the same during both the swing and stance phase. Cycle times are generally in the range of 1 to 1.6 seconds, with stair gait cycle times in the upper portion of this range.

2.3.3 Muscular Activity

Muscle activity is generally measured from electromyographical signals (EMG). Although these signals indicate which muscles are active and when, their proportionality to actual muscle tension is not as yet clearly established. Thus, only general trends of muscle activity can be recorded corresponding to gait cycle phases.

For walking gait, the results of two studies [Morrison (1970) in Figure 2.8 and Mann and Hagy (1980) in Figure 2.9] are reproduced. From these figures, a certain amount of variability is apparent. In both studies, just prior to heel strike, the hamstrings are activated to decelerate the lower limb in anticipation of ground contact. This activity is continued during heel strike with, in the case of Mann and Hagy's study, the antagonistic activity of the quadriceps. Antagonistic forces are assumed in general to be of minor amplitudes and serve a stabilizing purpose. Following heel strike, the knee flexes slightly complying to the braking action of the ground. In the case as shown by Morrison, the quadriceps are then reactivated to initially sustain the braking action which, in this case, is tending to flex the knee. This quadriceps action is continued to overcome the external flexing moment and re-extend the knee against it thus lifting and rocking the upper body forward. Little activity is noted from Mann and Hagy during this period. Thereafter, in both studies, the activity of the gastrocnemius ensues to apply a moment about the ankle to counteract the increasing moment induced by gravity as the center of gravity of the subject moves anteriorly from the ground contact point. In the case of Mann and Hagy's study, this gastrocnemius activity is initiated slightly earlier relative to the activity noted by Morrison. Then, according to both studies, controlled by the quadriceps action, the knee is allowed to start flexing again prior to the onset of the swing phase while the other leg, near the end of its swing phase, is being decelerated thus inertially pulling the body forward. In effect, the body is alternately rocking and falling forward from one step to another.

In stair gait, similar muscular activity is noted with increased activity of the extensors during the stance phase [Morrison (1969), Andriacchi et al. (1980)]. Heavier demands are placed on the extensors during stance in stair ascent as they are required to effectively lift the body about the knee. In stair descent, throughout the stance phase, the extensors are controlling the rate of knee flexion and the rate at which the body is lowered to the next step. As opposed to walking and stair ascent, during which energy is mostly expended, the extensor muscle group is absorbing relatively large amounts of energy and dissipating it in the form of heat during the stance phase portion of stair descent gait.

2.3.4 Joint Kinematics

As was mentioned previously, the relative motions between the bony components of the knee exhibit highly three-dimensional motion characteristics which are dependent both on the articulating surface geometries and the ligamentous structures as well as the forces acting on the knee corresponding to a particular activity.

Table 2.2: Reported Magnitudes of Degrees of Freedom of the Knee.

	Degree of Freedom	Hoffman et al. (1977)	Kettelkamp et al. (1970)	Milner et al. (1973)	Townsend et al. (1977)
Level Walking	Flexion (deg)	71.5 ± 7.6	67.2	55.0	61.0
	Int./External (deg)	14.1 ± 3.9	13.0	—	11.5
	Abd./Adduction (deg)	11.7 ± 4.0	10.8	—	1.2
Stair Ascent	Flexion (deg)	81.7 ± 7.9	N.A.	N.A.	N.A.
	Int./External (deg)	12.8 ± 4.2			
	Abd./Adduction (deg)	18.5 ± 5.1			
Stair Descent	Flexion (deg)	83.3 ± 9.1	N.A.	N.A	N.A
	Int./External (deg)	15.0 ± 4.5			
	Abd./Adduction (deg)	14.3 ± 4.4			

The three rotational degrees of freedom between the tibia and the femur which are illustrated in Figure 2.10 are: flexion/extension, internal/external and abduction/adduction rotations. Flexion/extension is the result of rolling and sliding at the tibiofemoral articulation. Internal/external long axis rotation is the rotation of the tibia along its long axis. Abduction/adduction rotation is the transverse or lateral swing of the tibia. Reported average magnitudes of these degrees of freedom for walking and stair gaits are included in Table 2.2.

It is the combination of many forces which contribute to these relative displacements thus producing dynamic equilibrium in the knee. Thus to reproduce in-vitro the anatomic response of the knee joint during gait activities, i.e. the resulting relative displacements and joint reactions, the muscle forces, the ground reaction and the gravitational and inertial forces must be simulated.

2.3.5 Joint Reactions

The described forces that act upon the knee during functional activity result in the total joint reaction force which comprises the patellofemoral and tibiofemoral reactions. The output of a simulation run should result in anatomic joint reaction force time-histories being reproduced as would be measured under in-vivo conditions.

Presently, the tibiofemoral joint reaction force corresponding to a particular activity is calculated by investigators based on a simplified mathematical model of the knee where measured ground reaction and limb relative position time-histories are the inputs. Often the predictions are verified with electromyographical measurements. Although the joint reaction has components in all three directions, the compressive load in the direction of the tibial long axis is by far the largest component. Reported tibial long axis compressive load time- histories by three investigators are reproduced in Figure 2.11. As may be noted from the figure, there are discrepancies between the depicted results. These differences may be attributed to biological variances with regard to the articular surface geometries, the ligamentous structure, the configuration of the muscles and the subject's gait habits. They may also be attributed to each investigator's particular technique of solving the dynamic equilibrium equations of the knee. Because there are many more unknowns than equations, due to the large number of muscles which span the knee, optimization techniques are required involving the use of objective functions. The choice of the objective functions varies somewhat between investigators.

In spite of the discrepancies between the results in Figure 2.11, the overall trends and shapes predicted for the joint reaction force are approximately constant with generally only the magnitudes of the variables differing substantially.

Computed tibiofemoral joint reaction time-histories for stair activities may be found in the literature [e.g., Morrison (1969)].

With regards to the patellofemoral joint reaction corresponding to dynamic activity, a study by Reilly and Martens (1972) yields estimates for this force for a variety of activities. A highly simplified mathematical model was assumed and an experimental validation was not performed. This area of study seems to be lacking even though the patellofemoral joint reaction is of great clinical significance.

2.4 Summary

The contributions of the muscular activity, the reaction of the ground, the inertial and gravitational forces result in the relative motions and reaction forces between the tibia, the femur and the patella during a given functional activity. Furthermore, since the articular surface geometry and the ligamentous structure of each knee joint specimen are unique, due to biological variance, each joint will have a correspondingly unique response to a single activity. This characteristic of uniqueness must be respected for an in-vitro simulator to be physiologically faithful, i.e., for it to simulate in-vivo conditions.

Chapter 3

DESIGN APPROACH

3.1 Introduction

In this chapter, the basic approach and the underlying motivations behind the design of the key features and loading scheme of the simulator are discussed.

As was elaborated in the previous section, because of biological variance, each knee joint has a unique dynamic response characteristic under the conditions of functional activity. Thus the means of applying the loads that act upon the knee must be such that the natural and conjunct passive motions of the knee are unconstrained. In view of the technical complexities, it is not feasible in a simulator to apply all the independent forces which act upon the knee. In the present study, only the more important contributors which are active during normal gait activity in the plane of motion are considered. The simulator presented herein comprises the capability of generating four independent time-varying loads on a knee joint specimen. These include the actions of the two main lumped muscle groups (the extensor and flexor groups) in controlling the flexion angle histories, and the tibial axial force and flexing/extending moment components of the ground reaction force. The dynamic functions to be simulated and the loading scheme used are each further discussed in this chapter.

Also discussed in this chapter are the adjustability and versatility features incorporated into the simulator's design. These are essential since the simulator must apply the loads in such a manner as to be commensurate with the uniqueness of each specimen. A final section is reserved for specimen preparation. The procedure must be such that the tibiofemoral and the patellofemoral articulations are conserved.

3.2 Four Force Simulation

The primary function of the knee is to flex or extend as the rest of the body interacts with the ground surface such that the overall motion (e.g., of gait) is produced. This in effect results in cyclical flexion angle and concurrent ground reaction time-histories. These patterns are primarily dependent on the activity being performed and are generally repeatable from cycle to cycle. Furthermore, the flexion angle and ground reaction characteristics of gait are readily available in the literature. It is also important to note that these characteristics are directly measured in-vivo as opposed to muscle forces which are inferred. In view of the foregoing, the underlying concept of the dynamic simulator is to have the main muscle groups, which contribute to the flexion/extension action of the knee, reproduce flexion-angle time-histories on a knee while it is also subjected to the concurrent ground reaction time-histories. The flexion/extension action is produced by two displacement vs time controlled actuating systems. Each system independently simulates the lumped effects of the extensor and flexor muscle groups and acts through steel cables such as to not constrain the other degrees of freedom of the knee, viz, abduction/adduction, long axis rotation, and three dimensional relative translation (Fig. 3.1). In order that the lines of action of these lumped forces be as close as possible to the net effect of all the individual muscles, the lumped estimation is derived in the following manner:

i. the muscle attachment points are estimated to be at the centroid of the attachment areas as depicted in anatomy texts (section 2.2.3),

ii. the individual muscle lines of action are assumed to be straight lines between estimated origin and insertion points,

iii. the contribution of individual muscles are assumed to be proportional to their cross-sectional area,

iv. the net line of action of a muscle group is the weighted average of the individual lines.

Other flexor and extensor mechanism details are further discussed in the following section of this chapter.

As was established in the introduction, the simulated components of the ground reaction include the flexing/extending moment and the tibial axial force. The flexing/extending moment component has been selected since it is generally the larger contributor to the joint reaction during functional activity. It is this moment that the flexor or extensor muscles must counteract in order to lift or push/pull the body during functional activity. The forces generated in these muscles in response to this moment may be shown to account for 50% to 70% of the joint reaction force during level walking.

The tibial axial force component of the ground reaction has also been selected in view of its relative significance with respect to its contribution to the joint reaction. Generally, during normal functional activity, the leg joints position themselves so as to minimize the moment components of the ground reaction thus reducing the required muscle forces and relieving the joint reactions. More specifically, the ground reaction force orients itself to a large extent along the tibial axis since that portion which acts perpendicular to the tibia at the heel will result in a large moment about the knee joint. This force may be shown to account for 20% to 50% of the total joint reaction during level walking.

As to the manner in which the ground reaction loads are applied in the simulator, the employed schemes are depicted in Figure 3.2. The tibial axial component of the ground reaction is applied to the tibial fixation bucket through a steel cable and pulley system, to another cable which distributes the load evenly to each side of the tibia. A set of sheaves attached to the frame is adjusted to ensure that the line of action of the force is parallel to the tibial axis and coincident with the flexion axis of the joint, regardless of the flexion angle. Although not constrained, a fixed flexion axis is assumed. Deviation of the joint's flexion axis from the one assumed will result in a parasitic flexing/extending moment being generated. Furthermore, parasitic long axis twisting moments will also be generated given that tibial long axis rotation relative to the femur is expected (Figure 3.3). However, given proper adjustment, these stray effects may be minimized. Corresponding to level walking, the magnitudes of both these parasitic moments were estimated to be less than 5 Nm and are therefore assumed to be of negligible effect. These estimations were obtained by assuming reported tibial long axis rotation magnitudes during the stance phase of level walking (Chao et al.,1983) and, the locus of the flexion axes as estimated from Walker et al. (1972) in correspondence to the stance flexion amplitude

As to the flexing/extending moment component of the ground reaction, a specially designed linkage system, acted upon by a linear actuator, is implemented to apply a transverse force (anterior/posterior) to an extension of the tibial shaft beneath the tibial fixation bucket (refer to Fig. 3.2). The actuating force is applied to a long lever arm whose rotational axis is aligned with the average flexion axis of each specimen. The lever arm extends distally to connect with the tibial extension through a specially designed linkage which only permits the transfer of a transverse force on the tibia while not constraining the tibia's three dimensional degrees-of-freedoom Assuming the flexion axis of each joint to be constant and coincident with that of the lever arm, the transverse tibial force should act with an approximately constant moment arm and futhermore, the rotation of the lever arm should equal the flexion rotation of each specimen. The moment arm of the transverse force is adjustable and in this study, it was adjusted to 44.7 cm. This moment arm is approximately equal to the lower shank length and thus the transverse force application is approximately equivalent to a base-of-foot application. As in the actuation of the tibial axial force component, a constant knee flexion axis is assumed but deviation of the true axis from the one assumed is unconstrained. In the case of the moment actuating system, deviation of the flexion axis, as estimated from Walker et al. (1972), will only result in

2% deviation from the sought moment time-histories corresponding to level walking. This is because of the relatively large moment arm chosen for the applied transverse force.

Since the desired moment is obtained by applying a transverse force on the tibia, a parasitic transverse force of equal magnitude and sense will also be transmitted to the joint. This parasitic force will be evaluated in the next section.

As can be seen in Figure 3.1, the femur is rigidly fixed to a force plate permitting the measurement of the joint reaction time-histories while the tibia is free to move under the actions of the applied forces. However, during functional activity, the femur also moves substantially about the hip joint. Therefore, as was discussed in the introduction, only the relative accelerations and corresponding inertial forces between the shank and thigh are reproduced. The gravitational forces are only approximated since the femur is held fixed in an average upright position.

3.3 Selection of the Simulated Dynamic Functions

For normal level walking, the target flexion angle versus time function which has been selected in this study is reproduced in Figure 3.4 (Mann and Hagy, 1980). The cycle time was chosen to be 1.25 seconds with stance occupying 64% of the cycle (0.8 sec).

The ground reaction time-histories are usually found in the literature in terms of the vertical and fore-aft component time-histories, these directions being with respect to the ground's surface, along with their point of application under the foot (center of pressure). The set of functions assumed in this study is reproduced in Figure 3.5 (Grundy et al., 1975). To obtain the corresponding moment and tibial axial components of the ground reaction, the time-histories of the given reaction components and the location of their point of application under the foot must be coupled with corresponding limb segment position time-histories. The flexing/extending moment due to ground reaction is obtained by taking the cross product of the sum of the reaction forces in the plane of motion with the position vector joining the point of application of the reaction force to the approximate rotational axis of the knee joint. The required limb segment orientation time-histories (ankle, knee and hip) used in the computations are those published by Mann and Hagy (1980). The limb segment lengths that are assumed in the calculation were found in anatomy texts and the upper torso orientation, which was also required in the computations, was assumed to be vertical throughout the walking gait cycle. The resulting target time-histories of the flexing/extending moment and tibial axial force components of the ground reaction are depicted in Figure 3.6.

As can be noted from the figure, the moment component of the ground reaction remains a flexing moment throughout the stance cycle and the maximum magnitude is approximately 110 Nm. Other investigators have published the 'net' torque amplitudes and senses which the flexor or extensor muscle groups must counteract during level walking. However, it must be mentioned that these published values of 'net' torques could not be adopted in this study as the target moments because they include inertial and gravitational forces. They may be used for comparison with the computed moments in this study during the stance phase assuming inertial and gravitational effects are negligible during this phase. Winter (1980) has compiled the results of various investigators and the review is reproduced in Table 3.1. According to that study, considerable variability exists with respect to the moment time-histories which the knee must sustain during walking gait both in terms of magnitude and sense. It appears plausible that a given individual gait pattern may result in a moment time-histories about the knee as computed in this study. However, the computed peak magnitude seems to be rather on the high side and an extreme case. The corresponding results by Patriarco et al. (1981) also seem to indicate that the moments computed in this study are overestimated. To avoid excessive loading, the target moment time-history that was adopted in this study for simulation is as depicted in Figure 3.6, only the magnitudes are halved as indicated on the figure. The obtained pattern closely matches the pattern measured by Patriarco et al. (1981).

Design considerations of the actuating system assume the larger amplitudes (i.e.,

Table 3.1: Flex./Ext. Moment Variability (Winter, 1980)

	Peaks of muscle moments - flexion (f), extension (e) Knee (N.m)	
	Wt. accept	Push off
Elftman (1939)	40(e)	50(e)
Bresler &	48(e) + 40(f)	15(e) + 37(f)
Frankel (1950)	16(e) + 75(f)	48(e) + 35(f)
	5(e) + 42(f)	50(e) + 15(f)
	5(e) + 85(f)	17(e) + 85(f)
Paul (1966)	100(e)	25(f)
Morrison (1968)	48(e) + 35(f)	28(e)
Morrison (1970)	2(f)	7(e) + 2(f)
	1(f) + 5(e)	10(e) + 2(f)
	7(e)	17(e)
Morrison via	25(f) + 30(e)	25(f)
Paul (1971)		
(10 subjects)		
Pedotti (1977)	30(f)	65(f)
	40(f) + 40(e)	50(f) + 25(e)
	50(f) + 80(e)	10(f)
Johnson &	110(f)	65(e)
Waugh (1979)		

110 N.m. flexing moment amplitude) in the event that such load magnitudes are considered for simulation in future studies. It is understood that the simulator is entirely programmable. Functions with somewhat different characteristics than those adopted here may also have been used as the input functions.

The time-histories of the tibial transverse force component of the ground reaction were also computed and are illustrated in Figure 3.7. Also included in the same figure for comparison is the applied transverse force to the base of the tibia resulting from the generation of the flex./ext. moment time-histories (see previous section) During heel contact, the applied force is consistent with the 'normal' force Thereafter, however, they deviate as the point of contact moves towards the toes. Although it is not possible to reproduce the normal transverse force as well as the moment component of the ground reaction with the described moment applicator, it was nevertheless approached by adjusting the moment arm of the applied transverse force on the simulator. In any event, the magnitude of the resulting transverse force which will also be transmitted to the joint remains negligible. The force is only about 1/3 of body weight maximum, in comparison to the total joint reaction magnitude of 3 times body weight as estimated from Morrison (1970) during walking gait.

3.4 Specimen Fixation and System Versatility

An underlying criterion in the design of the simulator in which knee joint specimens are to be loaded, is that the location and orientation of the lines of action of the applied forces be adjustable, so as to accommodate each specimen's specific characteristics. The specimen fixation components of the simulator are basically the same as implemented in the prototype. The proximal end of the femur and the distal end of the tibia are both potted with fiberglass resin in metal sleeves. The femoral sleeve attaches to the force plate via a bracket which incorporates sufficient adjustments for femoral positioning. An added feature is that the femur may also be oriented skewed relative to the plane of motion which is also defined by the main plane of the simulator's frame. This added adjustment was deemed necessary since the femur is in fact normally skewed with respect to the plane of motion by up to 10°. On the tibial sleeve, cable attachment brackets, each with independent adjustment capability, were designed to be fixed to each side of the sleeve for attachment of the tibial axial reaction cables, and to the rear for attachment of the flexor actuating cable. The flexor actuating cable may also be adjusted proximally to assure a correct line of action. A bracket was also designed to affix a cylindrical extension of the tibial axis which transmits the tibial transverse force generated by the moment actuating mechanism. The actual point of application of the transmitted tibial transverse force used to generate the required moment may also be independently adjusted as needed. The extensor muscle cable attaches directly to the patella but its line of action may be adjusted proximally as required. Hence, the lines of action of the four simulated forces may be varied and adjusted. Not only does this allow for specimen variation but also permits the lines of action of the applied forces to become experimental variables.

Versatility must also be incorporated into other aspects of the simulator design. The actuating system must be entirely programmable so as to allow for variable target function simulation. Although single target functions were described in the previous section, the actuating system must be capable and programmable to simulate walking gait patterns with differing characteristics as well as other activities. The actuating systems were designed specifically to also accommodate the simulation of stair ascent and descent. A description of functional activity programming is presented in Chapter 6.

3.5 Specimen Preparation

This final section is a description of the specimen preparation procedure. Since the musculature is artificially reproduced in the simulator, all muscle tissues are removed, along with the skin and subcutaneous fat. The preparation is such that the passive soft tissues of the joint, the ligaments and cartilage, and the patella with its tendon and capsular attachments remain intact. Care is also taken not to damage the tibiofibular joint since the lateral collateral ligament is partially attached to the fibular capsule. The femur and tibia/fibula components are cut to length as per fixation design and then potted in their respective sleeves or fixation buckets as was described in the previous section. A patellar cap is screwed into the patella so that the extensor cable may be attached. The reader should refer back to Figure 3.1 for clarification. Thus the tibiofemoral, the patellofemoral, as well as the tibiofibular joints are left intact.

As in the intact specimen, the extensor loads are taken up by the patella and the load thereon distributed to the femur (patellofemoral reaction) and the tibia via the patellar tendon. The flexor mechanism, however, is totally artificial. No actual attachments are made to the joint bone components.

3.6 Summary

The simulator is a four actuator design. Two actuators mimic the effects of each of the flexor and extensor lumped muscle groups to flex or extend the knee, according to given flexion angle time-histories, while the base of the tibia is subjected to the two main components of the ground reaction in the plane of motion. The two main components of the ground reaction are the flex./ext. moment and the tibial axial force. The application of these two load time-histories are accomplished by two independent actuating systems. All forces are applied either through steel cables or special mechanisms such that their lines of action can be adjusted according to specific specimen configurations and such that passive and conjunct joint motions are not constrained.

The scope of the present simulator evaluation is limited to normal level walking of which the target functions were presented. The design of the simulator also takes into consideration the simulation of more stringent activities, namely stair ascent and descent, and hence programmability, as well as other necessary versatility features, are incorporated into the design.

The specimen preparation is such that the tibiofemoral and patellofemoral articulations are retained in their intact states and thus the overall knee joint response, in terms of joint reaction forces, pressure distributions and relative displacements, may be assumed to approach that of the intact in-vivo specimen under the aforementioned dynamic loads.

Chapter 4

SIMULATOR ACTUATION SYSTEM: DESIGN AND PERFORMANCE

4.1 Introduction

In chapter 3, the criteria for the design of the simulator's actuation system were formulated. In this chapter, the implemented actuation system components and their relevant characteristics are presented.

It is recalled that the flexor and extensor actuators control the positions of each of the flexor and extensor load cables such as to reproduce the flexion angle time-history of the knee joint. The actuators of choice are stepping motors. Stepping motors possess accurate positional characteristics (i.e., one step resolution) even when coupled with just an open-loop controller, and are capable of speed/torque relationships comparable to standard D.C. motors. Hence two industrial stepping motors, with suitable stepping motor drivers and speed reducers, were selected to actuate the two muscle load cables. A special two-axis open-loop controller was designed and fabricated to independently control each of the motors, such that given flexion angle time-histories may be accurately reproduced. The muscle actuation system components are further discussed in the following section.

The tibial axial force and flex./ext. moment actuators must each reproduce given load time-histories. Electro-hydraulic actuation systems possess good dynamic response characteristics and high load generation capacity comparatively to other actuation system types. Two electro-hydraulic actuators were salvaged from the prototype simulator, in which they were used as muscle force actuators. Coupled with a programmable voltage source in a closed-loop load pressure control system, these actuators were implemented and their control systems suitably configured to apply given load time-histories. It was also necessary to modify the hydraulic power supply unit as well as other more minor components to accomplish the given task in view of the problems which limited the capacity and range of the hydraulic actuation system in the prototype.

4.2 Muscle Actuation System: Design and Performance

A stepping motor actuation system includes a stepping motor which upon reception of a suitable D.C. voltage waveform from a stepping motor driver will advance to its next incremental rotor position (one step). This process is activated by a pulse and direction signal sent to the driver. Hence, the generation of a pulse stream of variable frequency with corresponding directional reference signals will result in the near continuous and precise repositioning of the motor output shaft with respect to time. A programmable controller serves to generate the required pulse stream and directional reference signals. As the rated torque is available at relatively high rotor speeds the output shaft must be coupled to the load through a speed reducer.

4.2.1 Stepping Motor/Driver/Speed Reducer Combination

The stepping motor/driver/speed reducer combination must be such that the required torque of the motor at a given motor speed be less than the rated torque of the motor as specified by the manufacturer. Initially the load torque requirements of the load were estimated from the target functions presented in Chapter 3. The load torque of either the flexor or extensor actuator is the net moment about the knee due to either the extensor or flexor muscle force (Fig. 4.1) and is given by the following equation:

$$T_L = M_G - I\alpha - m \cdot g \cdot l \cdot \sin\theta. \tag{4.1}$$

where

T_L: net load torque, either flexing or extending

M_G: moment due to the ground reaction

I: moment of inertia of the lower limb ($\approx$ 0.17 kg$\cdot$ m^2)

α: angular acceleration of the lower limb

m: lumped mass of the lower limb ($\approx$ 4.3 kg)

g: gravitational acceleration constant (9.81 m/s^2)

l: lumped mass pendulum length ($\approx$ 0.2 m)

θ: flexion angle.

According to this equation and Figure 4.1, a positive torque corresponds to an extension torque and a negative torque corresponds to a flexion torque. Antagonistic effects are neglected in this estimation and hence when a net flexion torque is calculated, a null extending torque is assumed or vice-versa.

A speed reducer is interspaced between the load and the motor. According to the gear ratio (r), the load torque is geared down and the speeds geared up to bring them to within specified stepping motor capacities. The motor torque (T_M) requirements are then estimated according to equation 4.2 taking into account the inertia of the rotor (I_M) and the forward and reverse efficiency of the speed reducer ($\mu_{f,r}$).

$$T_M = \left(\frac{b}{a}\right) \cdot \left(\frac{1}{r}\right) \cdot \left(\frac{1}{\mu_{f,r}}\right) \cdot T_L + I_M \cdot \alpha \cdot \left(\frac{a}{b}\right) \cdot r \tag{4.2}$$

where

b: torque arm of the muscle load cable about the output shaft of the speed reducer

a: torque arm of the muscle load cable about the knee joint. The flexor and extensor torque arms are assumed equal ($\approx$ 5 cm, [Szklar, 1985; p. 130])

r: gear ratio of the speed reducer

$\mu_{f,r}$: forward or reverse efficiency of the reducer

T_L: load torque according to eqn. 4.1

I_M: motor rotor inertia

α: angular acceleration of the lower limb.

After a lengthy iterative procedure, the commercially available combinations that were selected based on their rated torque/speed capacities are as follows:

Flexor actuation: MH112-FJ4201 stepping motor with a series windings configuration, 1.8^o full step mode/ DRD-004 driver (both by Superior Electric) with a 721 (Boston Gear) worm gear speed reducer

Extensor actuation: same motor and driver as flexor actuation but with a 724 worm gear speed reducer which has a higher torque capacity.

The pertinent specifications as per eqn. 4.2 for both flexor and extensor sides are:

$b = 5$ cm (hence output shaft rotation of speed reducer is approximately equal to knee flexion rotation)

$r = 25$

$\mu_f = 0.85$ (Boston Gear specifications)

$\mu_r = \frac{1}{.4}$, estimated based on average braking speed, lead angle and gear ratio [Merritt (1971)]

$I_M = 8\ 05$ kg$\cdot$ cm^2 (Superior Electric specifications)

The estimated motor torque/speeds requirements corresponding to level walking for both the extensor and flexor actuating motors are depicted in figures 4.2 and 4.3.

Superimposed on these graphs are the rated capacities of the stepping motor/driver combinations. In view of the depicted safety margins between the required torques and rated torques, these actuation systems may be safely assumed to induce on the muscle load cables the given displacements-vs-time functions while sustaining the loads corresponding to a level walking simulation.

In the selection of the muscle actuation system, the requirements of stair ascent and descent simulation were also considered. Although an equivalent detailed analysis was performed, based on the reported flexion angle and ground reaction load time-histories for both stair gait patterns by Andriacchi et al. (1980), only salient points of interest are included in this report. For both stair gaits, although the required motor torques were found to be of the same magnitudes as those determined for level walking, the speeds at which these must be developed were somewhat higher.

Stair ascent:

max. stall torque:	- extensor $\approx$ 2.4 Nm
	- flexor $\approx$ negligible
max. speed:	$\approx$ 5200 steps/sec for both motors with negligible torque requirements
max. power:	- extensor $\approx$ 3.8 Nm @ 2785 step/sec
	- flexor $\approx$ relatively little power requirements

Stair descent:

max. stall torque:	- extensor $\approx$ 2.2 Nm
	- flexor $\approx$ negligible
max. speed:	$\approx$ 5600 steps/sec for both motors
max. power:	- extensor $\approx$ 2.4 Nm @ 4775 steps/sec
	- flexor $\approx$ 2.15 Nm @ 4775 steps/sec

The torque safety margins were determined to be greater than two for all three gaits. Although these stepping motor/driver combinations are completely bi-directional in that rated torques in either direction are available to drive or brake the load (thus either expending or absorbing energy), their capacity to absorb energy is subject to another constraint beyond their rated torque/speed specifications. Energy absorbed in the windings when the motor is either braking the load and/or decelerating its own rotor inertia is dissipated in a coiled resistor in the driver units. This resistor is rated up to a 650 watts peak dissipative capacity with a 50 watts average capacity. This constraint is of special interest in stair descent simulation. An estimated 60 watts of energy was determined to be absorbed by the extensor motor on average during stair descent. However, since the peak capacity rating is substantial (650 watts), this will limit only the number of stair gait cycles that can be simulated concurrently during a single run. A certain cool off period must be allowed between runs. It is interesting to note that the poor efficiency of worm gear speed reducers when backdriven by the load, is a beneficial factor in this situation. In effect, the large braking torques which the muscle forces must generate about the knee during stair descent are largely absorbed in the reducer itself with little actual braking torque required at the input shaft. This energy absorption constraint was found to be of no consequence in the simulation of walking or stair ascent as energy is mostly expended in these.

4.2.2 Stepping Motor Controller

Industrial stepping motor controllers are designed to position loads via programmed constant velocity or acceleration segmented profiles and thus in a 'non-continuous' fashion. Furthermore, the time scales of the profile segments and the resolution of the velocity or acceleration parameters are relatively coarse. Such controllers are not suitable for the application at hand. A precise as well as a nearly continuously variable reference pulse stream frequency, under program control, is required not only to simulate given continuous functions, but also to prevent the generation of large antagonistic forces on the knee specimen by both the flexor and extensor actuators (refer to Figure 3.1 for clarification). Taking advantage of gait like function characteristics, a suitable 2-axis controller was designed and implemented to independently control the motions of both the extensor and flexor stepping motor actuators.

The controller basically consists of a microprocessor which is programmed to sequentially issue reference pulse and direction signals to each of the motor drivers at specified time intervals (time duration between each pulse). The consecutive time durations between pulses and the associated directions for a complete cycle are stored in the controller's memory banks (one for each motor). The microprocessor continuously cycles through the memory banks downloading each time duration and direction bit to two sets of dedicated hardware. Each set automatically sets the direction, and issues the pulse to each of the drivers once the specified time durations have been counted down. The smallest base unit or resolution of the time durations, which is switch selectable, is 2.727 μsec (30/11 μsec). The control algorithm cycle time of the microprocessor is such that each driver may effectively be issued up to 10 000 steps/sec independently. A maximum of 8192 pulses for each axis is allowed per gait cycle based on the size of the memory banks. The maximum time duration for a given pulse is slightly under 90 msec (i.e. $(2^{15} - 1) \times 30/11$ μsec) assuming the smallest base unit and the 15 bit length of each time duration. The information for each pulse is 16 bits long of which the last bit is the associated direction bit. With respect to the application, the foregoing specifications are interpreted as follows. Less than half of the maximum number of pulses was estimated to be required for walking or stair gaits. The maximum allowed time duration of 90 msec corresponds to about 11 steps/sec or approximately a minimum speed of less than 1 degree of knee flexion per second. The maximum speed for any of the gaits was estimated to be less than 6000 steps/sec which is safely less than the specified maximum 10 000 steps/sec permissible by the controller.

As to the procedure by which each time duration is determined, each knee joint is calibrated statically in terms of motor rotation vs flexion angle. Once the knee joint is positioned in the simulator and the muscle lines of force fixed, the number of pulses required to position each of the stepping motors corresponding to given flexion angles are recorded. Some cable pre-tension is necessary to ensure correct mechanism functioning and therefore the motor shafts are positioned such that about 22 N of antagonistic muscle force is present at each position. The procedure is repeated until the full flexion range is scanned. Intermediate points are interpolated by assuming a cubic spline function between measured points and thus establishing the relationship between each motor's step position and flexion angle. This information is then coupled with the target flexion angle time-histories to obtain the required consecutive time durations and step directions which are then downloaded to the controller's memory banks. Details regarding the interpolation functions and the time-duration/step-direction determinations, will be further discussed in Chapter 6.

4.2.3 Muscle Actuation System Performance Characteristics

A series of flexion angle vs time functions were simulated to establish the performance characteristics of the muscle actuation system. Initially the system's accuracy and output torque capacity were verified. Upon completion of given function simulation runs, the rotors returned to their initial positions to within plus or minus one step (1.8^o) demonstrating the system's accuracy. The available motor output torques were verified only at low speeds and found to agree with rated specifications. The operating constraints which are specific to stepping motors had to be considered. Stepping motors resonate at very low speeds resulting in unpredictable rotor rotations. The analysis of this characteristic is extremely complex and usually the speed range during which this problem may arise is determined experimentally under operating conditions. In this study, this range was determined to be between 100 and 250 steps per second. To avoid the resonance problem, the step position time-histories of each motor were adjusted locally wherever speeds lower than 250 steps/sec were encountered. Another important characteristic to be reckoned with is that the rotational direction of the rotor cannot be changed instantaneously. More explicitly, to reverse the polarity of the windings, the rotor must first come to rest and remain idle for about 20 to 30 msec depending on the inertial and stall load torques. This problem is resolved by increasing the time durations by up to 30 msec before any pulse is issued in a new direction. This artificially introduces a dwell time in the flexion angle time-history whenever a directional change occurs. Both these characteristics or constraints do not significantly affect the overall flexion motion.

The more important problem that hindered the performance of the muscle actuation system is the elasticity in the muscle load cables and in the connecting soft tissues on the extensor side which were initially unaccounted for in the command function generation. During walking gait simulation runs, although the output shafts of the motors followed input profiles with precision, the actual measured flexion angle response deviated about the target function significantly especially during stance. The calibration procedure by which the input profiles are generated is a static one in which only the gravity effects are included. However, according to eqn 4.1, in addition to the torques generated by the muscle actuator themselves, the flex./ext. moment of the ground reaction as well as the inertial torques due to the angular acceleration of the lower limb will also affect the flexion angle time-history depending on the elasticity of the load cable and connecting soft tissues. Each knee was calibrated statically to establish the relationship between flexion deflection and applied moments about the knee at various flexion angle. A linear relation (correlation factor $R^2 = 99$) was determined (see Table 4.1). This relationship was found to be negligibly affected by the flexion angle and hence was assumed constant As the deviations from the target input functions were found to be relatively small during the swing phase when inertial forces are prevalent, the motor input profiles were only adjusted to nullify the deflections due to the applied moment component of the ground reaction.

Table 4.1: Elasticity in Extensor Mechanism

Specimen # 1	.25°/Nm *	(used .20°/Nm)
Specimen # 2	.20°/Nm	

* This factor was arbitrarily reduced by 20% since it was judged that a more conservative factor would be appropriate for a first attempt in view of the stiffening effect of dynamic loads on viscoelastic passive soft tissues.

4.3 Ground Reaction Actuation System: Design and Performance

The electro-hydraulic actuation system (2 actuators) implemented in this study to simulate the ground reaction components is partly depicted in Figure 4.4 and consists in the following:

- two flow-control servovalves (MOOG A076-231 SERVOVALVE), which in response to an input current, proportionally displace a spool providing openings for both pressure and return lines to and from the actuators.
- two actuators (MOOG A085-1-BM-2 ACTUATOR), which are acted upon by the fluid flow to displace the load. Each actuator is symmetric and double acting (bi directional).
- each actuator is equipped with an adjustable metering orifice (AMO) which serves as a variable bypass restriction to mechanically adjust the dynamic response of each actuator. It attenuates load pressure excursions by opening some of the valve flow to the return line depending on its setting and load pressure.
- each actuator is also equipped with a differential pressure transducer which measures the pressure across the pistons.

- a 2-axis servoamplifier/signal-conditioning card which amplifies the pressure transducer signals, subtracts them from the reference input signals and proportionally to the difference, issues the corrective actions or currents to the servovalves such that a two axis closed-loop load pressure system is obtained.
- a constant pressure power unit which supplies the pressurized fluid to the system and consists mainly of a motor, a pump, a constant pressure relief valve, a bladder accumulator (N2), heat exchangers and a resevoir.

The system just described is basically the same system which served in the prototype simulator design. However problems were encountered in the prototype which limited the system's capacity to perform gait like functions. In view of the more stringent functions which are considered in this study, the pump, the supply pressure, the accumulator charge pressure, and transd omponents had to be either changed or modified. This will be further discuss next section.

Each of the actuators was configured to act upon the knee joint through two separate and different linkages or couplings, thus forming the two entirelv different systems which are the tibial axial force and moment actuation systems. Initially the load flow versus load pressure time-histories were estimated according to gait simulation requirements. Then the gains (servoamplifier and signal conditioning) and the AMO openings were set such as to obtain a suitable response. Each system was then calibrated to establish their overall gains (load force versus input voltage). Futhermore, each system was modelled for the purpose of theoretical analysis as well as to give insight into their dynamic responses.

4.3.1 Hydraulic System Modifications

Szklar (1985), reported in his thesis on the prototype simulator that a 'debilatating' problem limited the hydraulic systems capacity. Due to valve resonance or 'squeal', which is the self sustained excitation of an oil line at its natural frequency with valve interaction and results in a standing pressure wave pattern in the concerned line, the AMO's were opened until the pressure waves were effectively damped out. However, the AMO settings that were necessary to produce this effect were such that large proportions of the available flow were bypassed back to the return lines and thus reduced the net power available to the load. Only gait frequencies of up to .5 Hz and having a 40^o flexion range could then be simulated. Not only did this problem limit the system capacity but it also tied up the AMO whose adjustment could be used to improve the actuator responses by effectively introducing apparent load viscous damping.

This problem was also initially encountered in this study. The frequency of oscillation of the squeal was measured to be around 1000 Hz. The first natural frequency of an oil line length is given by the following equation:

$$f_N = \frac{c}{(4 \cdot l)} \tag{4.3}$$

where

- c: speed of sound in oil $\approx$ 1400 m/s
- l: length of line

According to this equation, an oil line of about 35 cm would have a natural frequency of 1000 Hz. An oil line of approximately this length was located. It was the rigid tube which connects one side of the actuator manifold to one port of the differential pressure transducer. This line was unnecessarily long and hence its length was reduced to a minimum decreasing it by about 30%. It was hoped that this action would in effect increase the natural frequency of this line beyond the bandwidth of the servovalve, decreasing the likelihood that its natural frequency would be self-sustained by the dynamic closed-loop interaction between the valve and the pressure transducer. Upon performance testing, within the requirements of this study, the problem was never again encountered. Hence the AMO adjustment was free to adjust the normal response of the system while not overly reducing the net amount of fluid power available to the load.

In view of the stringent activities considered in this study, accurate dynamic control of the hydraulic actuators was necessary. It can be shown that the higher the operating supply pressure the better the speed of response of hydraulic systems. In the prototype, the operating pressure was set at 8.0 MPa (1150 psi). It was determined that a pressure setting of 17.3 MPa (2500 psi) would be more suitable in this study. The vane pump which was used in the prototype simulator was only compatible with low operating pressures and high flow rates. Even at the moderately low operating pressure of 8.0 MPa, this vane pump was beyond its design point giving rise to poor pump efficiency. A gear pump (TKP-4/26-6.2 - DCI, Sundstrand) rated up to 20.7 MPa with a flow rate compatible with the given pump motor speed was implemented in this study. Given the speed of the pump motor (1150 RPM) and its 2238 watts (3 HP), the pump flow was calculated to be .101 l/sec at the 17.3 MPa operating pressure having taken into consideration the combined pump/motor efficiency of 0.80. Neglecting all losses including AMO losses, the average flow rates pertaining to walking gait and both stair gaits were estimated and are as follows:

Q walk, avg	= .037 l/sec
Q stair ascent, avg	= .065 l/sec
Q stair descent, avg	= .065 l/sec

Hence, the pump may be assumed to supply enough flow on average to simulate all three gaits.

The flow rates given above are on an average basis. During gait simulation, however, instantaneous flow rates are expected to exceed the pump flow rates. Accumulators are designed to attenuate pump flow variations giving best results when precharged to operating pressure as was done in the study of Szklar (1985). However, by reducing the precharging pressure, accumulators may also be used to store various amounts of pressurized hydraulic fluid and may thus supply the load when the pump flow is deficient. The accumulator is replenished by the pump during those parts of the operating cycle when load flow requirements are reduced. The accumulator was precharged to half the operating pressure in this study. Thus when the system is activated, half the total volume (3.8 litres) of the accumulator will be filled with fluid at the operating pressure. The actual operating pressure will of course fluctuate about a mean since the accumulator oil volume fluctuates during an operating cycle depending on flow requirements. The measured pressure fluctuations during walking gait simulations and a discussion of their effects will be given in section 4.3.5. They were found to be minimal and did not seem to significantly affect the system's performance during walking gait simulation.

4.3.2 Tibial Axial Force Actuation System

The hydraulic actuator in this system acts through a system of steel cables on the tibial pot. The reader is referred back to Figure 3.2 for clarification. Through a system of pulleys, the load is evenly distributed to each side of the tibial pot and directed along the tibial axis through the approximate flexion axis of the knee joint specimen. The load time-histories which this system must duplicate are, for walking gait, as per Figure 3.6. The maximum load magnitude which the actuator must apply is in the order of one body weight which corresponds to less than 10% of the supply pressure ($7.1 \times 10\text{-}4$ m^2 piston area). Furthermore, as tibial motion along its long axis is negligible, the load flow requirements are also negligible. For stair gait simulation, relatively small load pressures combined with negligible flow requirements were also estimated. As the available hydraulic power greatly exceeds the load requirements in this instance, only the control aspects of the system remain to be examined.

Initially, the step response of the system was measured and adjusted until satisfactory performance during normal operating conditions was established. The available adjustments are the servoamplifier gain which amplifies the difference between the reference input signal and the feedback signal, the feedback gain which amplifies the load pressure transducer signal, the AMO restriction setting which determines the amount of bypass flow from the valve away from the load at a given load pressure, and finally, the reference input signal gain which amplifies the input signal before subtraction with the feedback signal such that full scale loads may be achieved with the available range of input signals. After much iteration, the servoamplifier gain was set at 42.76 ma/V, the feedback gain at 0.187 mV/N, the input signal gain at 0.04254 V/V and a suitable AMO restriction setting determined. The actual bypass flow through the AMO restriction as a function of load pressure was not explicitly determined in this study. The step response to a 2.5 volt step input with the above settings was measured and is reproduced in Figure 4.7 As can be seen in the figure, less than 5 msec are required before the output reaches 90% of its steady state output at which point some oscillations of relatively small amplitude are noted. The oscillations quickly die out and thereafter the output smoothly rises to its steady state output. Although the overall response time is seemingly long at about 150 msec, the rise time and overall damping are satisfactory. The response to different levels of input was also measured and although the system's steady state gain below 2 volts input was somewhat reduced, an overall constant gain of 85 N/V was assumed throughout the required range of output force. It should be noted that the time delay between the input step and the onset of response was not measured.

Modelling: The servovalves employed in this study are flow control servovalves The control flow Q_V (output) is both dependent on input current and load pressure drop according to the characteristic square-root relationship for sharp edge orifices.

$$Q_V = K_V \cdot i \cdot \sqrt{(P_S - P_L)} \tag{4.4}$$

where

K_V: valve sizing contant

i : input current

P_S: supply pressure

P_L: load pressure

The bypass flow Q_O through the AMO restriction is given by the following equation.

$$Q_O = K_O \cdot \sqrt{P_L} \tag{4.5}$$

where K_0: orifice setting.

The net flow to the load (Q_L) is the difference between the valve control flow (Q_V) and the bypass flow (Q_O). These relationships are illustrated in Figure 4.5.

Hence, for a given input level, the control flow decreases as the load pressure increases in a highly nonlinear fashion. This relationship was linearized assuming a given set point such that a complete linear mathematical model of the actuation system could be formulated. The valve's dynamic characteristics are reflected in its first order approximation assuming low operating frequencies. The block diagram corresponding to this closed-loop control system is depicted in Figure 4.6 for which:

E_c: command reference signal [V]

K_A: servo amplifier gain [mA/V]

K_V: no-load flow gain of servovalve [l/sec/mA]

τ: valve time constant

A: actuator piston area [m2]

K_2: pressure sensitivity gain [l/sec/Pa]
(i.e. loss due to load pressure drop)

$\frac{\Delta P}{A}$:force feedback gain, includes transducer gain and signal conditioning gain.

K_T: combined elasticity of hydraulic fluid in piston and steel cable [N/m]

K_S: piston damping constant [N/m/sec]

K_1: input signal gain [V/V]

s: Laplace operator

F_a: actuating force [N]

Numerical computations of the model parameters are included in Appendix A. This model is the same model which Szklar determined in his thesis for his force servo (Szklar, 1985; p. 54) except that a piston damping force has been included here. Szklar experimentally determined later in his thesis that to induce a given amount of piston ram speed, a piston force was proportionally required to overcome kinetic friction (Szklar, 1985; p. 71). The constant of proportionality assumed in this study was estimated from his findings. The load flow reduction due to both the valve characteristics and losses through the AMO restriction is reflected in the pressure sensitivity gain K_2. This parameter was determined by applying the Final Value Theorem to the system transfer function thus obtaining a theoretical expression (Equation 4.6) for the steady state gain of the system, which was experimentally measured to be 85 N/V:

$$\frac{F_A}{E_C} = \frac{(K_1 \cdot K_A \cdot K_V \cdot A)}{(K_2 + K_A \cdot K_V \cdot \Delta P)} \tag{4.6}$$

This linear mathematical model was then loaded into the control system analysis software package MATLAB$^{\text{TM}}$ (Math Works) along with the numerical values for the measured gains and model parameter values. According to this model, the step response, and the frequency response (each to a 2.5 V input amplitude), in terms of both the amplitude and phase lag, were computed and are graphed in Figures 4.8 and 4.9 respectively. Comparing Figures 4.7 and 4.8, the transients of the computed step response do not correspond with the measured response transients although the settling time of 150 ms does match. Many factors could partially explain the discrepancy between the theoretical and experimental responses such as static ram friction, the linearization process and assumed model parameter values. It is felt, however, that losses in the valve's secondary stage were occurring resulting in off-design performance and that valve servicing is required. Although partial misfunction is suspected here, the system still provided satisfactory performance during simulation run conditions.

According to Figure 4.9, the theoretical bandwidth of the system is approximately 10 Hz. Assuming the model to be valid, such a frequency bandwidth should be sufficient in the simulation of normal functional activities since the frequencies which characterize them are relatively low. The measured static gain of the system can therefore be assumed constant in the computation of the required reference command signals corresponding to the sought time varying loads. Furthermore, since the operating frequencies and system bandwidth are much lower than the valve's bandwidth, estimated at about 180 Hz (MOOG^R 4076 SERVOVALVE CATALOG 762568), the valve's first order representation in the system's model is appropriate. The phase lag as depicted in Figure 4.9 is negligible within the system's bandwidth.

4.3.3 Flex./Ext. Moment Actuation System

In this system, the linear hydraulic actuator used must apply a force to a lever arm which is rigidly coupled to an extension of the tibial shaft (refer to Figure 3.2 for clarification). The coupling to the tibial extension is such that only a transverse force may be transferred to the tibia since all other relative motions between the tibial extension and the lever arm are unconstrained. Therefore, assuming sufficient force is generated to overcome the linkage's inertial, gravitational and frictional forces, the applied actuation force will result in a net transverse force on the tibia and a corresponding moment about the knee. The linkage's main rotary axis is aligned with the approximated rotational axis of the knee and hence, the distance or moment arm between the resulting tibial transverse force and the rotational axis of the knee is approximately constant. It is recalled from section 3.2 that the moment arm of the applied transverse force is adjustable and that, in this study, it was fixed to 44.7 cm. The relationship between the applied actuator force and the flex./ext. moment about the knee is according to the following equation and figure 4.10 : - Taking moments about the central rotary axis and neglecting frictional losses -

$$F_a \cdot r \cdot \cos\phi = I \cdot \alpha + m \cdot g \cdot l \cdot \sin(\theta - \theta_p) + M_G \tag{4.7}$$

where

- F_a: actuator force
- ϕ: angle between actuator force and linkage's radial axis from the perpendicular position
- r: radial distance between the point of application of actuator force on linkage and central axis.

I: mass moment of inertia of linkage system about central axis.

g: acceleration due to gravity.

m: mass of linkage

l: distance between central axis and the center gravity of the linkage

θ_p: see Figure 4.10

θ: flexion angle

α: angular acceleration of lower limb

M_G: flex./ext. moment

In view of the construction, the flexion angle acceleration is also the rotational acceleration of the linkage. The angle ϕ is of important consideration since it is also a function of the flexion angle and is given by the following equation:

$$\phi = \tan^{-1} \frac{b - r \cdot \cos(\theta - \theta_p)}{a + r \cdot \sin(\theta - \theta_p)} - \theta + \theta_p \tag{4.8}$$

where a, b, r and θ_p are as defined in Fig. 4.10,

$$\begin{aligned} a &= 7.2 \text{ cm}, \\ b &= 5.19 \text{ cm}, \\ r &= 2.86 \text{ cm}. \\ \theta_p &= 0.3316 \text{ rad}. \end{aligned}$$

This geometric configuration allows up to 120° of knee flexion taking into consideration the maximum 5.08 cm range of motion of the linear actuator. Furthermore, the design is such that the required actuator load flow and pressure as per walking and stair gait simulations does not exceed the hydraulic power supply unit and servovalve/actuator capacities. The actuator load flow (Q_L) is a function of both the flexion rate and the angle ϕ according to equation 4.9.

$$Q_L = r \cdot \dot{\theta} \cdot \cos\phi \tag{4.9}$$

where $\dot{\theta}$ is the flexion rate [rad/sec] and r, ϕ are as per Figure 4.10.

According to the above equation and equation 4.8, and assuming the flexion angle and applied moment time-histories as per Figures 3.4 and 3.6 respectively, the load flow rate versus load pressure time-histories were estimated for walking gait simulation In this estimation flow losses (i.e. AMO losses) and frictional effects were neglected. These results are depicted in Figure 4.11 with the theoretical capacity of the servovalve/actuator superimposed and assuming the operating supply pressure of 17.3 MPa Stair ascent and descent requirements were also estimated Although approximately the same ranges in load pressures were estimated, up to 50% higher flow rates were noted. Hence, assuming it feasible to nearly close the AMO restriction and neglecting other possible losses, the actuation system described here should be capable of applying the sought moment time-histories given an appropriate control scheme

In a similar fashion to the tibial axial force actuation system, the actuator force is controlled by a closed-loop control system. As was done for the tibial axial control system, the step response was adjusted by setting the amplifier and load pressure feedback gain as well as by adjusting the AMO restriction opening in order to obtain a suitable response. The final settings that were adopted in this study are 52.4 ma/V for the amplifier gain and .15 mV/V for the feedback gain. The AMO restriction was also set such that during a walking gait simulation run, the total flow requirement would not exceed the capacity of the power unit which would have resulted in a noticeable drop in the supply pressure. The step input was applied to the linkage coupled to a mechanical knee joint (described in Appendix B) flexed at 30°. Although no active motion was concurrently applied by the muscle actuators, their passive flexible restraint to knee flexion was present as would be during a simulation run The measured step response (.5 volt step input) of the actuator force control system is shown in Figure 4.13. The response is fast with negligible overshoot and small high frequency oscillations which quickly damp out. The settling time is less than 10 msec. The linearity of response, with respect to varying input levels was verified (± 5%)

and an overall system steady state gain of 1346 N/V may be assumed.

Modelling: The method of modelling the servovalve characteristics is similar to the method used for the tibial axial force actuation system. In this situation, however, the piston force is applied to a rigid linkage which is itself rigidly coupled to the tibia. Motion of the tibia, and hence the load application linkage, is passively restrained by the muscle cables. In view of the non-negligible deflection in the flexion angle due to an applied moment, as was reported in Section 4.2.3, the inertial and gravity effects of the linkage and tibia and the rotary elastic restraints posed by the muscle cables were included in the model. The block diagram of the linearized model is shown in Figure 4.12 for which:

- K_1, K_A, K_V, τ, A, K_2, $\Delta P/A$, s, F_a: as listed for Figure 4.6.
- K_H: stiffness of the hydraulic volume of oil [N/m]
- I: rotary second moment of inertia of the load, that is the tibia and linkage mechanism, about the center of rotation [kg/m^2]
- M: equivalent gravity constant of also the total load as in I [N/m]
- a: effective moment arm of the actuating force about the center of rotation [m]
- K_θ: rotational spring, constant equivalent to the contribution of the muscle load cable in opposing load flexion rotation.
- C: rotational damping coefficient equivalent to the damping effect described in the text reflected to the load (i.e. $C = C_F a$).
- s is the Laplace operator
- F_a is the actuation force

A rotary damping coefficient is also included in the model Initially all damping effects were neglected. But during the system's functional tests, in which flexion angle time-histories were concurrently applied, it was noted that in order to obtain given moment time-histories, the actuator force time-histories had to be augmented by amounts approximately proportional to the flexion angle rates. Inclusion of the estimated constant of proportionality C_F (500 N.sec/rad when the leg is flexing and 400 N.sec/rad when the leg is extending) in the generation of the actuator force time-histories gave satisfactory results and, therefore, this contribution was included in the model. The piston damping force, as was reported in the previous section for the tibial axial force actuation system, can be considered to be included in this rotary damping coefficient in addition to the frictional contributions of the various rotational components of the actuation linkage itself.

The dynamic equations, by which the model characteristics were evolved, are included in Appendix B. Also included in the Appendix are the model parameter values which were estimated for the same operating conditions that prevailed during the measurement of the system's step response. K_2 was determined by applying the Final Value Theorem to the system's transfer function and assuming the system's measured static gain. The resulting steady state gain expression may be shown to be equal to the steady state gain expression of the tibial axial force actuation system as given by Eqn. 4.6.

Computations of the corresponding theoretical step response to a 0.5 volt input and the frequency response in terms of the steady state amplitude response and phase lag (0.5 volt amplitude input), were obtained in the same manner as the tibial axial force actuation system (i.e., using MATLAB$^{\text{TM}}$) and are shown in Figures 4.14 and 4.15 respectively.

The computed step response, according to the assumed model, shows a rapid rise time, as in the measured step response, but the transient oscillations, after the rise, are of larger amplitudes and last about 200 msec. In the measured response, the transients damp out within a few milliseconds. Although these discrepancies may, to an extent, be attributed to the model assumptions, the increased damping characteristics of the measured response are more likely attributable to the unaccounted friction characteristics of the actuator and linkage components This poor theoretical transient response stems from the presence of a low undamped natural frequency due to the high rotary inertia of the coupled tibia and lever arm. According to the computed amplitude and phase lag frequency response, the presence of this low resonant natural frequency is further illustrated in the computed frequency response characteristics. In the region of 5.7 Hz (36 rad/sec), which can be shown to be the theoretical natural frequency of the load (i.e., of the lever arm & tibia & elastic restraints), the amplitude response is reduced and the phase lag initially increases from negligible amounts, then decreases into regions of lead angle. It then reverses again and returns to negligible amounts. This interesting characteristic of the phase angle frequency response is due to the complex closed-loop response characteristics of the system components in the presence of a low resonant frequency. Accordingly, the theoretical bandwidth of the system is limited by this natural frequency. The frictional effects which were omitted in the modelling of the system may be assumed to slightly better the system response as they partially increase the effective damping factor associated with the system's low resonant frequency. In view of the foregoing, the system's ability to reproduce those components of the functions to be simulated with frequencies greater than 5 Hz may be assumed to be limited. Nevertheless, the measured overall system gain of 1346 N/V, which was obtained statically, is assumed applicable throughout for a first estimate.

4.3.4 Ground Reaction Actuation System Performance Characteristics

The tibial axial force actuation system performed satisfactorily during walking gait simulation runs as will be shown in Chapter 7. Few problems were expected since the combined flow and load pressure requirements were relatively low and operating frequencies much lower than the system's theoretical cut-off frequency (bandwidth). Under such conditions, linear system response can be assumed.

However, the moment application system requires substantially more power with the servovalve operating in regions where non-linear effects are no longer negligible. The effects of the system's low resonant frequency can only worsen the situation. As expected, application of eqn. 4.7, with the inclusion of the rotary damping force to calculate the required reference signal time-histories and assuming the static system gain as established in the previous section, resulted in off-target operation during walking gait simulation runs. During the stance phase, when the system must supply large forces, the moments generated were 20% to 40% lower than prescribed. During the swing phase, when no net moment is to be applied to the tibia and the system must only track the tibia without interfering with it, interference moments of up to 30 Nm were measured. This also resulted in significantly off-target flexion angle time-histories since the generation of the stepping motor command functions assumes the prescribed flex./ext. moment time-histories. The situation is further aggravated by the fact that the effective moment arm of the actuating force, and hence the net resulting moment to the knee with a given actuating force, is also a function of the flexion angle (Eqn. 4.7 and 4.8). To improve the performance, the command function from which the reference signals are generated were adjusted locally at given increments in time by an amount proportional to the difference between the sought moment and the measured moment still assuming the previously established system gain This process was repeated in an iterative fashion for each specimen until the levelling off of improvements while not exceeding the life span of the thawed specimens. Six to seven iterative runs were performed taking each about 45 minutes to complete. Thereafter, as will be shown in Chapter 7, the measured moments were on average within 20% of the prescribed moments and the interference moments during swing were on average less than 3 Nm. This corrective procedure also resulted in marked improvements in the flexion angle time-histories. Discrepancies in the reproduction of the flex./ext. moment time-histories can be attributed to the presence of the system's low natural frequency, sporadic frictional effects, inaccuracies in the stepping motor command functions, play in the actuation system components, and inaccuracies in the system's assumed geometric parameters. The fluctuations in the system pressure due to the accumulator characteristics were measured to be between 16.9 MPa and 17.3 MPa during walking gait simulation. The effect of the system pressure fluctuation on both hydraulic system responses was therefore assumed negligible.

4.4 Summary

Each muscle cable is acted upon by stepping motors to provide given flexion angle time-histories while sustaining the corresponding muscle tensions. In the command function generation, a measured static calibration function is assumed for each specimen and motor in which only the effects of gravity are included. The command functions are corrected to nullify the elastic deflections in the cables and connecting tissues due to the flex./ext. moments which are applied during a simulation run.

The ground reaction actuation systems are electro-hydraulic based The hydraulic power supply unit, previously used for the muscle actuation system of the prototype simulator, was modified according to estimated flow and load pressure requirements. The line squeal problem, which hindered the system's capacity in the prototype, was also resolved. The tibial axial force component is directly controlled in a closed-loop control system according to a static calibration with satisfactory dynamic performance. In the case of the flex./ext. moment, only the actuating force is controlled in a closed-loop control system. The actuating force acts on the tibia through an intermediate lever arm linkage system resulting in an applied moment on the knee specimen. Due to second order dynamic effects (i.e. due to the linkage's low natural frequency and high load pressure and flow requirements) significant off-target performance was initially measured. Corrective action was implemented, resulting in a substantial performance upgrading.

Chapter 5

INSTRUMENTATION AND FACILITY DESIGN

5.1 Introduction

In this chapter, the instrumentation used to measure the simulator's performance is described. A force plate measures both the axial and anterior/posterior force components of the joint reaction. The flexion angle is measured by a potentiometer incorporated into the flex./ext. moment actuation linkage. The moment is measured by a load cell incorporated into the coupling interspaced between the moment actuating lever arm and the distal extension distally. These three items will be described in further detail. The differential pressure transducer components of the hydraulic actuating systems are standard items and will not be described here. These pressure transducers were used in establishing the hydraulic actuation system step responses and, in the case of the tibial axial force actuation system, also served to measure the applied tibial axial force time-histories during simulation runs.

5.2 Force Plate

The force plate used in this study is exactly the same one which served in the prototype design without any modifications. The femur is mounted under the plate which is totally supported by four load cells. The geometric disposition and the Wheatstone-bridge connections are such that the femoral axial and anterior/posterior (A/P) force components of the total joint reaction can be measured. Design details may be found in Szklar (1985), p. 74-78.

The calibrations that were performed in this study yielded 18.19 N/mV and 19.13 N/mV sensitivities (± 2%) to axial and A/P loads respectively, after amplification. The transducer outputs were verified to be relatively insensitive (± 2%) to the moment arm length of the A/P loads.

It is understood that the loads measured with this instrument comprise the sum of the forces transmitted to the femur by both the tibia and the patella. It must be mentioned that in numerous gait studies (Figure 2.11), the 'joint reaction' reported is frequently only the tibiofemoral portion of the total joint reaction along the tibial axis.

During the stance phase of level walking, the tibial axis is nearly aligned with the femoral axis and the patellofemoral joint reaction may be assumed to be negligible since the patellar tendon and extensor line of force are also nearly aligned with the femoral axis. Hence, for the purposes of comparison, the total femoral axial joint reaction may be assumed to be approximately equal to the tibiofemoral axial joint reaction during the stance phase of level walking .

5.3 Flexion Angle Potentiometer

The flexion angle is measured by actually measuring the rotation of the main lever arm of the moment actuating linkage. A one-turn precision potentiometer (± 1% linearity) is rigidly linked to the main rotary shaft of the arm which is aligned with the approximated constant flexion axis of each knee joint. The design of the actuating linkage system is such that it is effectively equivalent to a six-degrees-of-freedom goniometer with only the main rotation about the assumed fixed rotary axis being monitored. Secondary flexion of the tibia relative to the arm, which is unconstrained in the simulator, is small because the locus of instananeous centers of flexion are confined to a relatively small and stationary area (Walker, 1972). Referring back to Figures 3.2 and 4.10, it may be shown that if the knee joint were in fact a joint with a fixed rotary axis exactly aligned with the actuating system's lever arm, its rotation would be exactly given by the arm's rotation. A 6 D.O.F. goniometer was attached to the tibia of each specimen used in this study and the true flexion angles were compared to the potentiometer readings with the differences increasing from very small amounts at full extension to about $\pm 4^o$ at 75^o flexion. In view of their close correspondence, the flexion angle, as measured by the potentiometer, is assumed in this study as the actual flexion angle to be controlled in the simulator by the muscle actuators. The calibration factor of this transducer is 77.68 [deg/V] given a 5V power supply.

5.4 Flex./Ext. Moment Load Cell

The applied flex./ext. moment is obtained by measuring the tibial shearing force transmitted to the tibial extension by the moment actuating system and by multiplying this force with the distance between the constant point of application and the assumed location of the flexion axis. Using the same reasoning as in the previous section, the actual moment arm length of this force would be constant only if the knee joint were in fact a pin joint with a fixed axis of flexion exactly aligned with the axis of rotation of the actuating system's lever arm. The mechanical coupling between the tibial extension and the distal end of the moment actuating lever arm is such that only a force transverse to the tibial extension in the plane of motion may be transmitted without constraining the other degrees of freedom or dictating the knee's natural flexion axis. Relative translations and rotations are permitted by the implementation of linear and radial bearing assemblies.

The load cell is integrated into the design of this coupling. The tibial shearing force is transmitted through a central column to a thin circular plate perpendicular to its line of action and held at its boundaries resulting in plate bending deflections. Four resistor strain gauges are mounted on the plate's exposed surface (column side) and wired into a four-active-arm Wheatstone bridge circuit for maximum sensitivity and temperature compensation. The bridge is powered with a 5 volt supply unit and its output signal is amplified with a suitable differential voltage amplifier set for a gain of about 50 V/V. The complete transducer system was calibrated yielding an overall sensitivity of 19.13 N/mV (± 3% linearity) equally for tensile or compressive loads. The safe range of the transducer was estimated at about 700 N in tension and 325 N in compression to avoid buckling failure.

Chapter 6

SIMULATOR HARDWARE INTERFACE AND OPERATION

6.1 Introduction

The simulator is interfaced with two microcomputer systems operating in real time. One system oversees and synchronizes the run- time operation of the actuating systems while the other is dedicated to logging the applied input functions and the concurrent joint reaction time-histories. Each system and how they are organized with respect to the simulator will be further described in the second section. The third section is a description of the procedures and various software programs used to generate the input command functions.

The next section is a description of the operating routine. The routine is downloaded to the main controller to generate, in real time, the sequential output of the ground reaction command signals, while overseeing the functioning of the stepping motor controller. The final section contains a description of the selected data acquisition channel configuration and a discussion of its run-time routine.

6.2 Hardware Interface

A complete schematic of the various simulator control and data acquisition components, along with the information flow directions, is presented in Figure 6.1. At run time, a microcomputer (IBM-AT compatible) equipped with an analog interface card (LABMASTER^{TM}, Scientific Solutions) and a parallel communication port (Intel-8255) oversees the system's functioning in real time. The analog interface system comprises two 12 bit digital to analog converters (DAC) and serves to issue the command reference signals to the two-axis servoamplifier/signal conditioner. The parallel port serves to communicate with the stepping motor controller Initially the flexor and extensor command functions are downloaded to the stepping motor controller memory banks. The main operating routine is then loaded into the main controlling computer and, upon reception of a start signal issued through the keyboard, the stepping motor controller is activated to begin cycling through its memory banks issuing the prescribed pulse streams and step directions to each of the two stepping motor drivers. The prescribed reference command voltage levels are concurrently clocked out by the main controlling computer to the hydraulic system's two axis servoamplifier/signal conditioner. Gait actuation cycles are repeated indefinitely until interrupted by the operator

The operating routine and the manner in which event timing and synchronization is achieved is discussed in Section 6.4. It is understood that the reference command voltage to the hydraulic actuation system is not varied in a continuous manner per se. However, the rate at which the reference signals are clocked out in an incremental step fashion is such that near continuous output force variations are obtained. The operating routine allows 11.5 msec before each signal is changed This time increment is of the same order as the rise times of each hydraulic actuating system and thus rippling of the output forces is minimized

The resulting applied input functions to which the knee joint specimens are subjected to, as well as the joint reaction forces, are monitored by the instrumentation system described in the previous chapter and logged for future analysis by a dedicated data acquisition system. A second microcomputer (IBM-AT compatible) equipped with a data acquisition card (ACPC-12-16^{TM}, Strawberry Tree) was used to perform this duty. This data acquisition card comprised 16 × 12 bit analog to digital channels which can be configured for various input voltage ranges (± 50 mV, ± 250 mV, etc ...). Furthermore, each ADC has a cut-off frequency of 10 KHz and thus partially filters electrical noise The system is entirely programmable and sufficient channels are available such that it can also be used to record other knee joint characteristics at run time. How the system was configured for the purpose of this study is described in Section 6.5.

6.3 Command Function Generation

6.3.1 Stepping Motor Command Functions

The generation of these functions requires extreme caution since both muscle actuators are controlled in an open-loop fashion. The response of the muscle actuation system depends largely on an accurate calibration and the corresponding computation of each individual pulse time coordinate

Initially each motor's shaft rotation is calibrated with respect to knee flexion angle as described in Section 4.2.2 A special computer program downloaded into the main controlling computer serves to command the stepping motor controller to position each of the motor's shafts to discrete positions as chosen by the operator in a step-by-step fashion The step position of each shaft is displayed on the computer monitor and manually recorded along with the corresponding flexion angle as measured by the flexion angle potentiometer (Section 5.3) Once the flexion range is scanned, the complete calibration functions are constructed by using cubic spline functions between the discrete data points This procedure is accomplished through the use of a suitable software package (CUBE-FREE^{TM} routine, Turbo Pascal Numerical Toolbox) The information is stored in a file for future access

The target input functions to which the calibration data will be applied must be of a form such that the required time coordinate of each discrete motor shaft position can be precisely defined. A periodic cubic spline representation of the target flexion angle time-history was constructed because the intermediate 3rd order polynomial functions generated between given data points can be exactly solved for the time co-ordinates corresponding to each incremental motor shaft step position. This special periodic cubic spline procedure constrains the position, velocity and acceleration to be continuous from the end point of the cycle back to the initial point. The algorithm of this procedure may be found in Spline-Algorithmen zur Konstruktion glatter Kurven und Flachen (1973). The target flexion angle time-history shown in Figure 3.4 was initially digitized ($\approx$ 50 points) and the data downloaded to the described periodic cubic spline routine. Upon inspection, however, it was determined that the resulting functions displayed regions of extremely high accelerations which would result in instantaneous muscle forces beyond the capacity of the actuating systems or even that of a 'normal' in-vivo musculature. Localized irregularities probably stemming from the digitizing process were present. To resolve this problem, using the same data points, the target functions were approximated by a least square 10th order Fourier series fit (FOURIER.LSQ^{TM} routine, Turbo Pascal Numerical Toolbox). Previous investigations (Jackson, 1979) have demonstrated that Fourier series or even polynominal functions with an order greater than five are sufficient to represent gait like functions. Assuming this series representation then, the coordinates of about 300 points were computed and the described periodic spline procedure applied to them with satisfactory results. Thereafter, a specially designed computer program was used to combine the calibration interpolation functions with the flexion angle interpolation functions in order to produce the required stepping motor command functions.

These command functions must, however, be corrected such that the deflections in the motor cables and connecting tissues due to the applied flex./ext. moment time-histories are nullified (Section 4.2.3.). The target moments, as shown in Figure 3.6, remain in the sense of a flexing moment during the stance phase and are null during the swing phase. Hence only the stance phase portion of the extensor motor command function needed to be corrected. The moment time-histories were digitized and for similar reasons to the flexion angle time-histories, the given data points were fitted with a 10th order polynomial regression curve (POLY.LSQ^{TM} routine, Turbo Pascal Numerical Toolbox). A polynomial fit was adopted instead of a Fourier series since periodicity does not apply in this situation. According to this polynomial fit, the deflections were calculated at each time coordinate of the smoothed target function during stance by applying the constant calibration factor between angular deflection and applied moment as measured in Section 4.2.3. The new corrected flexion angle time-history of the stance portion was computed by subtracting the deflections from the smoothed target flexion angles. In keeping with the previous procedure, cubic spline functions were computed between these new target data points (CUBE-FREE^{TM}, Turbo Pascal Numerical Toolbox) without the constraints of periodicity. The produced corrected stance phase portion of the extensor's command function was then appended to the already established swing phase portion. The region between swing and stance required slight modification upon inspection to ensure continuity.

As discussed in Section 4.2.3, the time durations corresponding to steps in a new direction were increased by up to 30 msec, and the time durations corresponding to rotor speeds of less than 250 steps/sec were suitably corrected. These modifications were implemented such that the gross motion was negligibly affected and the total cycle times of each motor command function were equal. The cycle time of the target flexion angle time-history was initially 1.2 sec and once the corrections applied, the resulting cycle time increased to 1.25 sec for specimen 1 and 1.26 sec for specimen 2.

The computer routine which serves to download the command functions to the stepping motor controller requires the information to be stored in an ASCI file in the following form:

Total # of steps (flexor)

Δt 0 or 1 (0 for extending action and 1 for flexing action)

...

Δtn

Total # steps (extensor)

Δt 0 or 1 (0 for flexing action and 1 for extending action)

...

Δtn

The integer time durations (Δt) must be in the base time unit which is switch selected in the controller. The base unit selected for this study is the smallest one available (30/11 μsec) resulting in maximum resolution.

6.3.2 Ground Reaction Command Function Generation

The target functions of the tibial axial force and the flexing/extending moment components of the ground reaction from which the respective command functions were generated are shown in Figure 3.6.

The target functions were computed, as described in Section 3.3, such that discrete data points could be evaluated as required. The tibial axial actuating forces were directly obtained from the target tibial axial reaction time-histories. As to the flexing/extending moment actuating forces, they were computed by combining the target moment time-histories with the load requirements of the moment application linkage according to the following equation:

$$F_a = \frac{(I \cdot \alpha + C \cdot \dot{\theta} + m \cdot g \cdot l \cdot \sin(\theta - \theta_p) + M_G)}{(r \cdot \cos\phi)} \tag{6.1}$$

where

- F_a: actuating force
- M_G: target moment
- I, α, θ, θ_p, m, g, l, ϕ, r, are described as in equation 4.7.
- C: overall system kinetic friction constant.
- $\dot{\theta}$: flexion rate, or first time derivative of the flexion angle.

This is basically the same equation as was presented in Section 4.3.4. (equation 4.7) with the inclusion of the kinetic frictional force described in that section. The geometric term ϕ is computed according to equation 4.8. The flexion angle, and its first two time derivatives were obtained from the flexion angle functions (previous section). Computations were performed through the use of the Symphony^{TM} data manipulation software program

As was mentioned in Section 6.2, during a simulation, the reference command signals are varied in the discrete time domain every 11.5 msec by the main controlling computer. The operating routine, which controls the main controlling computer, requires that each of the ground reaction command functions be stored in their respective files on a computer diskette in the following ASCI form corresponding to a complete gait cycle.

> Force [N] at 11.5 (i.e. each force level, floating point decimal, is computed corresponding to the end of each 11.5 msec time increment)
>
> ...
>
> ...
>
> Force at T*

(filename: AX.PRN and SF.PRN for the tibial axial force and flex/extend moment respectively)

At run time, transformation of these tables to corresponding voltage level tables is performed by the operating routine. The last entry to each file, which is computed at the end of the last 11.5 msec time increment, will be correspondingly issued to the actuating system at that instant in time and held unchanged through to the end of the first time increment. Since the total cycle time will not in general divide itself exactly into 11.5 msec increments, the last entries will correspond to a time T* which will be less than 11.5 msec minus the total cycle time. In other words, the resolution at the very end and beginning of a cycle will in general be slightly coarser than the remainder of the cycle.

As was mentioned in Section 4.3.4., the command functions were corrected in an iterative manner after each simulation run until satisfactory performance was obtained. The average measured moments corresponding to each 11.5 msec time window were compared to the prescribed moments corresponding to the beginning of each 11.5 msec increment and the corresponding actuating force entries corrected according to the following equation:

$$\Delta F_a = \frac{(M_{Gmeas} - M_{Gtarg})}{(r \cdot \cos\phi)} \tag{6.2}$$

6.4 Operating Routine

The operating routine, of which a listing is included in the Appendix C, is written in the C programming language. This language was chosen as it compiles into efficient machine code with execution speeds approaching that of assembler code while still providing the user with the programming ease associated with higher level languages.

Before describing the operating routine, certain aspects of the analog interface card fitted to the main controlling computer will first be discussed as they bear relevance to the understanding of the operating routine. The interface card was configured in this study to be memory mapped with respect to the host computer. The fact that it is accessed as a memory location, as opposed to an $I/0$ port, results in faster access time thereby increasing the 'throughput' time of the operating routine. As to the digital to analog converters, their 12 bit digital inputs must be presented to them in two's complement code. They were switch configured in this study for $\pm$ 10 Volt output range. This range selection was done in conjunction with the setting of the input signal amplifier gains (K_1) on the servoamplifier/signal-conditioning card (see Sections 4.3.3. and 4.3.4). According to these settings and the static gains of the hydraulic actuating systems, it may be shown that more than half of the total ranges available are required for the simulation of walking gait and that the digital resolution of the tibial axial and moment actuating forces are 4 N and 6.5 N per bit change respectively. The analog interface card is also equipped with a 5 $\times$ 16 bit counter/timer chip (AMD 9513) and a 1 MHz source clock. As will be further described, two of these counter/timers were used in this study; one to perform system timing and the other to serve as a memory mapped switch to interrupt the simulation run.

The operating routine may be summarized as follows. Initially, both ground reaction command function files are read in to the computer's memory. Each entry is then transformed into its corresponding 12 bit digital voltage equivalent assuming the respective static gains of each system as listed in Sections 4.3.3. and 4.3.4. Next, the counter/timer chip is configured as follows (the reader is referred to Am9513A/Am9513 System Timing Controller, Technical Manual, 1985). One counter/timer is configured to count the source clock pulses (1 MHz clock). It counts up time to 65535 μsec in a cyclic fashion in 1 μsec increments. This timer serves to keep track of the passage of time such that each reference signal entry will be clocked out every 11.5 msec as will be shown later. The other counter/timer required in the control scheme is configured to count, once, a source edge issued to it on an external line which is hard wired to a switch with a 5 volt port. As will also be shown later, this timer serves to interrupt the control algorithm and terminate the simulation run. Having prepared the command function tables and configured the timer, the operator is prompted to switch on the motor windings. The motor windings are switched on directly from the computer's keyboard interface.

It is recalled from Section 6.2 that the stepping motor controller was loaded prior to a simulation run with the stepping motor command functions. Thereafter, it is controlled by the operating routine and main controlling computer through a parallel interface port. Various functional commands such as turn on or off the motor windings and start or stop the programmed stepping motor functions may be issued to the stepping motor controller. One line on the parallel interface port serves as a status line indicating to the operating routine each time the stepping motor controller has completed a gait cycle with another one about to begin.

Returning to the description of the operating routine, having switched on the motor windings the operator is then prompted to start the simulation run through an indicated keyboard entry. Once the process is initialized, the timers and the stepping motor controller are activated to start their programmed functions. Thereafter, the operating routine enters its control algorithm which consists in:

- reading the first timer's register
- comparing the new reading with the last reading which corresponded with an 11.5 msec time increment
- outputing the respective command voltage levels conditional with an 11.5 msec time elaspse
- verifying if the second timer has received a process interrupt signal.

The algorithm is repeated until all ground reaction command signal entries have been issued corresponding with a complete gait cycle simulation.

At this point, the operating routine waits for the stepping motor controller to complete its ongoing cycle, leaving the end portion, after the last 11.5 msec time increment, to be completed. Upon cycle completion, as indicated to the operating routine through the stepping motor controller status bit, the first timer is re-intialized and activated and the control algorithm re-entered to produce another cycle. Cycles are repeated indefinitely until the second timer indicates a process interrupt request. The interrupt routine consists in issuing null reference signals to the hydraulic systems and a command to the stepping motor controller to terminate its programmed function at the end of the ongoing cycle. Once the last cycle is finished, the operator is prompted to turn off the motor windings and the program is terminated.

The control algorithm cycle time was timed at 75 μsec for the host computer (10 MHz) used in this study indicating the timing resolution of the system.

Table 6.1: Data Acquisition Channel Configuration and Resolution

Channel	Measured parameter	Instrumentation Gain (see Chp.5)	Estimated max/min	Selected Range	Resolution
1	Flexion angle	66.589 deg/V	+ 1.582 V (0°) to +2.637 V (70°)	+5V	0.16 deg
2	Flex./ext. Moment transverse force	19.13 N/mV (moment arm of 44.67 cm)	0 mV (0 N.m) to + 65mV (55 Nm)	± 250 mV	2.33 N (1.04 Nm)
3	Tibial Axial Force	5.347 N/mV	0 mV (0 N) to + 131 mV (700 N)	± 250 mV	.653 N
4	Axial Joint Reaction	18.19 N/mV	0 mV (0 N) to 105 mV (2000 N)	± 250 mV	2.22 N
5	A/P Joint Reaction	19.13 N/mV	0 mV (0 N) to + 37 mV (700 N)	± 250 mV	2.33 N

6.5 Data Acquisition

The data acquisition system that was described in Section 6.2 is software configured and controlled in real-time by a supplied software package (Analog Connection PC, Strawberry Tree^{TM}).

The voltage ranges that were selected in this study, corresponding with the various parameters that were measured, are listed in Table 6.1. Also included in the table are the corresponding digital resolutions.

At run time, the operator is prompted to select the channels to be scanned, the approximate scanning frequency, the total number of readings to be performed, and the disk file name where the readings will be logged. Once the simulation run is underway, the data acquisition routine is started by the operator through the host computer's keyboard. Once the total number of readings are obtained, the measurements are then logged to the assigned disk file.

The exact time coordinate of each voltage entry is obtained by calibrating the system for its exact scanning frequency corresponding to the selected system configuration. This was performed by switching one of the input channels to a signal which varied according to a known time base.

All measurements that were obtained in this study were obtained at the data acquisition's maximum scanning frequency and total number of readings. This corresponds to 2000 readings for each channel at a rate of 370 Hz. Thus the time coordinate between each reading for all channels was 2.7 msec and the results of over 4 consecutive cycles were obtained. Even though the ADCs have a 10 KHz frequency cutoff (Section 6 2), low frequency electrical noise was found to be present on the mV range signals upon inspection of the resulting traces.

To resolve this problem, each six consecutive readings were averaged and the results assigned the middle time coordinate of the six readings. Ideally, the averaging of an even number of readings taken over a 60 Hz noise period should have been implemented to rid the signals of their 60 Hz noise content. The filtering of the noise's higher harmonics is achieved by increasing the even number of readings taken over the noise period. However, in this situation, the scanning frequency of choice, an even multiple of the assumed 60 Hz noise frequency, was not available and could only be approximated. The implemented scheme corresponds with the digital filtering scheme of a 61.7 Hz noise signal. Although approximate, satisfactory results were nevertheless obtained. All data manipulation to obtain filtered readings and final results, as presented in Chapter 7, were performed through the use of a mass data manipulation software package (Symphony$^{\mathrm{TM}}$).

6.6 Summary

The simulator is interfaced with a microcomputer to serve, at run time, as a programmable voltage source, sequencing the reference command signals to the ground reaction actuating systems, while synchronizing the functioning of the stepping motor controller which is pre-programmed to control the displacement time-histories of the muscle load cables. On the output side, the simulator is interfaced with a dedicated data acquisition system to scan and record the instrument readings corresponding to a simulation run.

The stepping motor command functions were obtained by combining calibration functions with the desired flexion angle time-histories taking into account the compensation required to nullify the angular deflections due to the applied moment time-histories. The ground reaction command functions were obtained from the target ground reaction time-histories and, in the case of the flex./ext. moment, by also taking into consideration the dynamic functional requirements of the actuating mechanism by superposition.

During a simulation run, the main controlling computer is controlled in real time by a specially devised operating routine which operates in the discrete time domain. The cycle time of the control algorithm is 75 μsec.

The data acquisition system is driven by a supplied software package. The limitation of the data acquisition system corresponds to a complete instrumentation scan being repeated every 2.7 msec for a total of 2000 scans. The system was configured for this maximum operating capacity to obtain the measurements required in this study.

Chapter 7

SIMULATION RUN: RESULTS AND DISCUSSION

7.1 Results

Two fresh-frozen specimens, one right and one left, were thawed and subjected to a level walking simulation as described in the previous chapters. Upon preparation, both joints appeared normal with the first specimen slightly bigger than the second An average body weight (b.w.) of 68 kg was assumed.

The applied functions as well as the resulting joint reactions were recorded over approximately four consecutive cycles. Apart from minute sporadic variations, repeatability was verified between cycles as well as between simulation runs.

As was mentioned in Section 4.3.4, simulation runs were repeated modifying each time the moment applicator's command function until satisfactory target function reproduction was obtained or improvements became marginal In effect, the limiting factor was the life span of the thawed specimens. Six to seven runs (≈ 4 hrs total) were required before the results as presented here were achieved. Although continuing with the procedure would have resulted in better function reproductions, the life span of a thawed specimen is limited.

Corresponding to a single cycle of a final 'satisfactory' run, the measured time-histories of the flexion angle, and the flexing/extending moment and the tibial axial force components of the ground reaction, are depicted in Figures 7.1, 7.2 and 7.3 respectively. The corresponding target input functions are superimposed for comparison. The stance portion is from 0 to .82 seconds with the swing phase occupying the remaining portion.

In general, the flexion angle functions achieved corresponded well with the target function. For specimen 1, the angle was generally greater than the target angle with a maximum difference of 5 deg. occuring at the peaks of the stance and swing phases. With specimen 2, slightly better results were obtained except that just before the first peak in the stance phase, the leg momentarily re-extended slightly unlike the normal flexion angle characteristic curve.

The measured flex./extend. moment time-histories demonstrate relatively satisfactory function reproduction. Although during the stance phase the maximum deviations were +12%/-22% for specimen 1 and +17%/-30% for specimen 2, the applied moments were on average within ± 5 Nm of the target moments. And during the swing phase, the portion during which the moment actuating mechanism must track the motion of the tibia while not transmitting any force to it, interference moments were less than 4 Nm.

For the tibial axial force, satisfactory overall performance was obtained. During the stance phase, some lag is initially noted between the measured and target force time-histories in both specimens. The maximum error noted thereafter was + 10%, near the end of stance. And for a brief period towards the end of the swing portion, the actuating system interfered slightly with the tibia (10% b.w.).

The corresponding axial compressive and anterior/posterior (A/P) components of the total knee joint reaction force along the femoral axis were also measured and the results are depicted in Figures 7.4 and 7.5 respectively. Although very similar reaction force characteristics are noted during the swing portion for both specimens, more important variations between specimens were measured during the stance portion and especially for the axial component. During the stance phase for specimen 1, two consecutive peaks of decreasing magnitudes (2.7 b.w. and 2 b.w.) were measured While for specimen 2, three defined consecutive peaks of increasing magnitudes (2.2, 2.7 and 2.95 b.w.) were measured during the same period During the swing portion, the axial joint reaction for both specimens remained approximately constant between .25 and .5 b.w. As to the corresponding anterior/posterior (A/P) component of the joint reaction force, similar overall characteristics were observed for both specimens The force remained anterior for specimen 1, oscillating between 0.1 and 0.5 b.w. during the stance phase, then remained approximately constant during the swing phase at about 0.25 b.w. For specimen 2, the maximums and minimums occurred in phase with those of specimen 1, but with slightly increased amplitudes. The two minimum magnitudes in the stance phase decreased sufficiently resulting in a change in sense giving rise to a posterior reaction force of up to 0.25 b.w. In late stance, the maximum magnitude of the A/P force recorded was 0.8 b.w. anteriorly

7.2 Discussion

In generating the stepping motor command functions, the target flex./ext. moment time-histories were assumed to determine the compensatory cable displacements (Sections 4.2.3. and 6.3.1.) Hence, if the applied moment time-histories deviate from those intended, the flexion angle functions will be affected in proportion In view of the relatively significant elasticity of the combined extensor cable and connecting soft tissues, the inaccuracies in the flexion angle function reproduction are, to a large extent, attributable to the inaccuracies in the moment function reproduction Other flexion angle reproduction inaccuracies may be attributed to the inertial effects which are not accounted for in the command function generation, inaccuracies in the statically obtained calibration functions due to dynamic effects, minute changes in the equilibrium points due to the presence of loads which are not present during calibration, and the hysteresis in the muscle cables and connecting tissues on the extensor side.

The problems which hinder accurate moment function reproduction were already discussed in Section 4.3.1. Theoretically, the iterative procedure adapted in this study could have been continued further until near exact function reproducibility was obtained. However, the time available to continue the procedure was limited as mentioned in the previous section. Thus, the acknowledged off-target performance of the moment actuating system and the inaccuracies in the flexion angle command function interact multiplicatively to adversely affect both the flexion angle and moment function reproductions. It is recalled that the moment-arm of the moment actuating force is a function of the flexion angle (Eqn. 4.8) and, as noted in the previous paragraph, the flexion angle itself is affected by the applied moment.

With respect to the tibial axial force component of the ground reaction, the inaccuracies in function reproduction are assumed to stem mainly from the partial misfunction of the servovalve. This was suspected to be the cause of the discrepancies between the theoretical and measured step response as discussed in Section 4.3.2. A somewhat sluggish response with a 150 msec settling time and a reduced proportional response to signals under 2 volts, both contributed to the off-target performance given an assumed constant gain

The joint reaction time-histories are not controlled functions but are a result of the applied muscle and ground reaction forces to the knee joint specimens, each possessing unique structural characteristics. Hence, discrepancies between the joint reaction force time-histories of each specimen are expected. The differences in characteristics between each knee specimen may also be attributed to the measured deviations between the controlled input functions of each joint. For instance, similarities in the characteristic shapes of the measured moments and compressive joint reaction time-histories of each specimen are noted during the stance phase.

In order to compare the joint reaction time-histories measured in the present study with those available in the literature, the corresponding ground reaction time-histories must also be compared. As was mentioned in Section 3.3, considerable variability in the joint moment histories exists depending on individual gait habits. Hence, variability in the joint reaction may also be expected to prevail. Comparison of joint reaction force time-histories is further complicated by the fact that other investigators generally publish the tibiofemoral joint compressive force time-histories along the tibial axis, whereas in this study, the total joint compressive force is measured along the femoral axis. This measured compressive force includes the patellofemoral contributions as well. However, as was shown in Section 3.3, both parameters are approximately equivalent during stance when the leg is near full extension. Taking into account these reservations, it is interesting to note the similarities between the joint reaction time-histories measured in this study and the joint reaction force time-histories reproduced in Figure 2.11. The maximum amplitude just below 3 b.w. during the stance phase, and the force generally below 0.5 b.w. during the swing phase, correspond with the results of Morrison (1970).

Chapter 8

SUMMARY AND CONCLUDING REMARKS

8.1 Introduction

In this chapter, the study is concluded by reviewing the simulator's overall design. The features and performance of the facility are summarized in the next section to establish whether the original design criteria have been satisfied. In a following section, examples of possible biomechanical investigations which may be undertaken with the present simulator are examined. Finally, recommendations on future development work that would improve the simulator's performance are given.

8.2 Design Evaluation

The aim of this study was to design, develop and test a system capable of reproducing on a knee joint specimen the various force histories which occur during normal ambulatory activities. The facility was envisaged to permit the study of knee joint mechanics corresponding to dynamic functional conditions.

To simulate the required dynamic conditions, four actuators have been adopted in the simulator. Two actuators each apply the extensor and flexor muscle forces such as to control the flexion angle time-histories of the joint. The remaining two actuators are used to apply the two main components of the ground reaction in the plane of motion. The selected components of the ground reaction are the tibial axial force and the flexing/extending moment. The actuation scheme permits the control of the main forces which affect the knee joint in the plane of motion corresponding to functional activity.

For a valid simulation, the manner in which these forces are transmitted to the joint is of primary concern. Each joint has a unique geometry, and soft tissue configuration, and thus each possesses a unique motion response to an applied force. Therefore, the load application must be such that the joint response is unconstrained. The muscle forces are applied through flexible steel cables allowing unconstrained transverse motions. The ground reaction loads are applied through a steel cable/pulley arrangement, in the case of the tibial axial force, and through a special linkage system, in the case of the moment component. In each case, the designs are such that they do not interfere with the natural three-dimensional motions of the joint members. In addition, the extensor cable is attached to the patella and thus the patellofemoral articulation is left intact as is the tibiofemoral articulation. Its contribution to the overall joint mechanics remains physiological.

In addition, special design features have been incorporated to take into consideration the variability of biological specimens and the wide range of possible functional activities which may be of interest to simulate in future studies. All lines of forces and specimen fixation components are entirely adjustable such that specimens may be loaded uniformly. This is further ensured by individually calibrating each specimen for the muscle cable displacements corresponding to a flexion rotation taking into account the elasticity in the flexor/extensor mechanisms as required. These are applied to obtain the actuator command functions in accordance with the target dynamic input functions. These procedures are possible through the implementation of an entirely programmable system. Through the use of microcomputers equipped with hardware interface cards and driven by either specially written computer programs or other commercially available software packages, the user has the capability to measure each specimen's characteristics, as required, to generate and modify the command functions. Necessarily for this purpose, the simulator has been equipped with instrumentation to measure the applied functions in order to verify and improve system performance. The system's programmability also allows for a wide range of possible functional activities to be simulated. All hardware equipment (i.e., actuators, mechanical components, ...) have been selected, or designed, to take into account the mechanical requirements associated with level walking and stair ascent and descent simulations; thus encompassing a wide range of possible activities (viz. inclined walking, deep knee bends, ...).

The final criterion to be satisfied once the aforementioned was met was that the system be capable of reproducing the chosen dynamic functions. Satisfactory function reproduction was measured for two specimens in the example of a level walking gait simulation.

Photographs of the simulator are included (Fig. 8.1).

8.3 Scope of Investigations

Numerous studies on both the tibiofemoral and patellofemoral articulations are possible with the dynamic knee simulator presented in this study. For instance, the kinematics of the joint or the relative displacements between the joint bone members may be measured. Such measurements can be done with six degrees-of-freedom goniometers. It may be of interest to correlate these measurements to the articular surface geometry and the ligamentous structure. A far reaching study could involve, for instance, the comparison of knee joint displacements, as measured in an intact joint, with those measured in the same joint, but of which the cruciate ligaments were sequentially severed. This would help determine the relative importance of the cruciate ligaments in the mechanics of the knee joint. Furthermore such kinematic studies could be enhanced by the measurement of the tension in the ligaments and soft tissue structures through the use of buckle transducers. Such an overall picture could yield valuable data for the design of prosthetic devices.

The simulator may also be used directly in the design of prostheses. The biomechanical consequences of various prothesis design features may be conveniently evaluated by measuring the joint characteristics of interest before and after implantation and design modification. Furthermore, the effects of implant misalignment can be evaluated.

Innovative surgical procedures may also be initially evaluated in- vitro, avoiding any risk to a patient. For instance, ligament reconstruction techniques (viz., relocation of ligament attachment points) may first be performed on a joint specimen and the procedure evaluated based on preliminary tests using the simulator.

All the aforementioned analyses may be performed for a variety of gait activities for a more thorough investigation. Although the simulator was only tested for walking gait simulation, a wide range of activities may be simulated as was mentioned in the preceding section. The simulator is also presently equipped with a dedicated data acquisition system able to record the time-histories of up to sixteen channels. Since the system is software driven, it may be reconfigured in a simple manner to record multiple transducer signals to measure the selected joint characteristics during a simulation run.

8.4 Future Considerations

The performance of the simulator could be improved if the accuracy of the flexing/extending moment function reproduction was increased. It is recalled that discrepancies in the moment actuating force command function interactively resulted in off-target flexion angle time-histories and corresponding increased deviations in the obtained moment. The procedure by which the command functions were corrected iteratively between consecutive simulation runs, resulted in improved function reproduction but could not be continued sufficiently due to the limited life span of the thawed specimens. An easily adopted solution to increase the accuracy of the moment function reproduction in walking gait simulations would be to start the corrective procedure assuming first the final command functions already determined in this study.

Another solution would be to control the applied moment in a closed-loop fashion by incorporating the moment transducer signal as a feedback signal. It is noted however that the implementation of a closed-loop control system in this situation would be complex. A robust adaptive controller would have to be considered since on one hand, a low natural frequency is present in the system (recall section 4.3.3.), and that on the other, the obtained moment for a given actuating force is a function of the flexion angle. The robustness of the suggested system would ensure system stability and its ability to 'adapt' would enable it to automatically compensate for flexion angle effects as well as other effects. For an example of such a control system as applied to an electro-hydraulic system, the reader is referred to Hori et al. (1988).

The flexion angle could also be controlled in a closed-loop manner by using the flexion angle potentiometer as a feedback transducer. This would, in addition to increasing the accuracy of the flexion angle reproduction, result in improving the moment function reproduction. Also, all specimen calibration procedures would become unnecessary. However, the design and implementation of such a system would be highly complicated. Proper synchronization of both muscle cable displacements could only be ensured by simultaneously monitoring the cable loads, and utilizing a control algorithm that would minimize antagonistic muscle forces, while still ensuring that the sought flexion angle time-histories are obtained. The dwell time and low speed resonance characteristics of stepping motor systems might complicate the scheme further.

Certain modifications could also be made to increase the physiological accuracy of the simulation. For instance, the muscle and ground reaction force array could be increased to simulate out-of-plane forces which are also present during ambulatory activity.

FIGURES

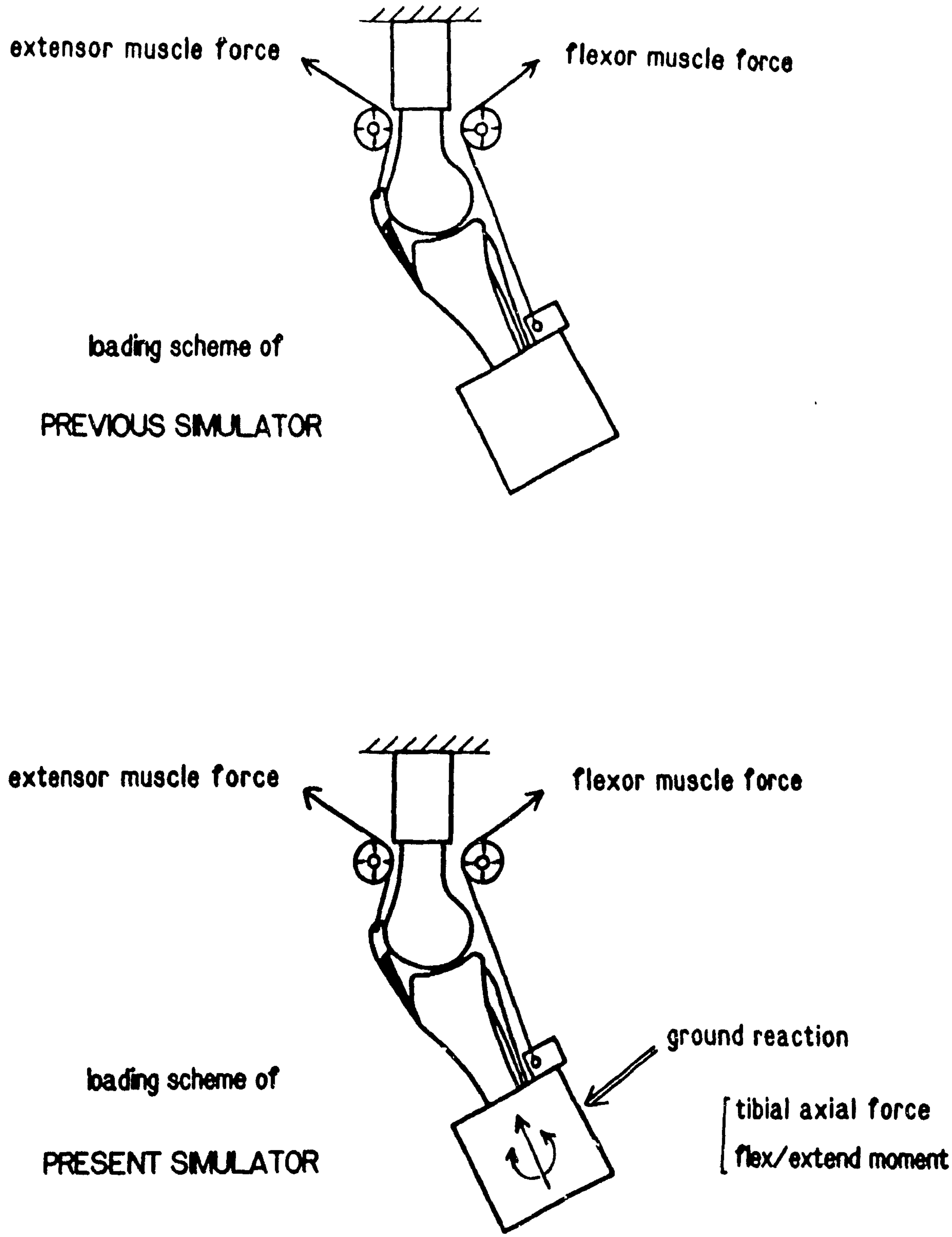

Figure 1.1: Simulated Forces

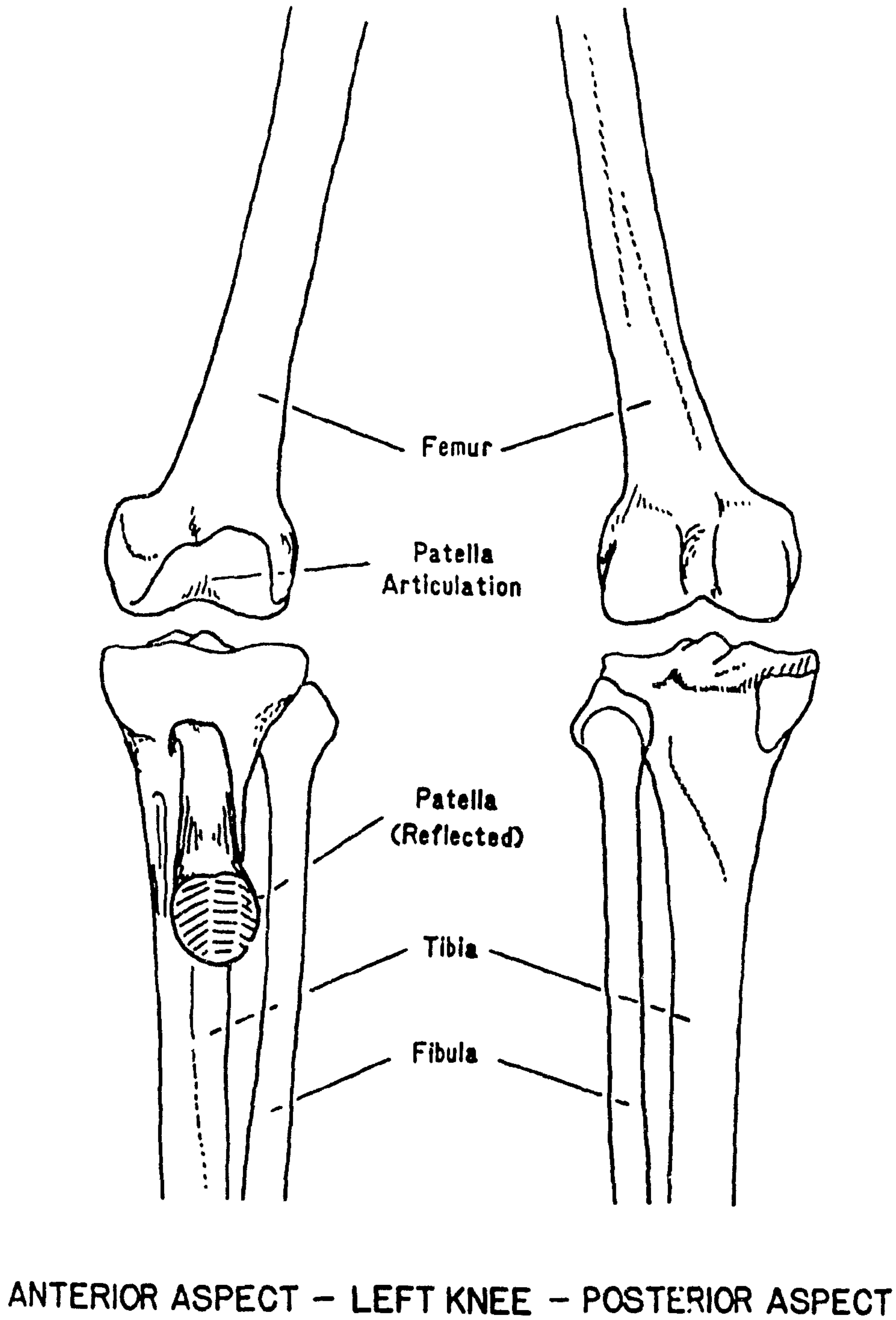

Figure 2.1: Articular Surfaces of the Knee (Szklar, 1985)

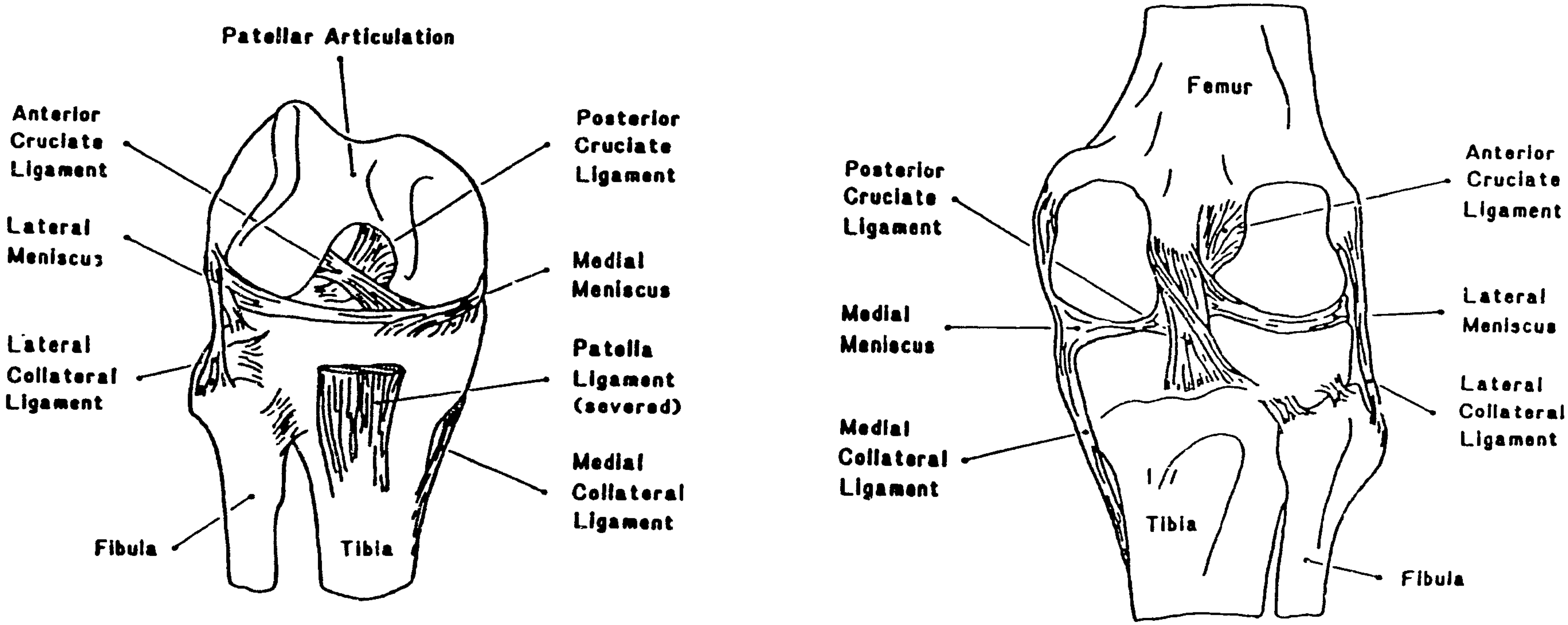

FULLY FLEXED RIGHT KNEE – ANTERIOR ASPECT

FULLY EXTENDED RIGHT KNEE – POSTERIOR ASPECT

Figure 2.2. Major Ligaments of the Knee (Szklar, 1985)

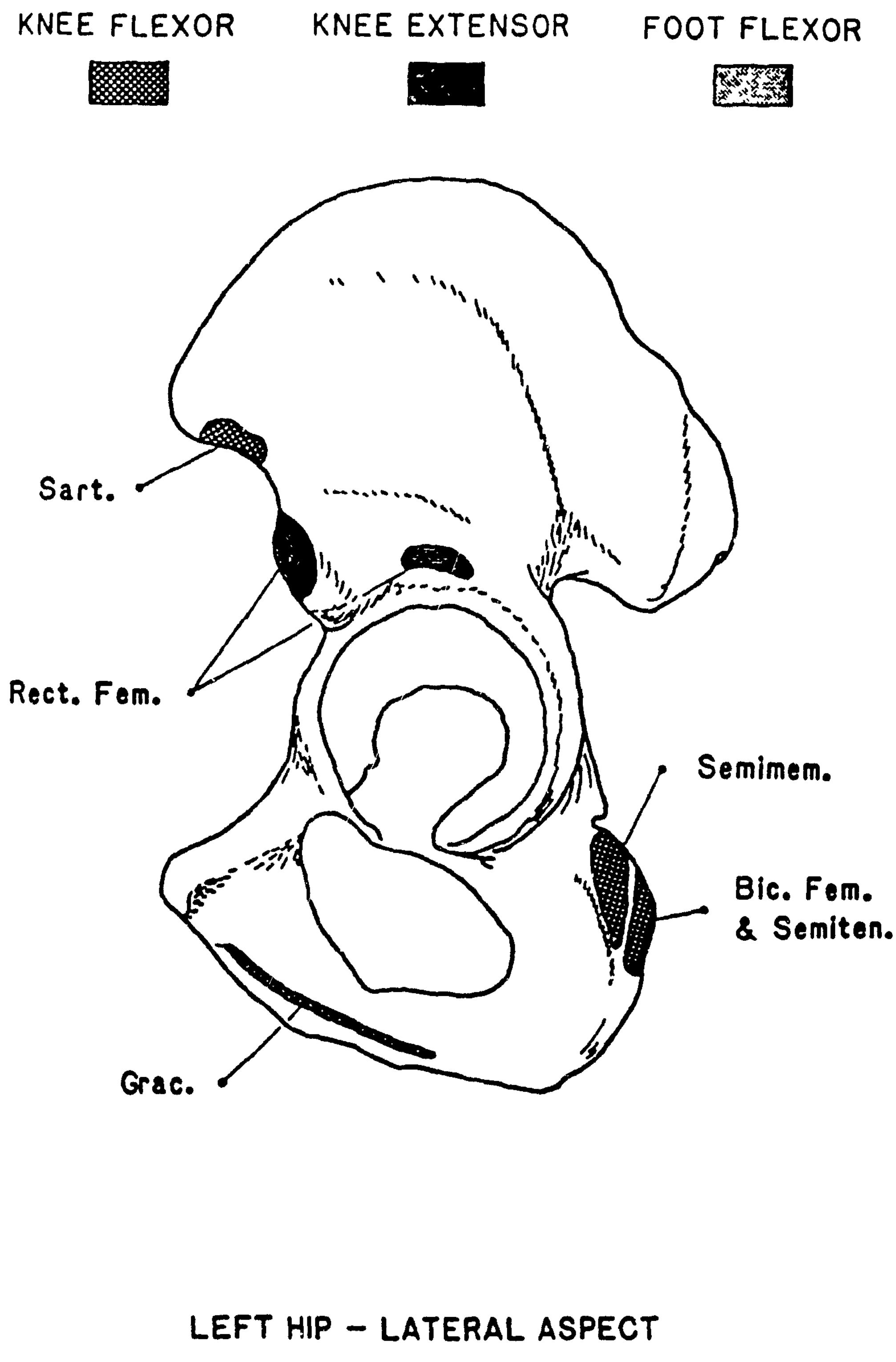

Figure 2.3: Pertinent Muscle Attachments of the Hip (Szklar, 1985)

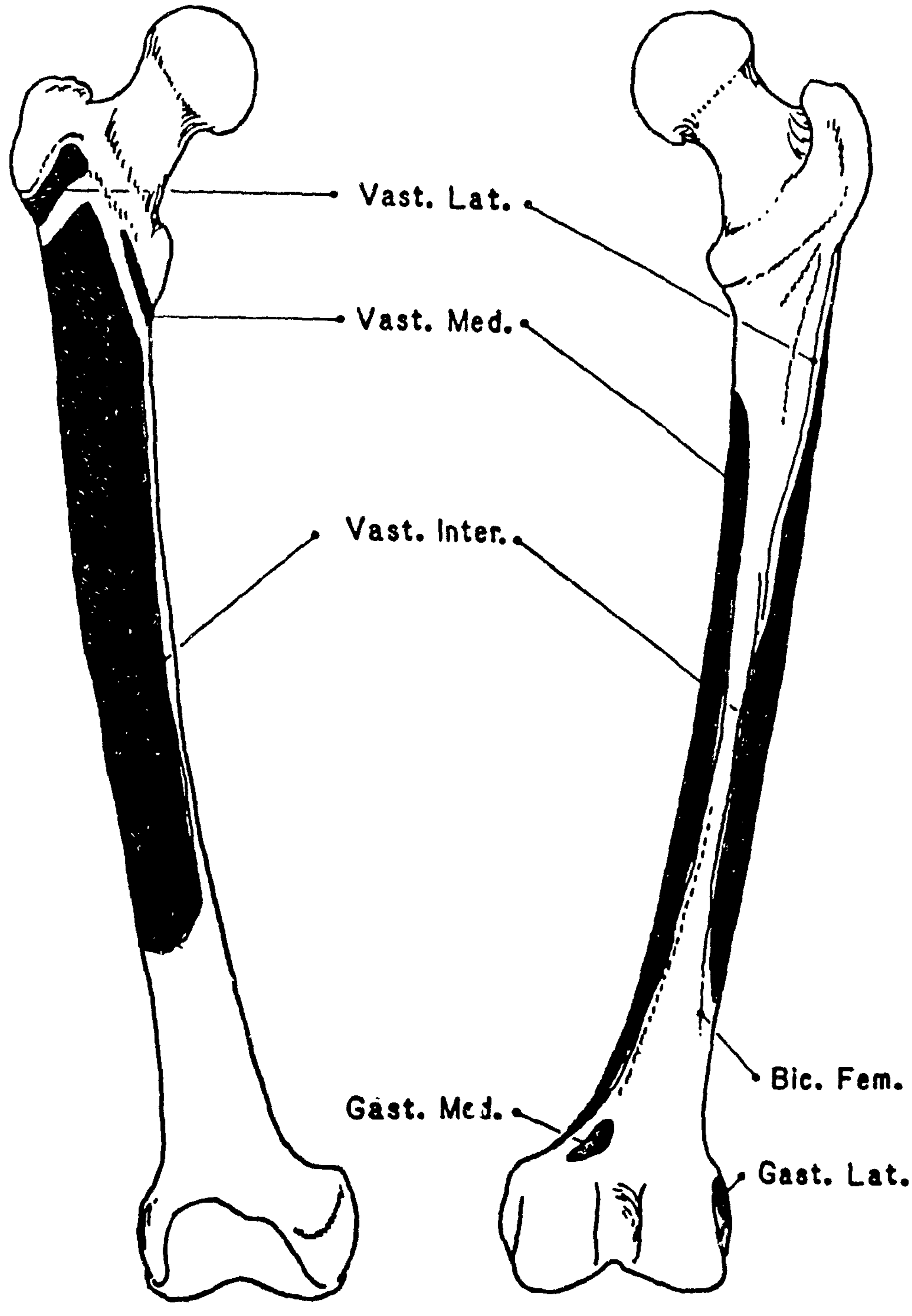

Figure 2.4: Pertinent Muscle Attachments of the Femur (Szklar, 1985)

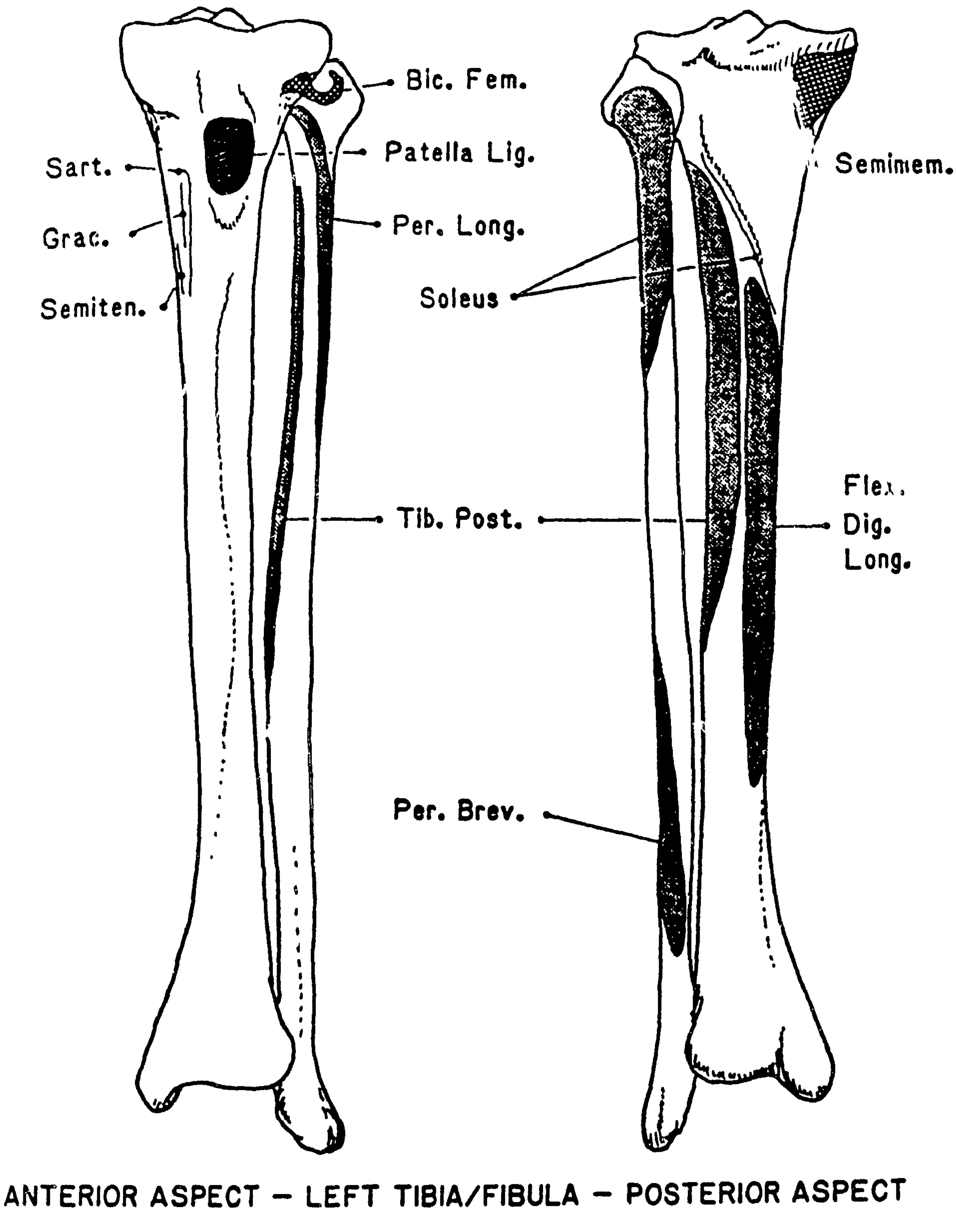

Figure 2.5: Pertinent Muscle Attachments of the Tibia/Fibula (Szklar, 1985)

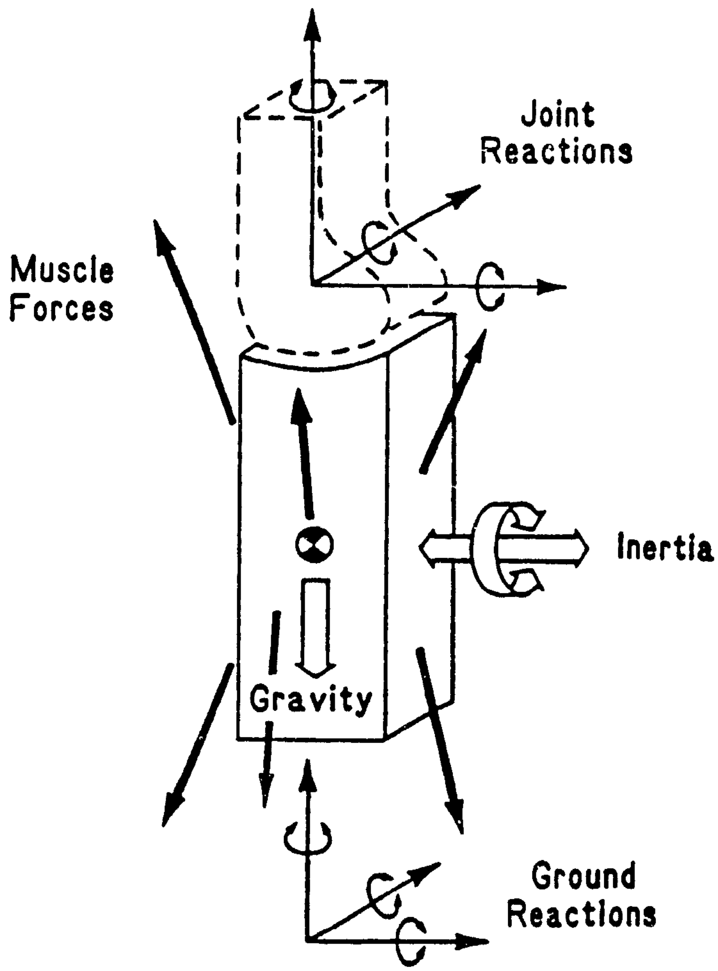

Figure 2.6: Free Body Diagram of the Knee Joint

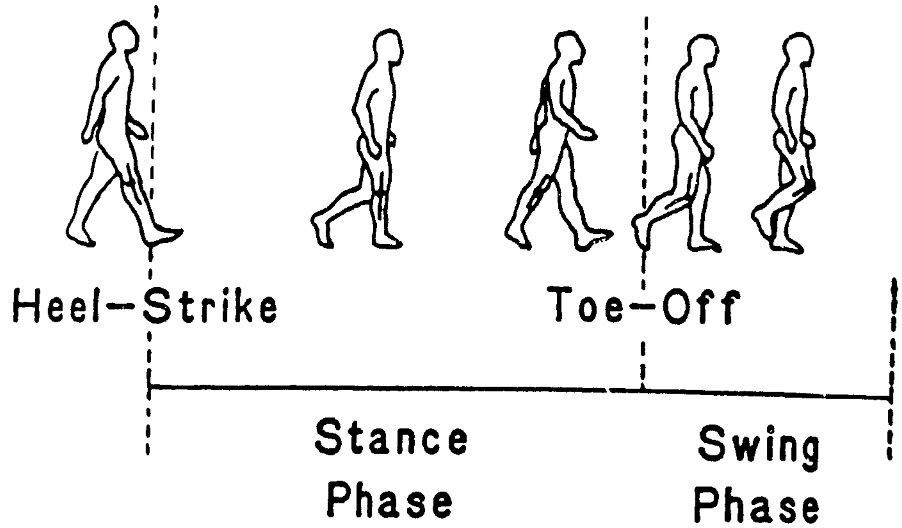

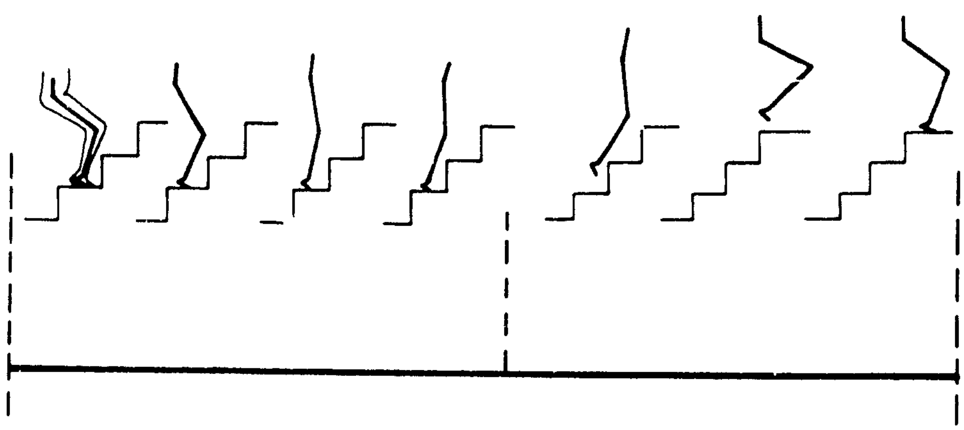

Figure 2.7: Stick Figure Representation of Walking and Stair Gaits

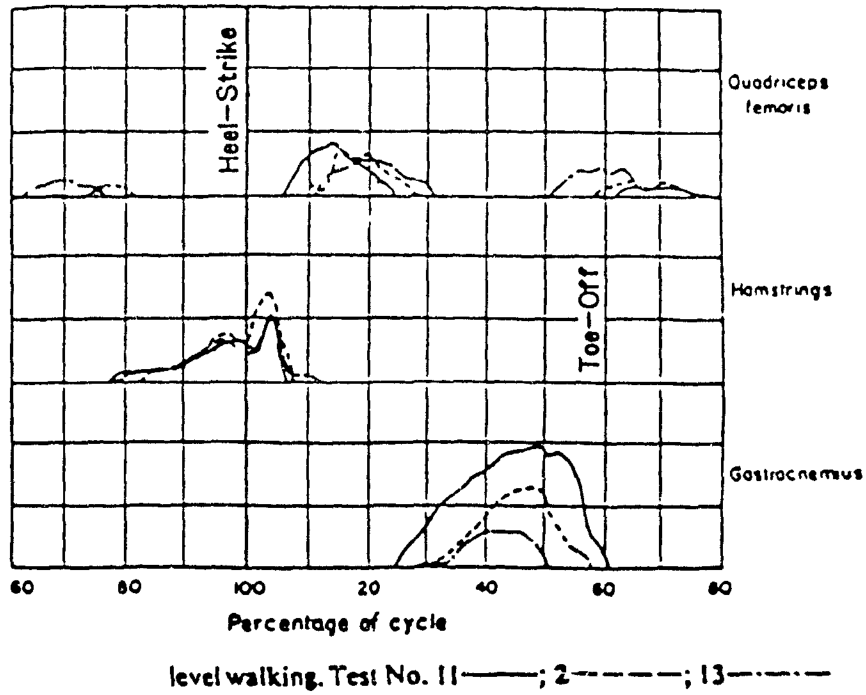

Figure 2.8: EMG Response during Walking (Morrison, 1970)

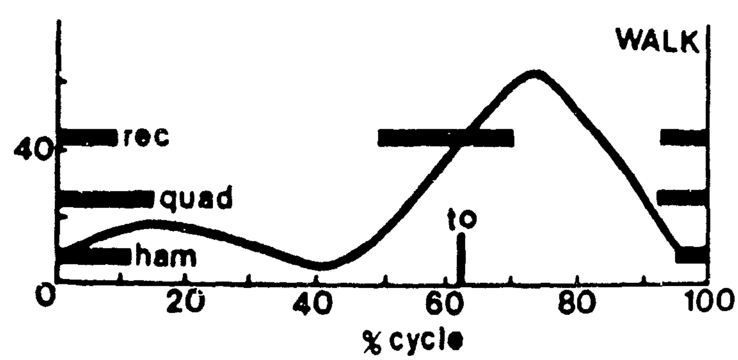

Figure 2.9: EMG Response during Walking (Mann and Hagy 1980)

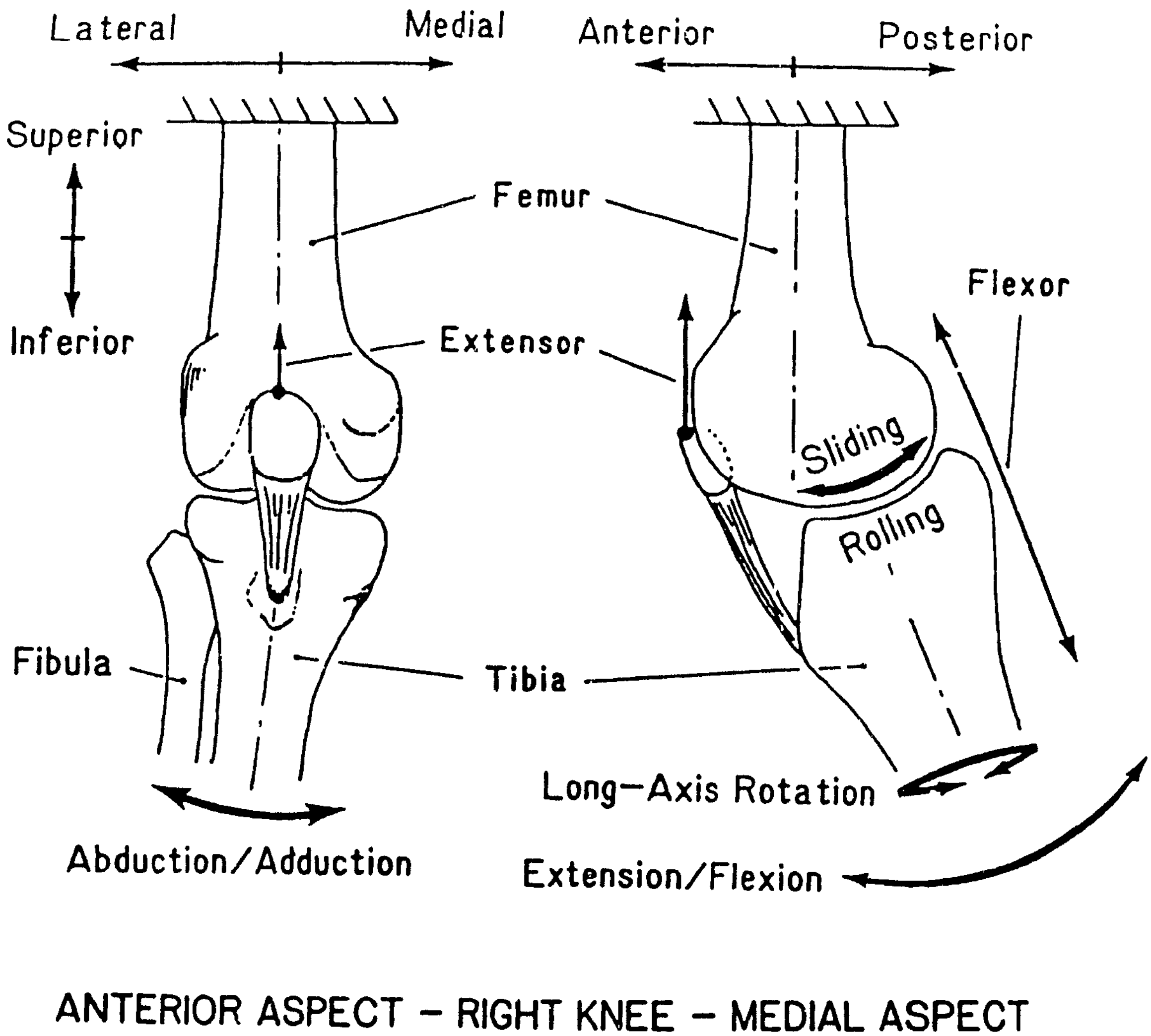

Figure 2.10: Degrees of Freedom of the Knee

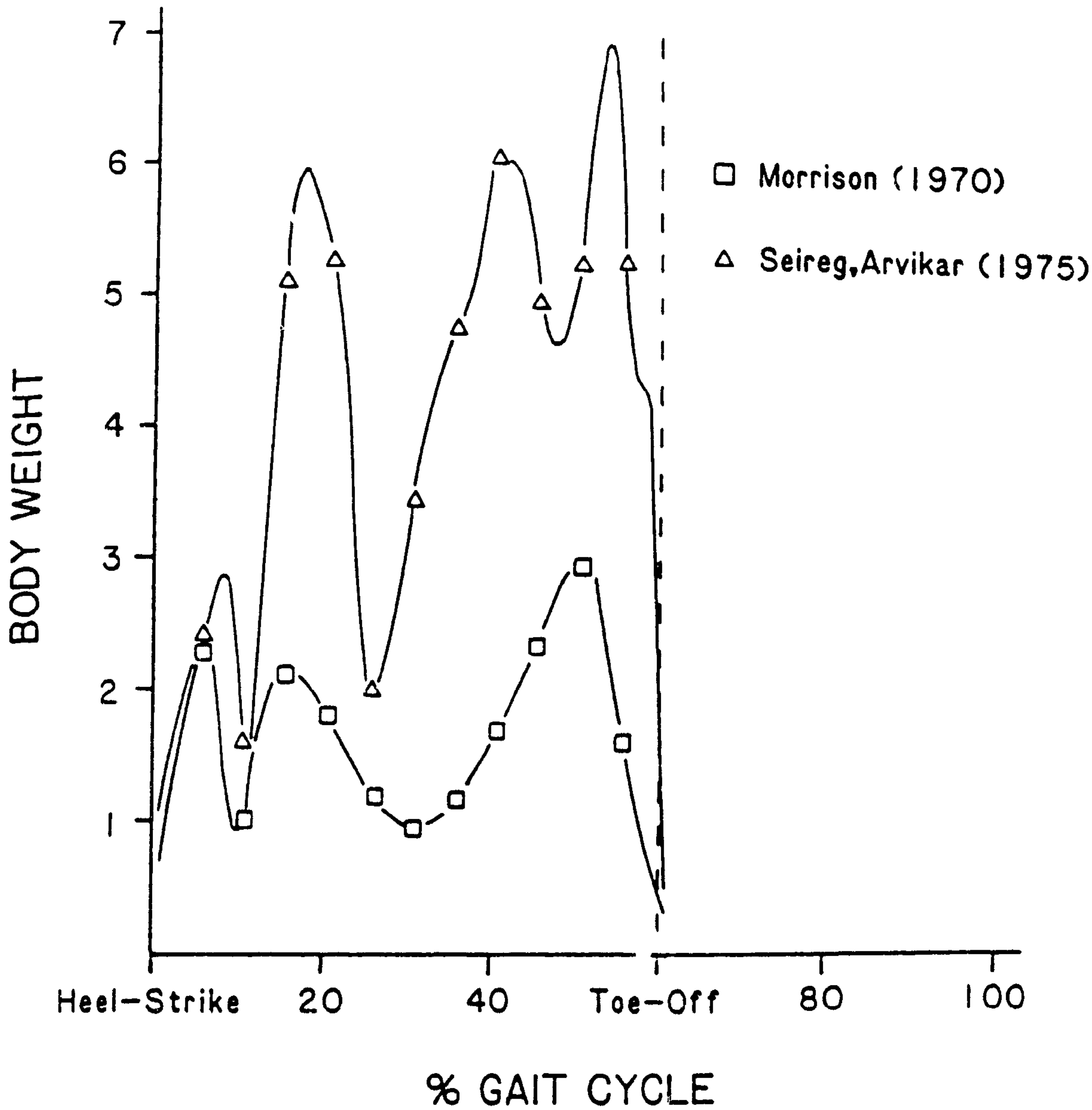

Figure 2.11: Comparison of Computed Axial Joint Reactions

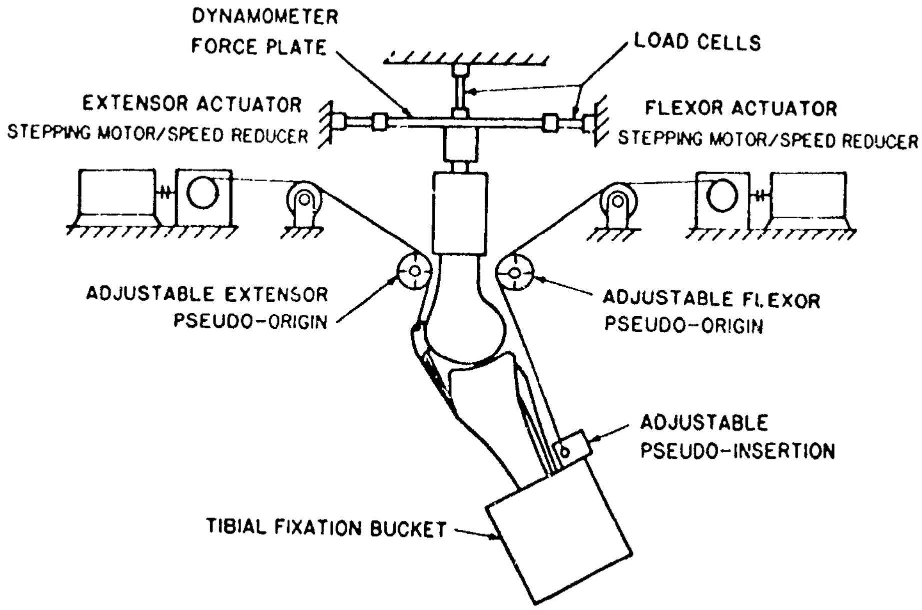

Figure 3.1: Muscle Actuation

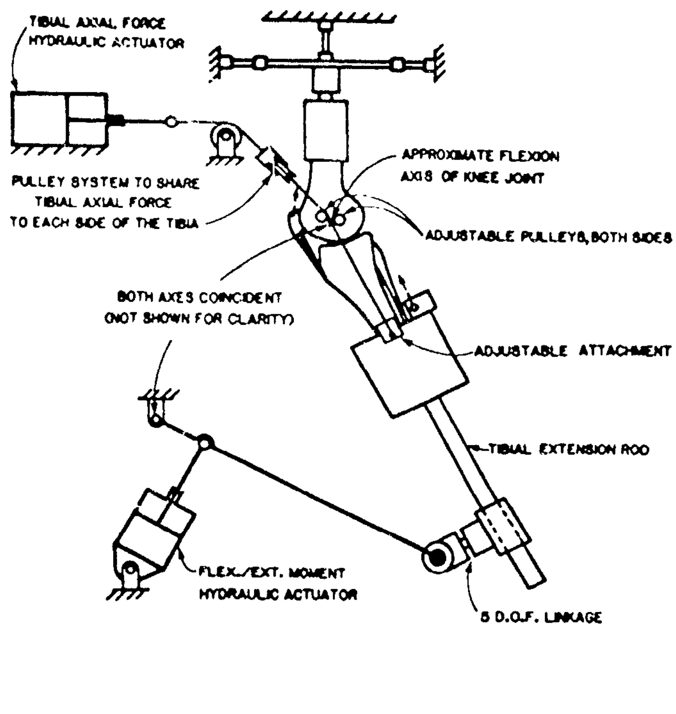

Figure 3.2: Ground Reaction Actuation

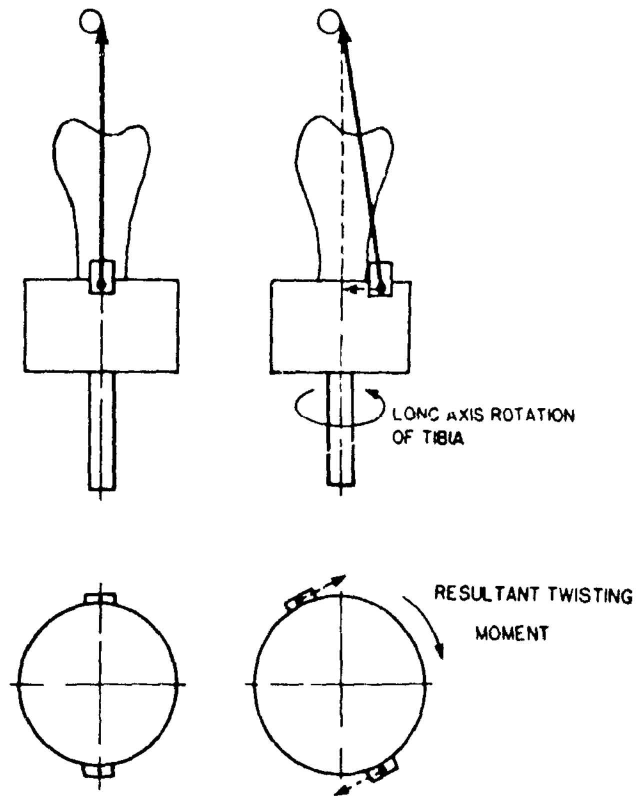

Figure 3.3: Parasitic Twisting Moment

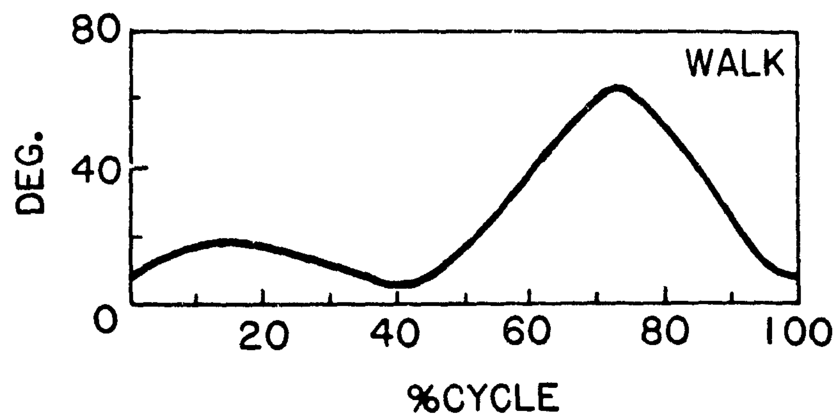

Figure 3.4: Target Flexion Angle (Mann and Hagy 1980)

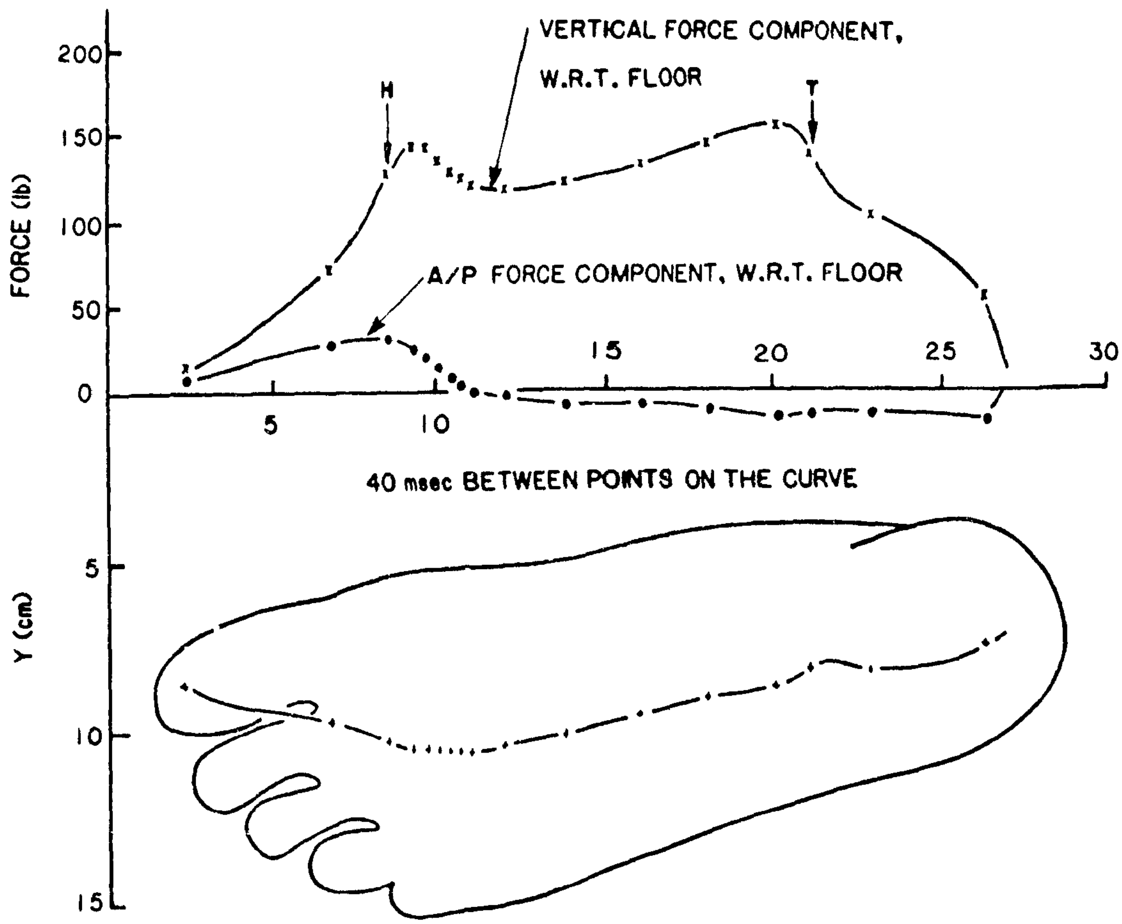

Figure 3.5: Input Ground Reaction Parameters (Grundy et al., 1975)

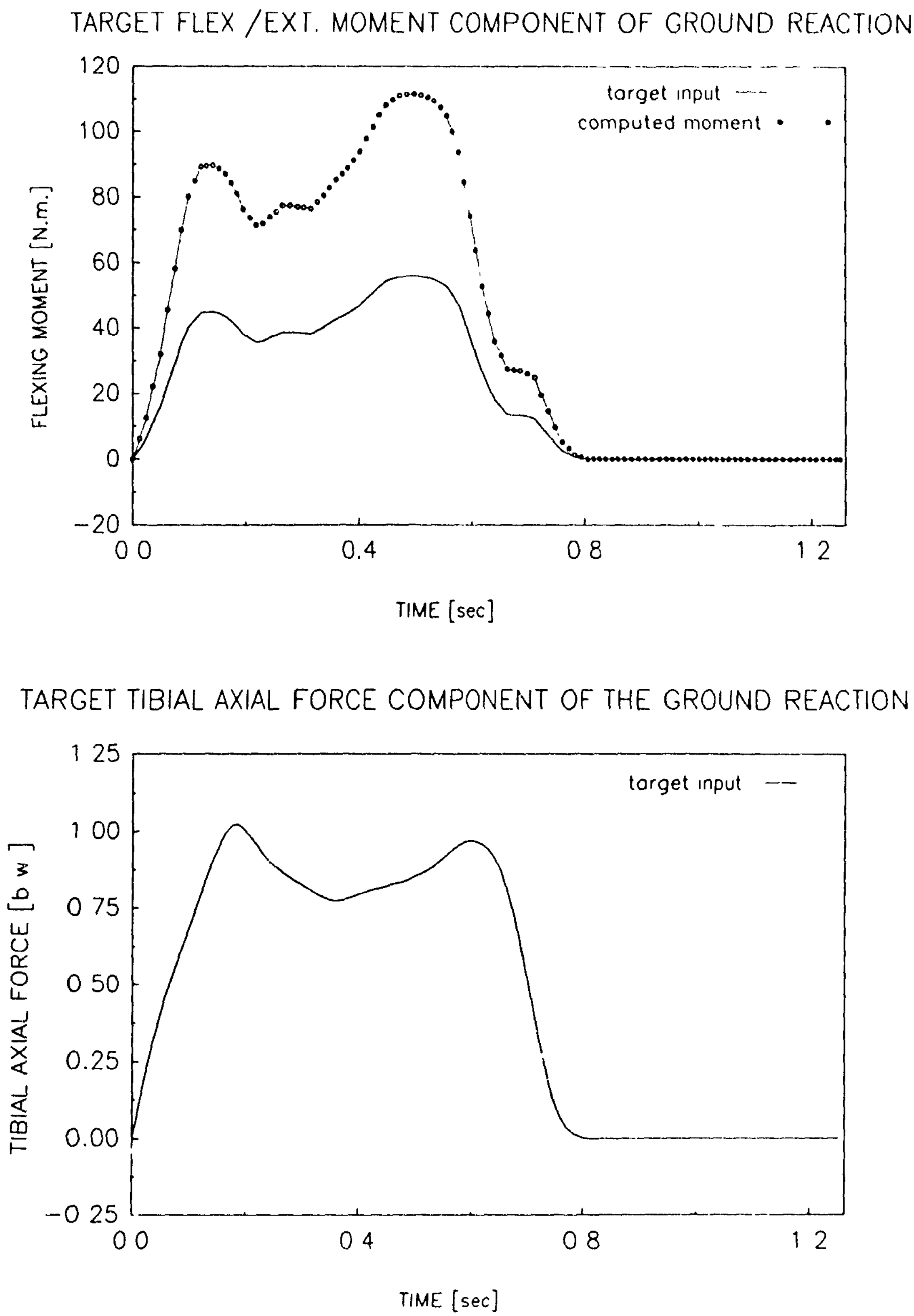

Figure 3.6: Target Ground Reaction Components

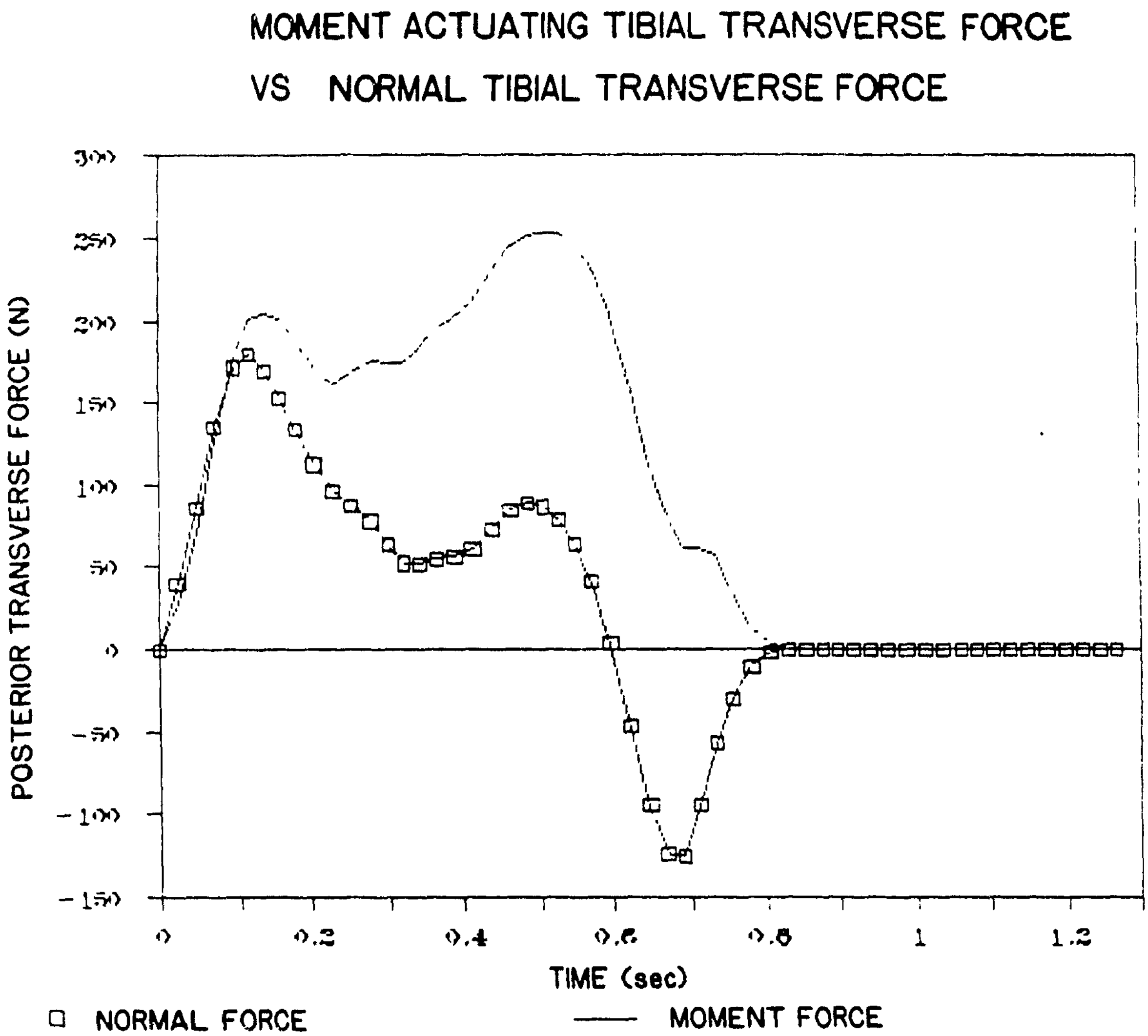

Figure 3.7: Parasitic Tibial Transverse Force Component

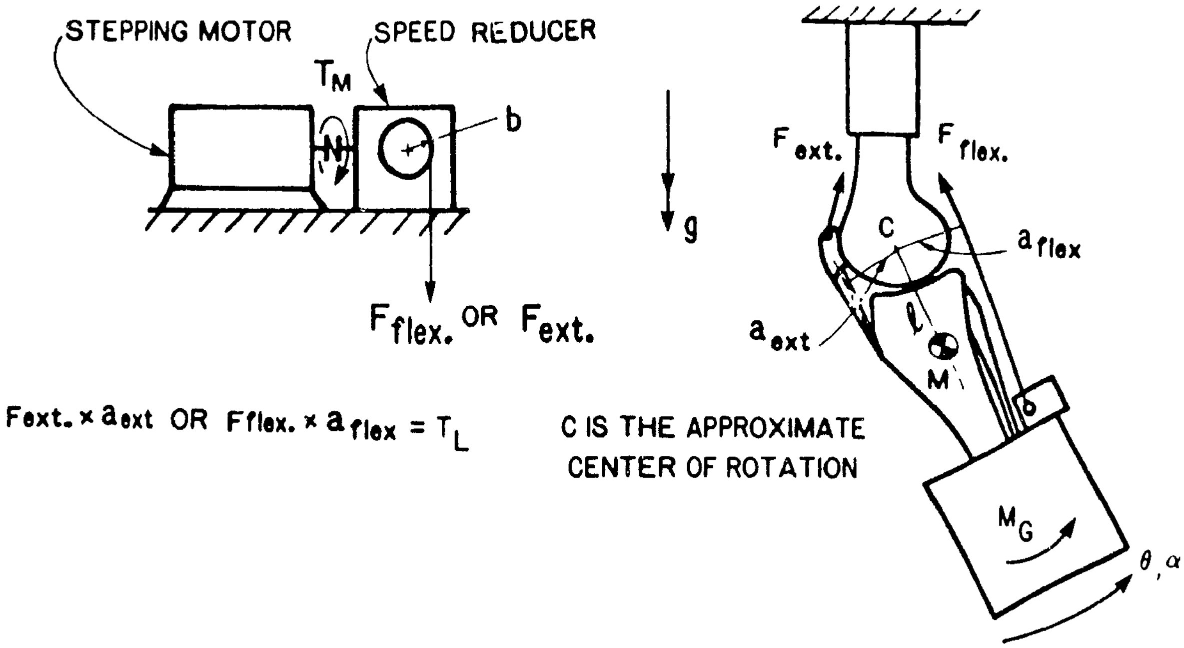

Figure 4.1: Muscle Actuation Parameters

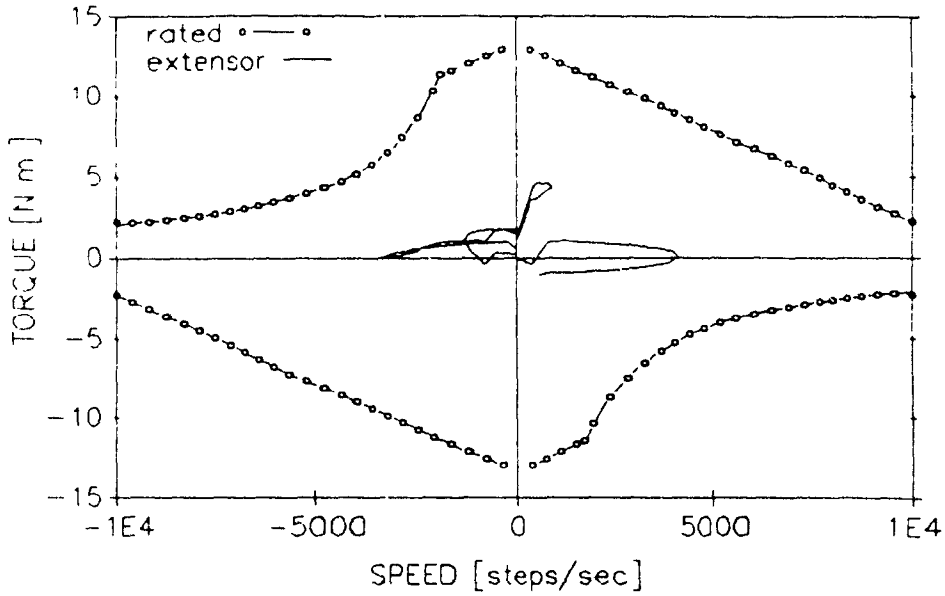

Figure 4.2: Torque/Speed Specifications; Extensor Motor

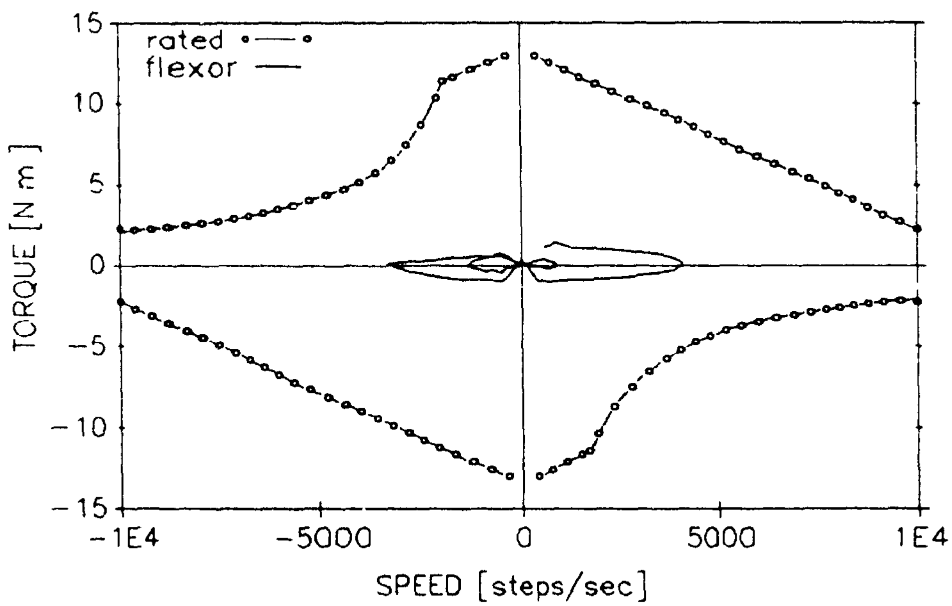

Figure 4.3: Torque/Speed Specifications; Flexor Motor

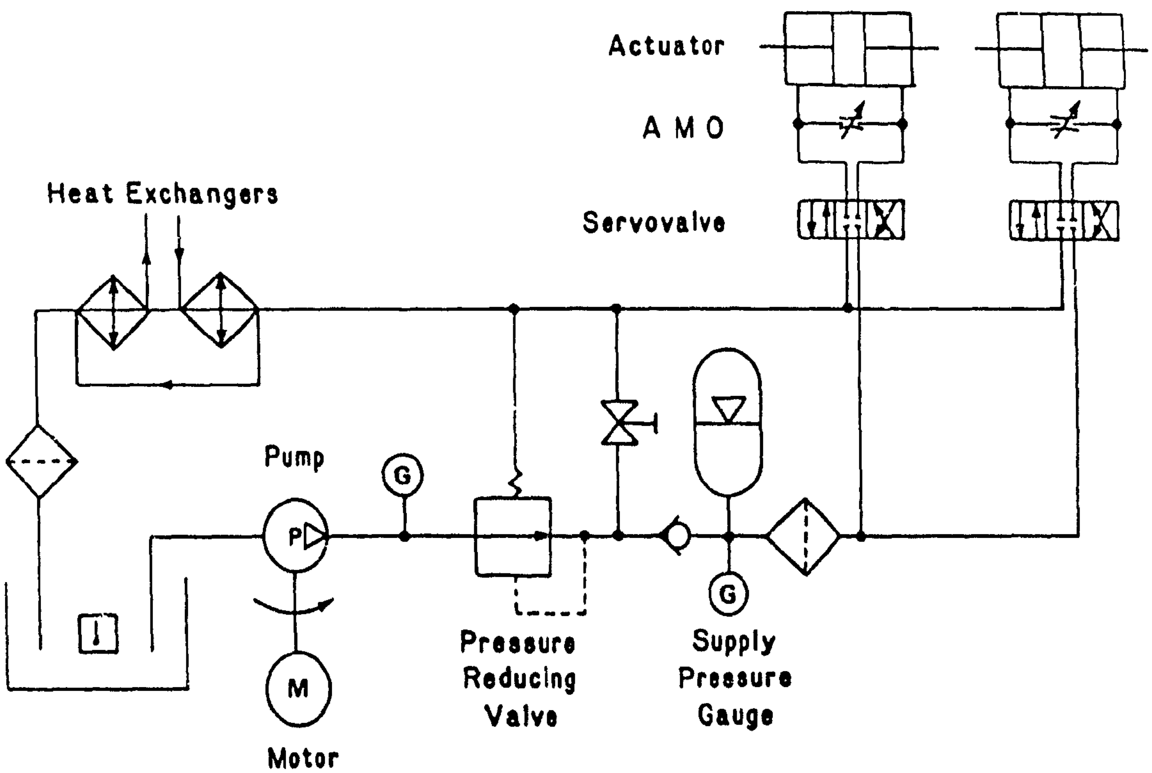

Figure 4.4: Hydraulic System Schematic

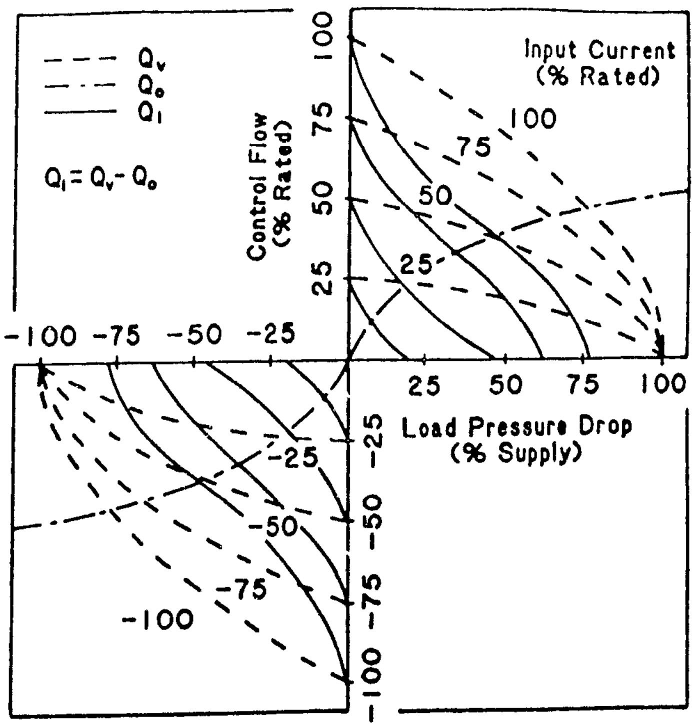

Figure 4.5: Flow-Load Characteristics of a Servovalve with Bypass Flow

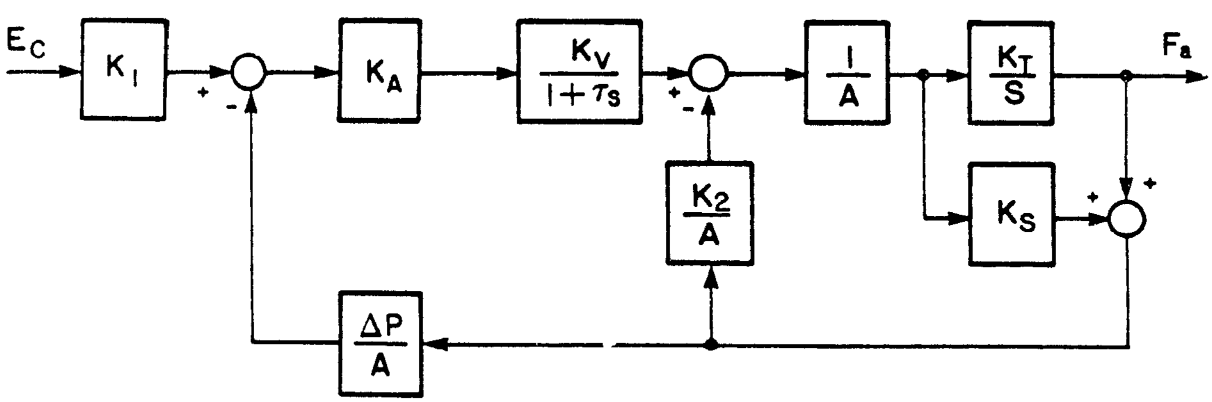

Figure 4.6: Block Diagram for Tibial Axial Force Actuation

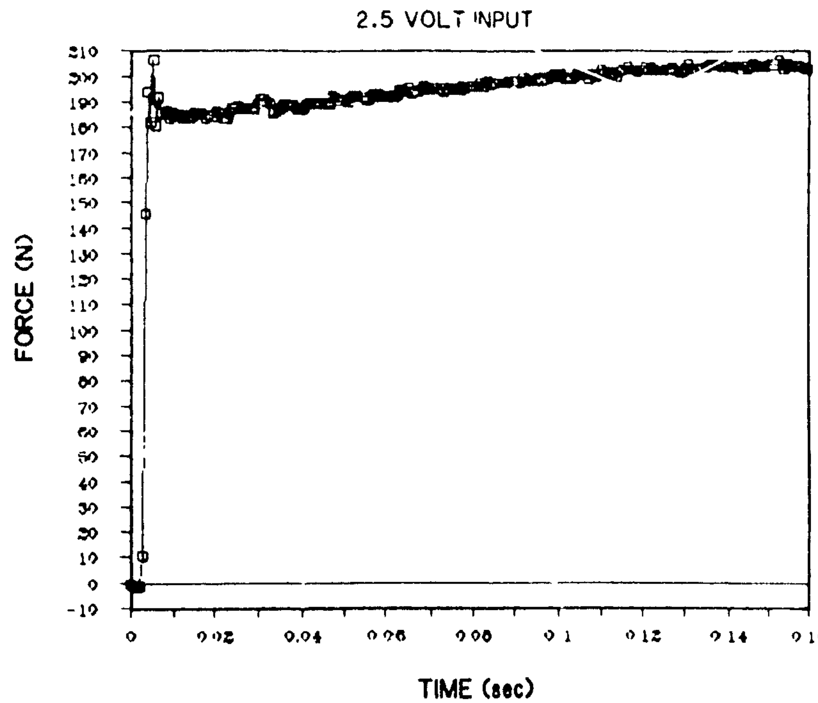

Figure 4.7: Measured Tibial Axial Actuation Step Response

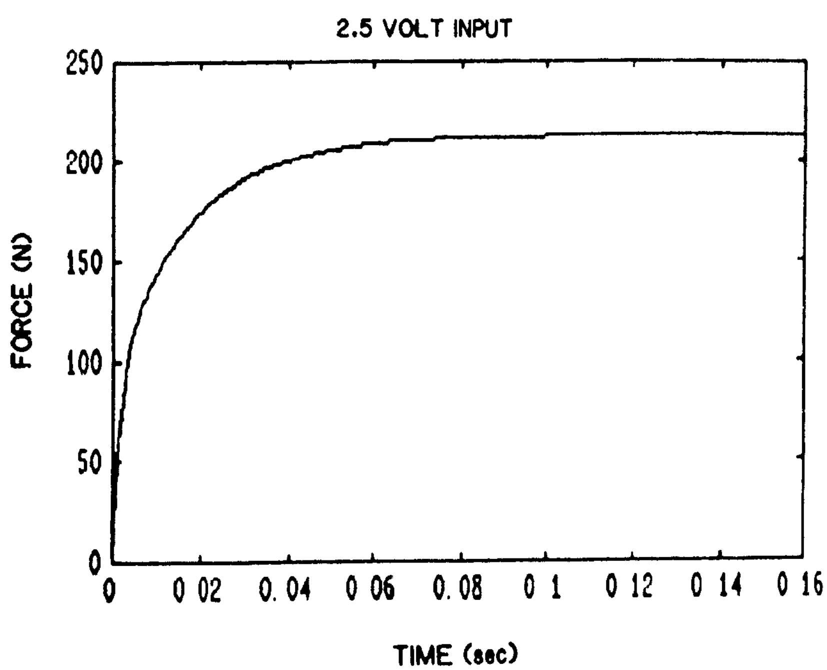

Figure 4.8: Computed Tibial Axial Actuation Step Response

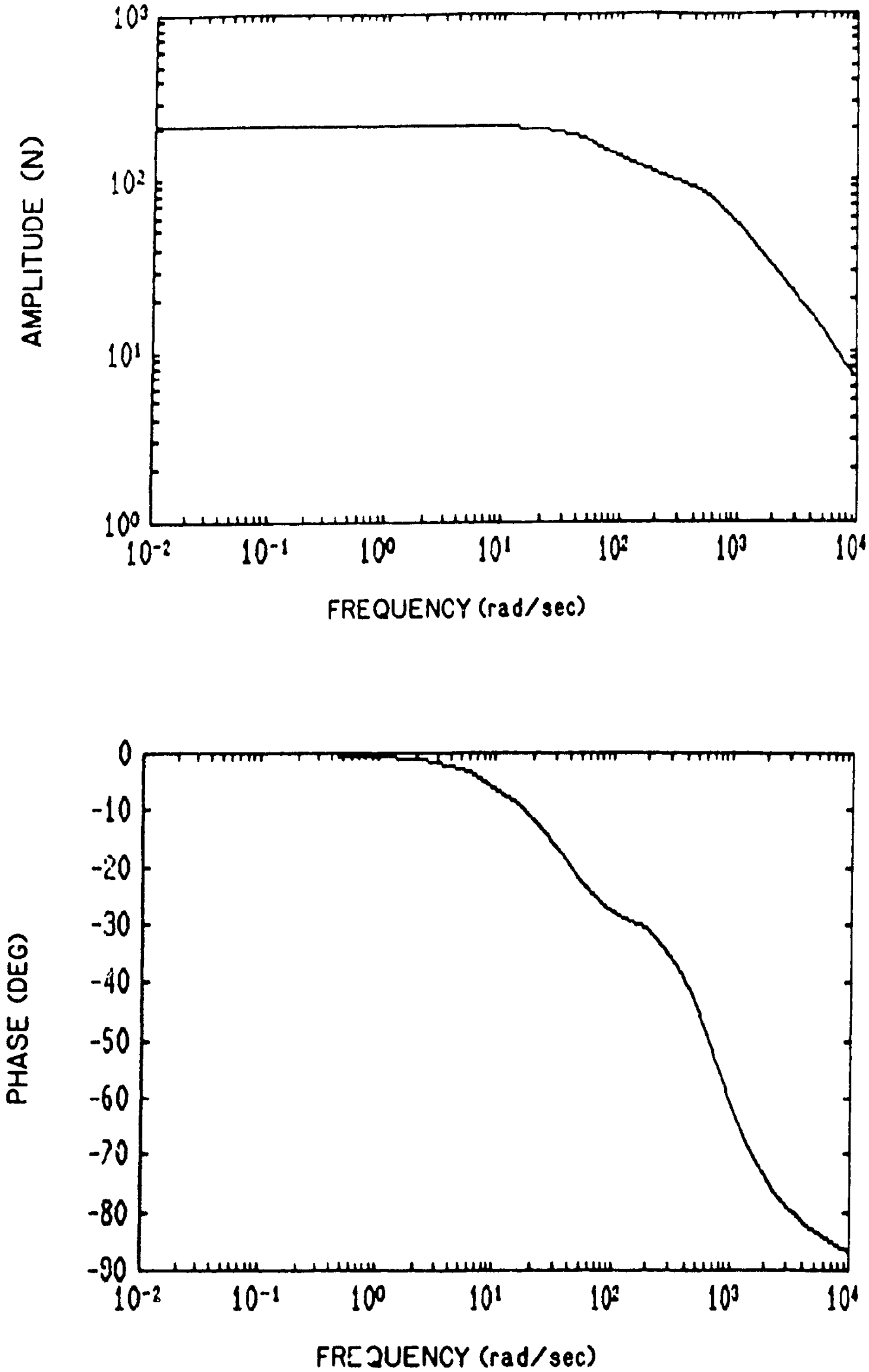

2.5 VOLT INPUT AMPLITUDE

Figure 4.9: Computed Tibial Axial Actuation Frequency Response

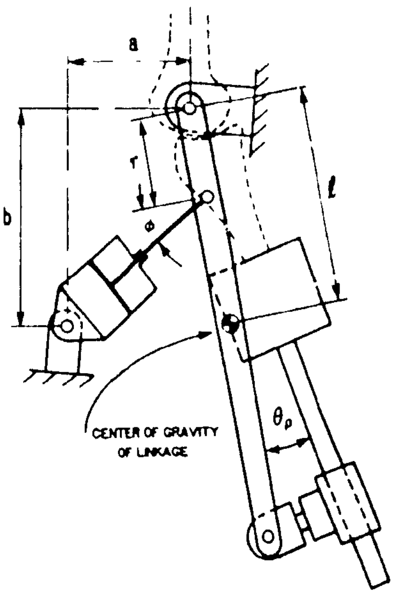

Figure 4.10: Flex./Ext. Moment Actuation Parameters

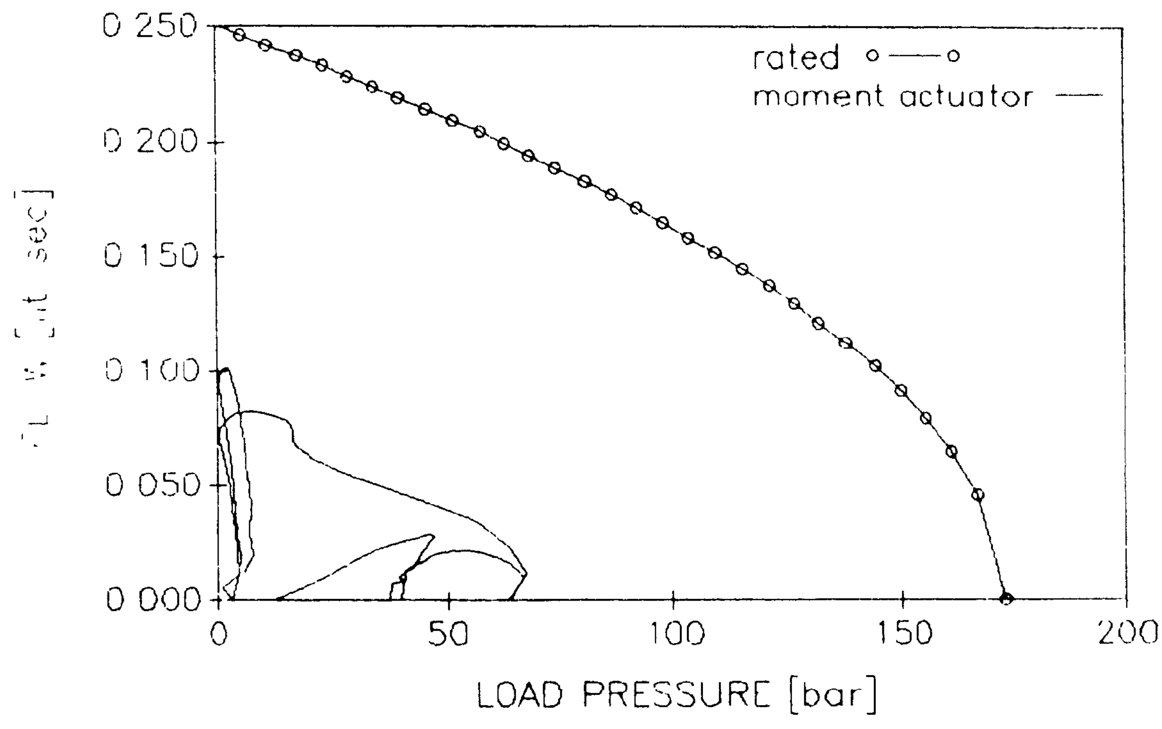

Figure 4.11: Flow/Pressure Specifications of Flex./Ext. Moment Actuation

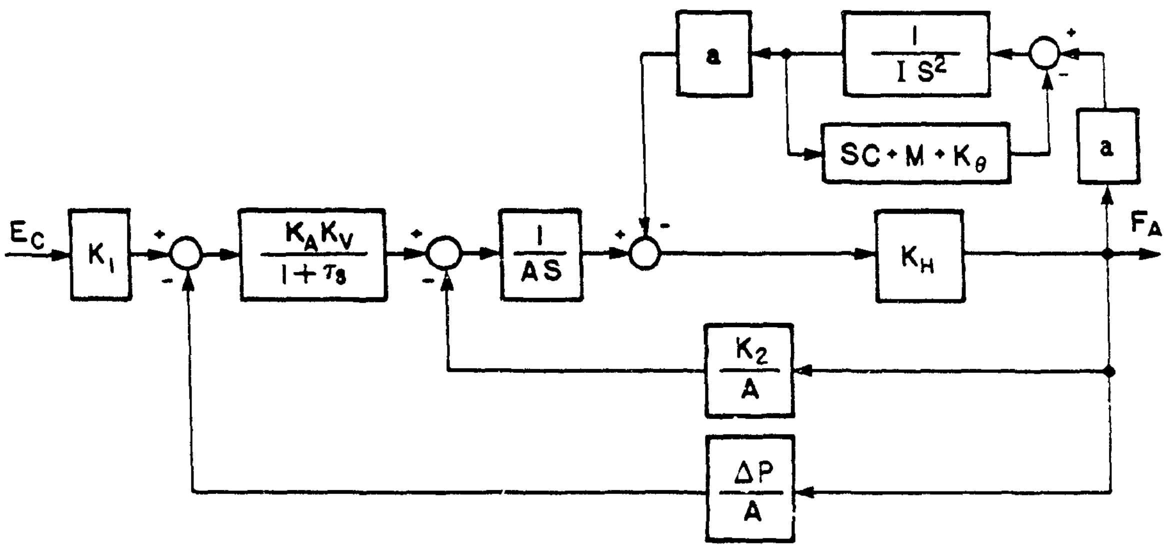

Figure 4.12: Block Diagram for Flex./Ext. Moment Actuation

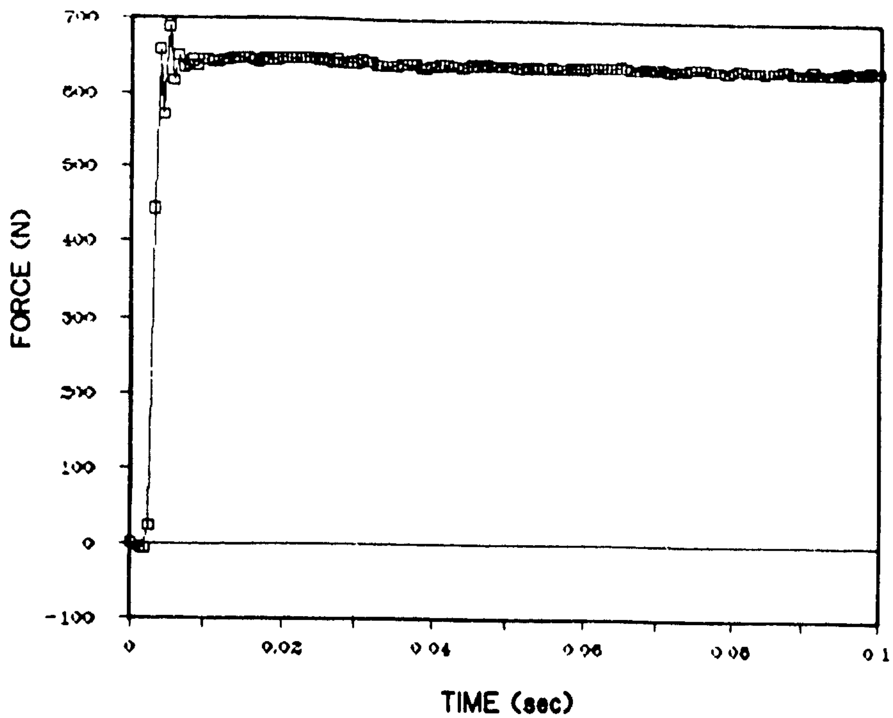

Figure 4.13: Measured Moment Actuation Step Response

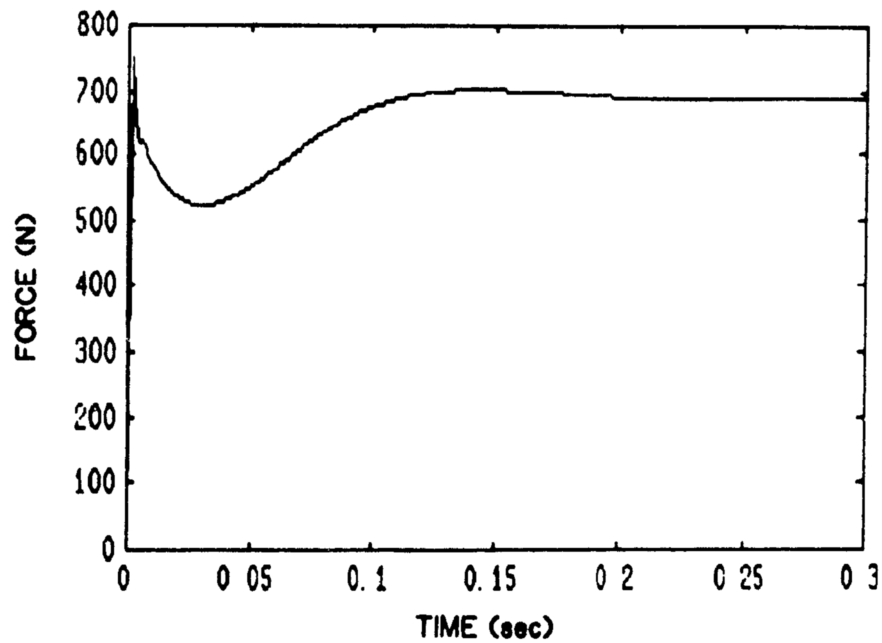

Figure 4.14: Computed Moment Actuation Step Response

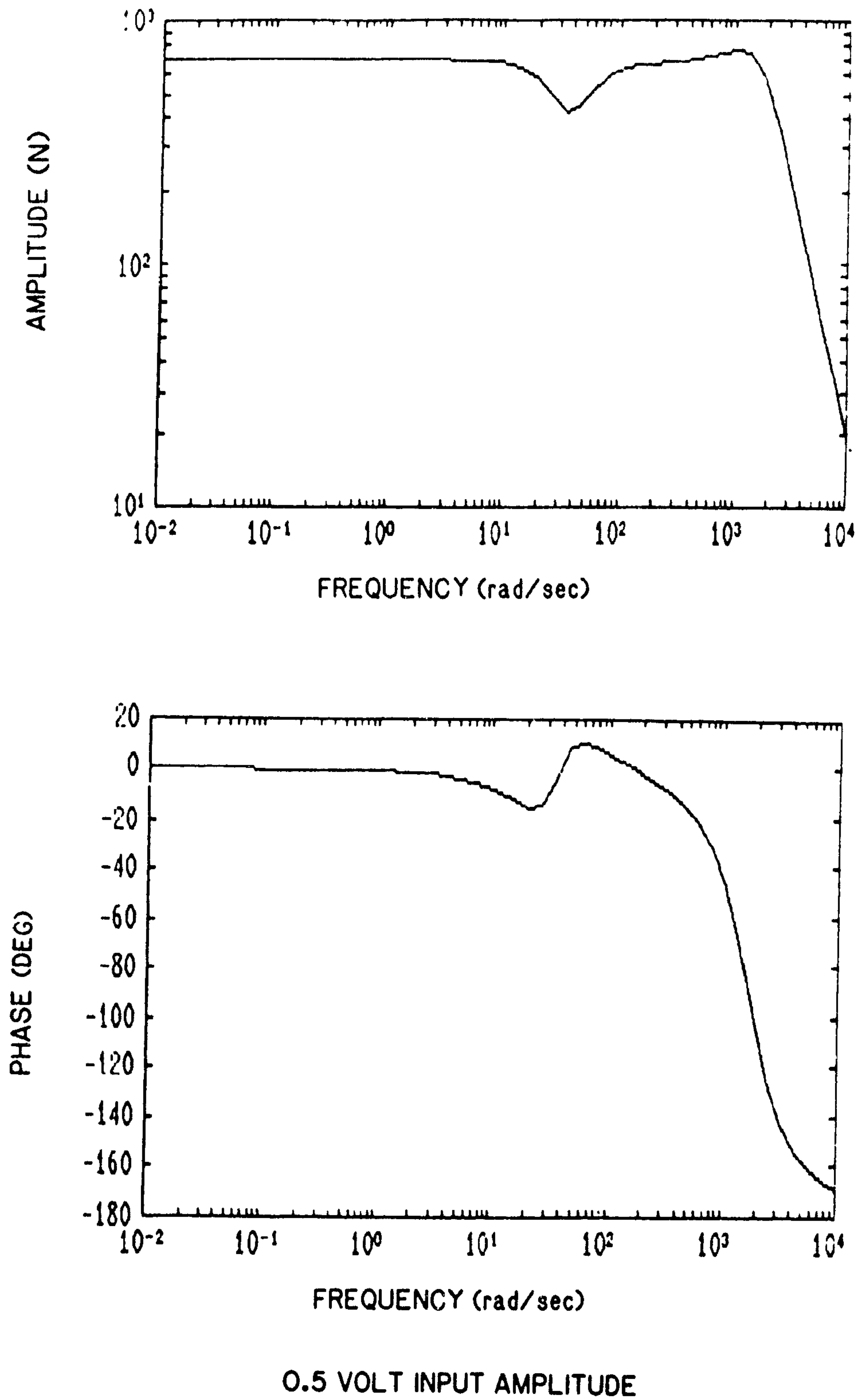

Figure 4.15: Computed Moment Actuation Frequency Response

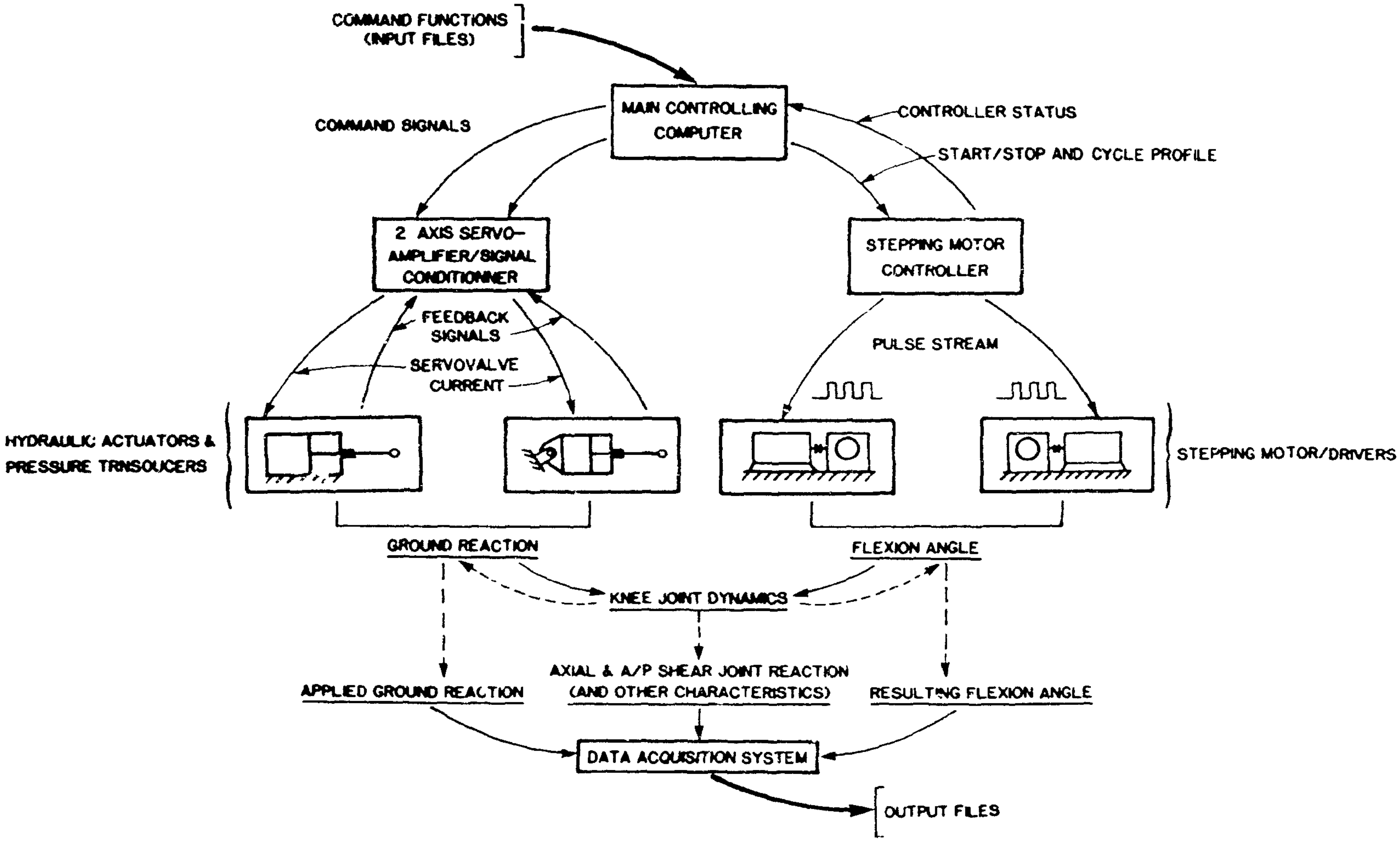

Figure 6 1: Information Flow and Hardware Configuration

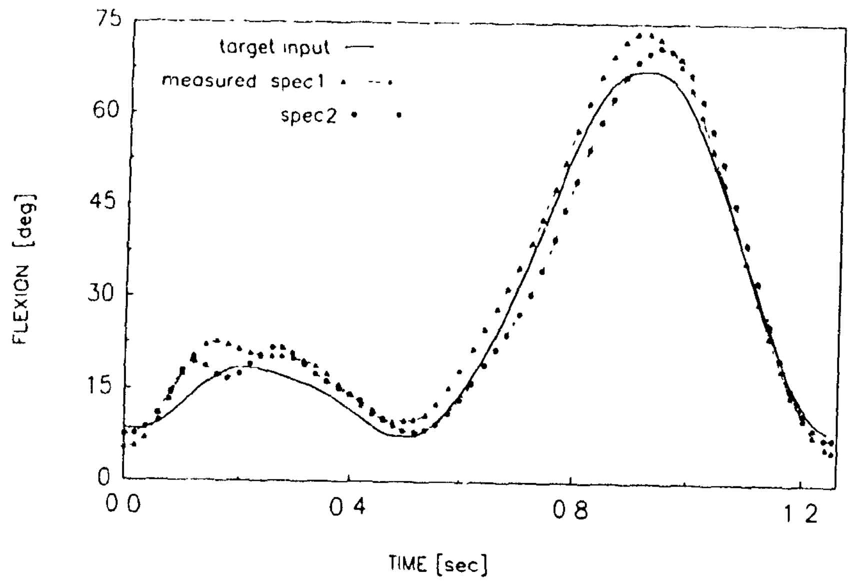

Figure 7.1: Flexion Angle Measurements

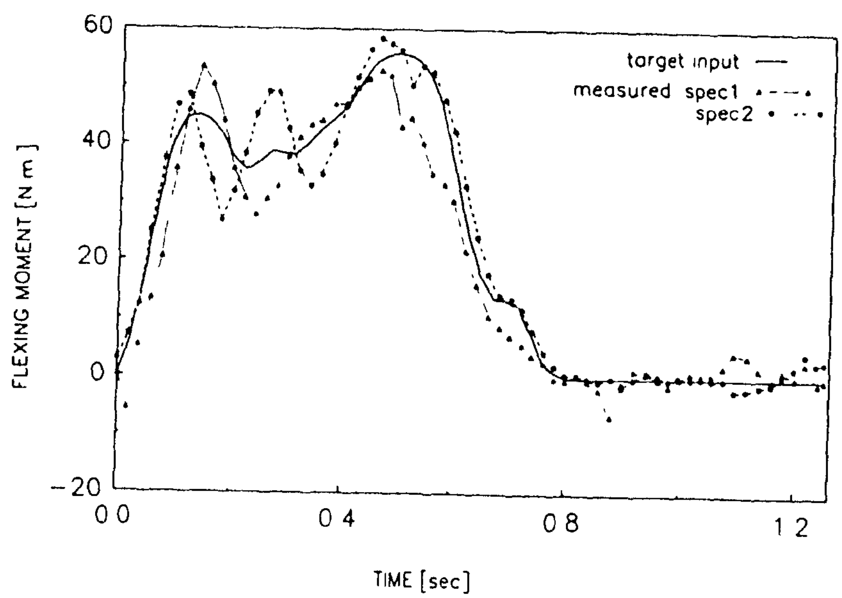

Figure 7.2: Flex./Ext. Moment Measurements

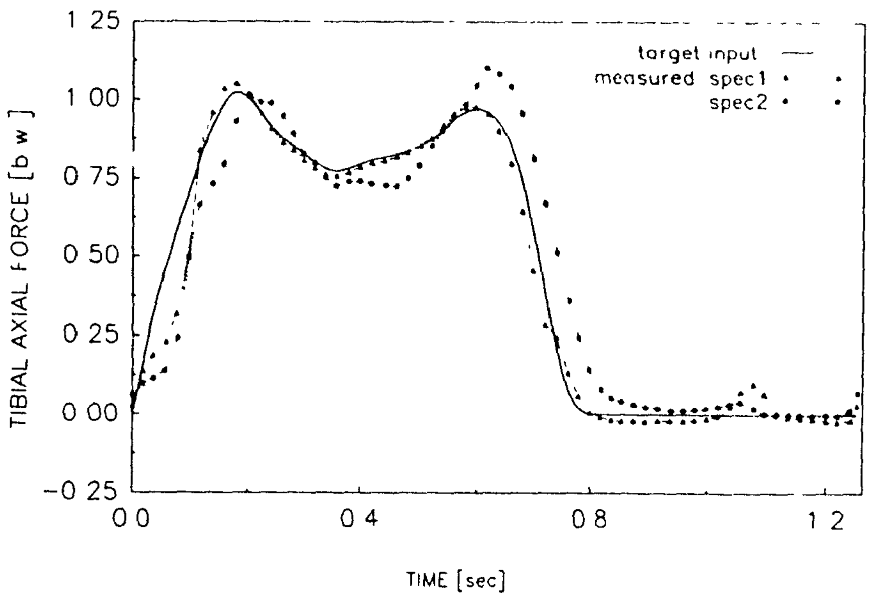

Figure 7.3: Tibial Axial Force Measurements

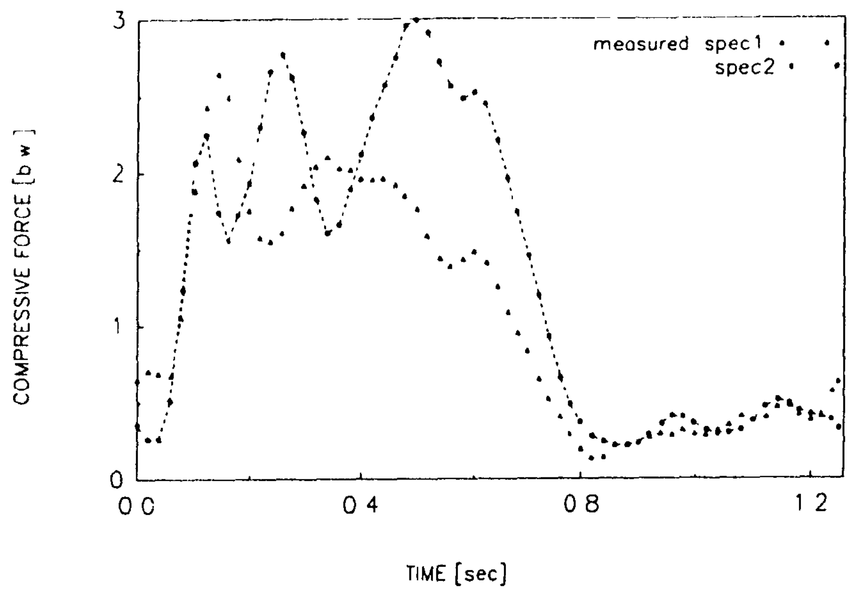

Figure 7.4: Femoral Axial Force Component of Joint Reaction

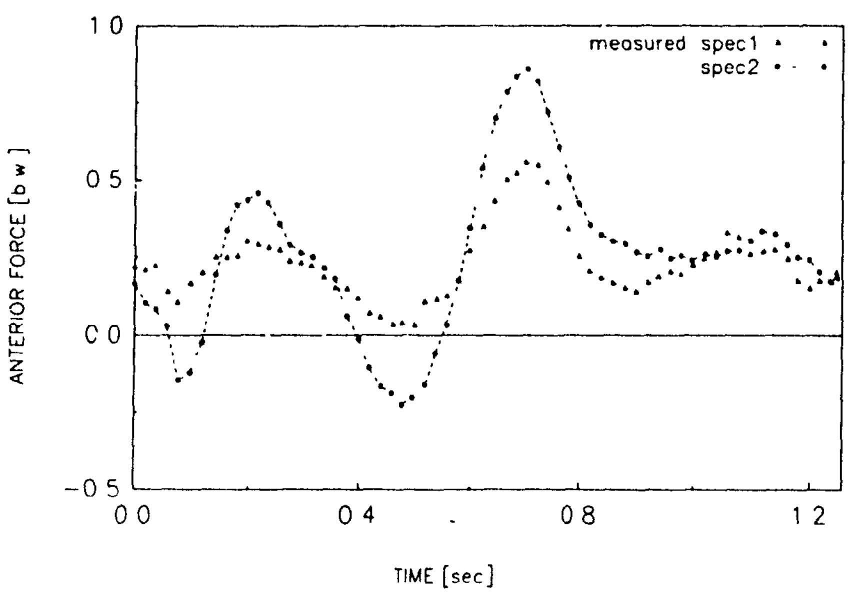

Figure 7.5: Femoral A/P Force Component of Joint Reaction

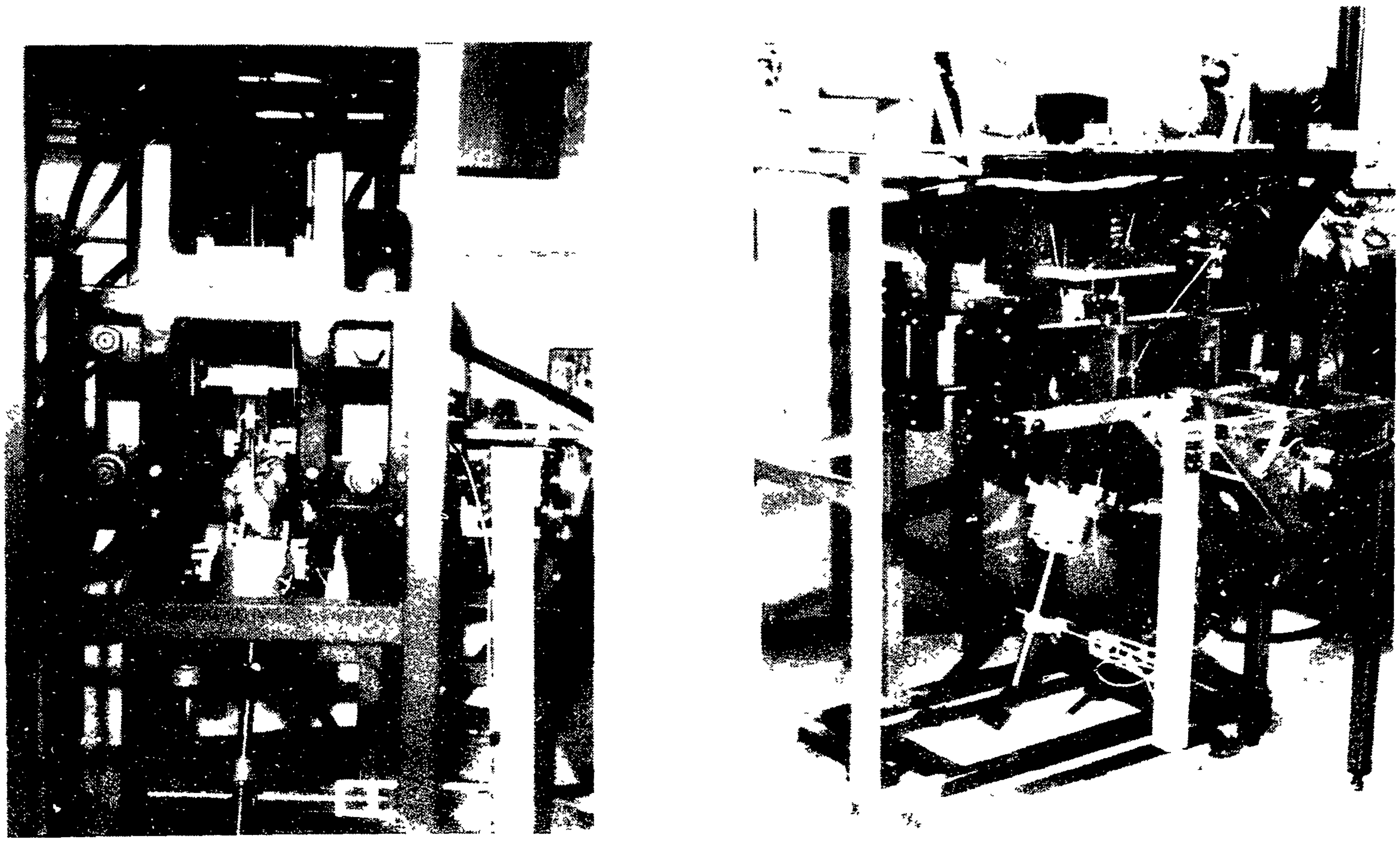

Figure 8.1: Photographs of the Simulator

REFERENCES

AM9513A/AM9513 SYSTEM TIMING CONTROLLER (1985). Technical Manual. Advanced Micro Devices, Sunnyvale, California.

ANDRIACCHI, T.P., ANDERSSON, G B.J., FERMIER, R.W., STERN, D., and GALANTE, J.O. (1980). A Study of Lower-Limb Mechanics during Stair-Climbing. *J of Bone and Joint Surgery*, Vol. 62-A, No 5, p. 749.

CHAO, E.Y , LAUGHMAN, R.K., SCHNEIDER, E., and STAUFFER, R.N. (1983). Normative Data of Knee Joint Motion and Ground Reaction Forces in Adult Level Walking. *J. of Biomech.*, Vol. 16, No. 3, p. 219.

GREER, K.W., (1979). Four Years of Wear Testing Experience on Three Joint Simulators. *Trans. 11th International Biomaterials Symposium*, Vol. 3, p. 80.

GRUNDY, M., TOSH, P.A., McLEISH, R.D., and SMIDT, L. (1975). An Investigation of the Centres of Pressure Under the Foot While Walking. *J. of Bone and Joint Surgery*, Vol. 57, No. 1, p. 98.

HOFFMAN, R.R., LAUGHMAN, R.K., STAUFFER, R.N., CHAO, E.Y. (1977). Normative Data of Knee Motion in Gait and Stair Activities. *Proceedings of the 30th Annual Conference on Engineering in Medicine and Biology*, Vol. 19, p. 186.

HORI, N., UKRAINETZ, P.R., NIKIFORUK, P.N., and BITNER, D.V. (1988). Robust Discrete-Time Adaptive Control of an Electrohydrolic Servo Actuator. *Proceedings of the 8th International Symposium on Fluid Power*, Birmingham, p. 495.

JACKSON, K.M. (1979). Fitting of Mathematical Functions to Biomechanical Data. *IEEE Trans. on Biomed.* Eng., Vol. BME-26, No. 2, p. 122.

KETTELKAMP, D.B., JOHNSON, R.J., SMIDT, G.L., CHAO, E.Y.S., and WALKER, M. (1970). An Electrogoniometric Study of Knee Motion in Normal Gait. *J. Bone and Joint Surg.*, Vol. 52-A, No. 4, p. 775.

MANN, R.A. and HAGY, J. (1980). Biomechanics of Walking, Running, and Sprinting. *American J. of Sports Med.*, Vol. 8, No. 5, p. 345.

MERRITT, H.E. (1971). Gear Engineering. Pitman, London.

MILNER, M., DALL, D., McCONNEL, J.A., BRENNAN, P.K., and HERSHLER, C. (1973). Angle Diagrams in the Assessment of Locomotor Function. *Supplement - S. Afr. J. of Lab. & Clin. Med.*, Vol. 47, Sup., p. 95.

MOOGR. 4076 Servovalve Catalog (762 578).

MORRISON, J.B. (1969). Function of the Knee Joint in Various Activities. *J. of Biomed. Eng.*, Vol. 4, p. 573.

MORRISON, J.B. (1970). The Mechanics of the Knee joint in Relation to Normal Walking. *J. of Biomech.*, Vol. 3, p. 51.

PAPPAS, M.J. and BUECHEL, F.F. (1979). New Jersey Knee Simulator. *Trans. 11th International Biomaterials Symposium*, Vol. 3, p. 101.

PATRIARCO, A.G., MANN, R.W., SIMON, S.R., and MANSOUR, J.M. (1981). An Evaluation of the Approaches of Optimization Models in the Prediction of Muscle Forces During Human Gait. *J. of Biomech.*, Vol. 14, No. 8, p. 513.

REILLY, D.T., MARTENS, M. (1972). Experimental Analysis of the Quadriceps Muscle Force and Patello-Femoral Joint Reaction Force for Various Activities. *Acta. Ortho.* Vol 43, p 126

RICHARDS MANUFACTURING CO. INC. (1978). In-Vitro of the RMCR Total Knee. Research & Development Technical Monograph. p. 10.

SEIREG, A., and ARVIKAR, R.J. (1975). The Prediction of Muscular Load Sharing and Joint forces in the Lower Extremities During Walking. *J. of Biomech.*, Vol. 8, p. 89

SHAW, J.A., and MURRAY, D.G. (1973). Knee Joint Simulator. *Clin. Orth. & Rel. Res.*, Vol. 94, p. 15.

TOWNSEND, M.A., IZAK, M., and JACKSON, R.W. (1977). Total Motion Knee Goniometry. *J. of Biomech.*, Vol. 10, p. 183.

TURBO PASCAL-NUMERICAL METHODS TOOLBOX-IBM VERSION (1986). Borland International Inc., Scotts Valley, Calif.

SPLINE-ALGORITHMEN ZUR KONSTRUKTION GLATTER KURVEN UND FLACHEN (1973). R. Oldenbourg Verlag, Munich.

SZKLAR, O. (1985). Development of an Unconstrained Two-Force Dynamic Simulator for the Human Knee Joint. M.Eng. Thesis, Dept. of Mechanical Engineering, McGill University, Montreal.

SZKLAR, O., AHMED, A.M. (1987). A Simple Unconstrained Dynamic Knee Simulator. *J. of Biomech. Eng.*, Vol. 109, p. 247.

WALKER, P.S., SHOJI, H., and ERKMAN, M.J. (1972). The Rotational Axis of the Knee and its Significance to Prosthesis Design. *Clin. Orth. Rel. Res.*, Vol. 89, p. 160

WINTER, D.A. (1980). Overall Principle of Lower Limb Support During Stance Phase of Gait. *J. of Biomech.*, Vol. 13, p. 923

Appendix A

Tibial Axial Force Actuation Modelling

Following are the dynamic equilibrium equations and parameter estimations used to model the tibial axial force actuation system.

a) Dynamic Equilibrium Equations:

Only the equations corresponding to the plant dynamics are given here. The servo-amplifier/signal conditioner and valve characteristics were described in the text.

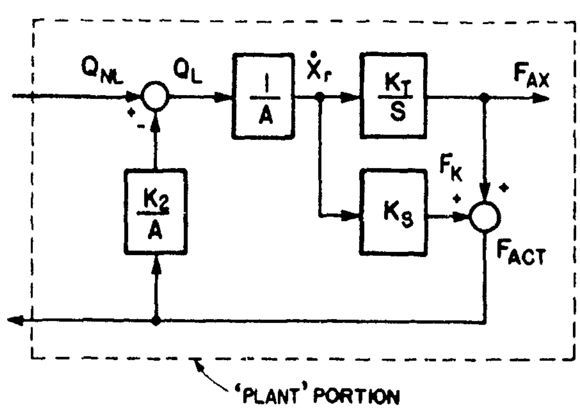

Corresponding to the above figure:

Q_{NL}: no load flow coming out of valve

Q_L: net actuation flow

X_r, $\dot{X}_r$: ram displacement/velocity

K_T: combined elasticity constant of cable (K_C) and hydraulic fluid (K_H)

F_{AX}: tibial axial force

K_S: piston damping force constant

K_2: flow loss factor

A: piston area

F_K: actuator force received to overcome kinetic friction

The plant may be represented as follows:

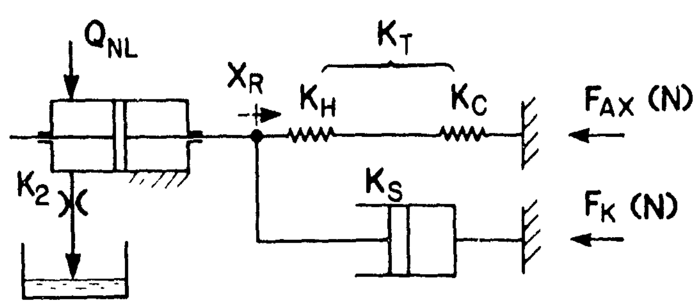

where $K_T = \frac{K_H K_C}{(K_H+K_C)}$; K_H and K_C are the spring constant equivalents of the hydraulic volume and steel cable respectively and $Q_L = K_2 \cdot \frac{(F_{AX}+F_K)}{A}$; $(F_{AX} + F_K)$ is the total force developed by the actuator.

Corresponding equilibrium equations:

1. $Q_{NL} - \frac{K_2}{A}\,(F_{AX} + F_K) = A\,\dot{X}_r$

2. $X_r\,K_T = F_{AX}$

3. $\dot{X}_r\,K_S = F_K$

b) Estimation of Model Parameters:

K_I $\frac{1}{23.51}$ V/V (reference signal amplification)

K_A: 42.76 mA/V (servo amplification)

K_V: 6.71×10^{-6} $m^2/(sec \cdot A)$

(servovalve no-load flow gain @ 17.3 MPa supply pressure)

T: 0.0019 sec (servovalve first order time constant, MOOG^R catalog 762578)

A: 7.1×10^{-4} m^2 (actuator piston area)

K_2: 6.32×10^{-11} $m^3/(sec \cdot Pa)$ (servovalve pressure sensitivity gain measured as described in section 4.3.2)

K_T: 5.138×10^5 N/m (combined spring constant of steel cable (K_C) and hydraulic fluid (K_H))

This parameter was determined as follows

$$K_T = \frac{K_H \cdot K_C}{(K_H + K_C)}$$

where the hydraulic stiffness is determined by

$$K_H = 4 \cdot B \cdot \frac{A^2}{V_T}$$

in which

B: bulk modulus

$= 1.379 \times 10^3$ MPa

A: actuator piston area

$= 7.1 \times 10^{-4}$ m^2

V_T: total fluid volume of actuator

$= 5.08 \times 10^{-5}$ m^3 (MOOG^R data sheet No. 850-1078)

therefore $K_H = 5.46 \times 10^7$ N/m and K_C, the cable spring constant, is given by $K_C = 2.529 \times 10^7$/effective length of cable in cm (N/m) (Szklar, 1985, p. 129) in which $l = 15 + \frac{60}{2} + \frac{15}{4} = 48.75$ cm according to the following schematic

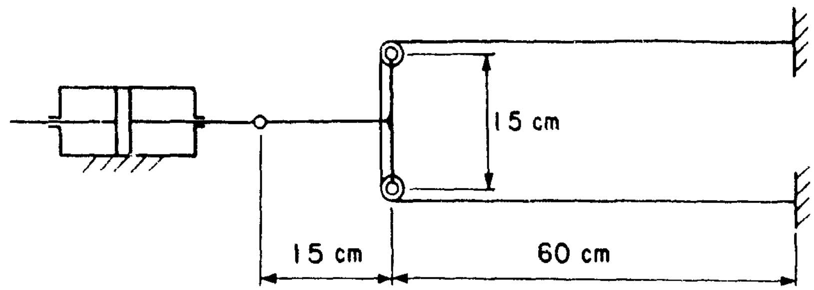

therefore $K_C = 5.187 \times 10^5$ N/m and $K_T = 5.138 \times 10^5$ N/m

$\frac{\Delta P}{A}$: 0.187×10^{-3} V/N (feedback transducer gain including signal-conditioner gain)

This parameter was obtained by assuming a calibrated pressure transducer gain of 0.947 mV/MPa and measuring the signal-conditioner gain (140 V/V).

K_S: 4762 N sec/m (actuator damping force constant)

This parameter was estimated from Szklar (1985), p.71, by combining the actuator velocity calibration factor of 0.084 cm/sec/mV and the force servo gain of 4 N/mV (Szklar, 1985; p.69) to determine the ram force required to generate a ram speed of 1 m/sec.

Appendix B

Flexing/Extending Moment Actuation Modelling

Following are the dynamic equilibrium equations and parameter estimations used to model the flexing/extending moment actuation system.

a) Dynamic Equilibrium Equations:

As for the tibial axial modelling (Appendix A), only the plant dynamics are given here.

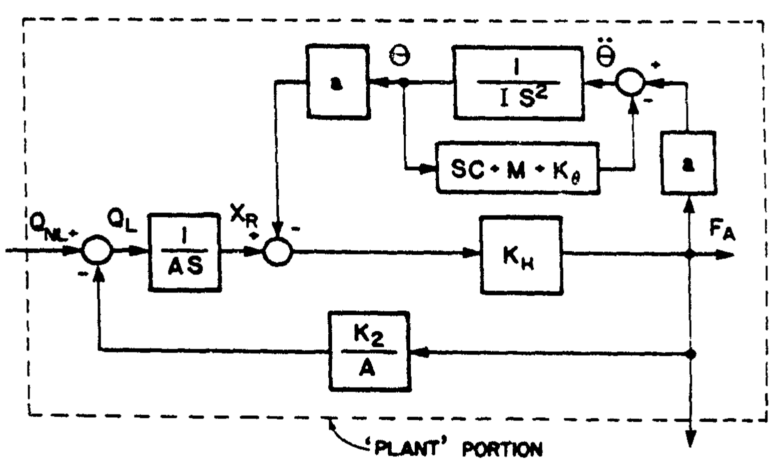

corresponding to this figure:

- Q_{NL}, Q_L, X_r, $\dot{X}_r$, K_H, K_2, and A are as described in Appendix A

- I, M, K_θ, F_a, S, C, and a are described in section 4.3.3, Figure 4.12.

The linearized plant about the set point (30° flexion angle) may be represented as follows:

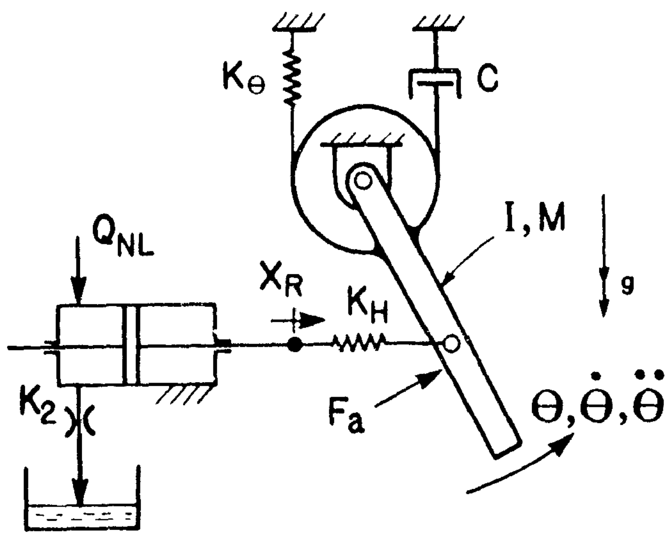

corresponding equilibrium equations:

1. $F_a = K_H\,(X_r - \theta \cdot a)$

2. $F_a \cdot a - M \cdot \theta - C \cdot \dot{\theta} - K_\theta \dot{\theta} = I \cdot \ddot{\theta}$

3. $\dfrac{Q_{NL}}{A} - \dfrac{K_2 \cdot F_a}{A^2} = \dot{X}_r$

where θ is the flexion angle and $\dot{\theta}$ & $\ddot{\theta}$ are its first and second time derivatives.

b) Estimations of Model Parameters:

$K_1 = \frac{1}{3.71}$ V/V (reference signal amplification)

$K_3 = 52.1$ mV/V (servo-amplification)

K_4, T, A, K_H: same as in Appendix A

$K_2 = 1.1 \times 10^{-11}$ $m^3/(sec \cdot Pa)$ (servovalve pressure sensitivity gain measured as described in section 4.3.3)

$\frac{\Delta P}{F} = 0.151$ mV/N (feedback transducer gain including signal-conditioner gain)

This parameter was obtained by assuming a calibrated pressure transducer gain of 0.947 mV/MPa and measuring the signal-conditioner gain (120 V/V)

$K_m = 600$ Nm/rad (reflected rotary spring constant from muscle steel cable)

This parameter was measured in a similar fashion to the parameters established in table 4.1, but for the mechanical knee joint. The features of this test joint may be found in Szklar, 1985; p. 89

$M = 13$ Nm/rad (linearized gravity moment of combined mechanical test joint and mechanical arm)

- linearized gravity moment of test joint $M_1 = \left[\frac{d}{d\theta}\,(m_1 \cdot g \cdot l_1 \sin\theta)\right]$, evaluated at set point of 30° flexion angle (θ) where

  - m_1: lumped mass of test joint, 4.3 kg (Szklar, 1985, p. 130)
  - l_1: length of lumped mass pendulum, 0.2 m (Szklar, 1985; p. 130)

- linearized gravity moment of mechanical arm $M_2 = \left[\frac{d}{d\theta}\,(m_2 \cdot g \cdot l_2 \sin(\theta - \theta_p))\right]$ also evaluated at set point, where

  - m_2: lumped mass of arm, estimated at 1.65 kg
  - l_2: length of lumped mass pendulum, 0.38 m
  - θ_p: offset angle between tibia and arm (see figure 4.10), 8.44°

– therefore $M_1 = 7.3$ Nm/rad and $M_2 = 5.7$ Nm/rad from which $M = M_1 + M_2 = 13$ Nm/rad

I: 0.16 kg m^2 (combined rotary inertia of test joint and mechanical arm)

The rotary inertia of each component was determined by assuming the lumped mass pendulum models used to establish M

a: 0.0284 m (moment arm of actuating force on mechanical arm at 30° flexion, see equation 1.8)

C: 12.8 Nm/(rad/sec) (approximate rotary damping coefficient)

This parameter was obtained by multiplying the measured actuating force required to generate rotary velocity of the mechanical arm, C_l (section 1.3.5), with the moment arm of the actuating force, a. Note that an average C_l, i.e. flexing and extending, is assumed.

Appendix C

Operating Routine Source Listing

```
/*                                                                  */
/*   control of hydraulics,step. motor controllers with switch */
/*     monitoring to terminate process at end of a cycle        */
/*                                                                  */
#include <math.h>
#include <stdio.h>
#include <stdlib.h>
#include <time.h>
#include <conio.h>
extern unsigned char readl(int);
extern unsigned char wwrite(int,int);
main()
{
FILE *infile;
char p;
unsigned char far *tcp,far *tdp,far *lsb_ad1,far *msb_ad1;
unsigned char far *lsb_ad2,far *msb_ad2;
float acti[3][135];          /* actuators                        */
unsigned int act[3][135];
unsigned int cycnt,n,n1,t,t1,dt;
float awo,pulse,w,r;
unsigned char fc,f3,k,tf3,tfc,tt,aw,msb,lsb;
int kk=1;
cycnt=0;
tcp=-1073741824+9;
tdp=-1073741824+8;
lsb_ad1=-1073741824;
msb_ad1=-1073741824+1;
lsb_ad2=-1073741824+2;
msb_ad2=-1073741824+3;
/*                                                                  */
/*  set analog outputs                                              */
/*                                                                  */
infile=fopen("b:ax.prn","rt");
for (k=1;k<109;k++)
```

```
   {fscanf(infile," %f \n",&acti[1][k]);}
fclose(infile);
for (k=1;k<109;k++)
{if(acti[1][k]<0) {act[1][k]=-acti[1][k]*2048/85.0/10;
                   act[1][k]=(~act[1][k])+1;}
   else act[1][k]=acti[1][k]*2048/85.0/10;  }
infile=fopen("b:sf.prn","rt");
for (k=1;k<109;k++)
   {fscanf(infile," %f \n",&acti[2][k]);}
fclose(infile);
for (k=1;k<109;k++)
{if(acti[2][k]<0) {act[2][k]=-acti[2][k]*2048/1346/10;
                   act[2][k]=(~act[2][k])+1;}
   else act[2][k]=acti[2][k]*2048/1346/10;  }
/*                                                              */
/*      configure timers: #1 switch,#3 hydraulics               */
/*                                                              */
wwrite(9,0xff);        /*  reset timer                          */
wwrite(9,95);          /*  dummy load to clear tc state         */
wwrite(9,0x03);        /*  point to mode register of #3         */
wwrite(8,0x28);        /*  1      mhz source                    */
wwrite(8,0x0b);
wwrite(9,0x0b);        /*  point to load register of #3         */
wwrite(8,0x00);        /*  clear                                */
wwrite(8,0x00);
wwrite(9,0x44);        /* load #3                               */
wwrite(9,0x01);        /* point to mode of timer #1             */
wwrite(8,0x02);        /* set output on rising edge of src 1    */
wwrite(8,0x01);
wwrite(9,0x09);        /* point to load of #1                   */
wwrite(8,0x03);
wwrite(8,0x00);
wwrite(9,0xe1);        /*  clear out #1 low                     */
fc=(inp(0x282)&32);
/*                                                              */
/*      go,start,begin                                          */
/*                                                              */
printf("RUN ? Enter 1 for yes, 2 for no: \n");
gets(p);
awo=atof(p);
if(awo==2.0) {goto end2;}
printf("JUST ONE CYCLE ? Enter 1 for yes, 2 for contineous
cycling: \n");
gets(p);
pulse=atof(p);
printf("WINDINGS ON? Enter 1 for off, 2 for on: \n");
gets(p);
awo=atof(p);
if(awo==2.0) {printf("windings are on \n");
              aw=(inp(0x280)^0x10);
              outp(0x280,aw);
              aw=(inp(0x280)^0x20);
```

```
            outp(0x280,aw);}
printf("RUN ? Enter 1 for yes, 2 for no: \n");
gets(p);
r=atof(p);
if(r==2.0) {goto end2;}
wwrite(9,0x61);        /* load & arm #1                          */
outp(0x283,0x03);      /* run stepper controller                 */
start: *tcp=0x44 ;     /* load & arm timer #3: process started   */
      *tcp=0x24 ;
t=0;
t1=0;
k=1;
if(pulse==1.0)   outp(0x283,0x02);
  while (k<109)
          { *tcp=0xa4 ;
            *tcp=0x13 ;
            lsb=*tdp    ;
            msb=*tdp    ;
           t=lsb+(msb<<8);
           if(t1>t) dt=65535-t1+t;
               else {dt=t-t1;}
           if(dt>=11500)
      {*msb_ad1=act[1][k]/256 ;      /*  msb   , actuator #1    */
       *lsb_ad1=act[1][k]%256 ;      /*  lsb                    */
       *msb_ad2=act[2][k]/256 ;      /*  msb   , actuator #2    */
       *lsb_ad2=act[2][k]%256 ;      /*  lsb                    */
       t1=t;
       k=k+1;  }
tt=((*tcp)&2);
      if(tt==2)    {*msb_ad1=0 ; /* kill all if switched */
                    *lsb_ad1=0 ;
                    *msb_ad2=0 ;
                    *lsb_ad2=0 ;
                   outp(0x283,0x02);
                   goto end;}  }
cycnt++;
if(pulse==1.0)     goto end;
*tcp=0xc4 ;                    /*  disarm  #3                   */
while((tfc=(inp(0x282)&32))==fc) { }  /* wait for cycle toggle */
fc=tfc;
goto start;                        /*  start cycle again        */
   end:     if(awo==1.0) goto end2;
printf("TURN WINDINGS OFF ?:1 for yes.\n");
       gets(p);
       w=atof(p);
       if(w!=1.0) goto end2;
                     aw=(inp(0x280)^0x10);
                     outp(0x280,aw);
                     aw=(inp(0x280)^0x20);
                     outp(0x280,aw);
end2:printf("end #cycles=%u \n",cycnt);
wwrite(9,0xc5);
}
```